
Electronic Thesis and Dissertation Repository

12-9-2021 9:00 AM

Investigating a Novel Receptor that Mediates Vasoconstriction in Mouse Femoral Arteries

Joselia Carlos, *The University of Western Ontario*

Supervisor: McGuire, John, *The University of Western Ontario*

A thesis submitted in partial fulfillment of the requirements for the Master of Science degree in Medical Biophysics

© Joselia Carlos 2021

Follow this and additional works at: <https://ir.lib.uwo.ca/etd>



Part of the [Medical Biophysics Commons](#), and the [Pharmacology Commons](#)

Recommended Citation

Carlos, Joselia, "Investigating a Novel Receptor that Mediates Vasoconstriction in Mouse Femoral Arteries" (2021). *Electronic Thesis and Dissertation Repository*. 8289.

<https://ir.lib.uwo.ca/etd/8289>

This Dissertation/Thesis is brought to you for free and open access by Scholarship@Western. It has been accepted for inclusion in Electronic Thesis and Dissertation Repository by an authorized administrator of Scholarship@Western. For more information, please contact wlsadmin@uwo.ca.

Abstract

The synthetic peptide trans-cinnamoyl-leucine-isoleucine-glycine-arginine-leucine-ornithine-amide (tcLIGRLO) causes smooth muscle contraction in mouse femoral arteries. The identity of the receptor that mediates this response is undetermined. We hypothesize that the novel mechanism for tcLIGRLO-induced contractions involves a G-protein coupled receptor (GPCR) and a G_q - Ca^{2+} signalling pathway. Chapter 2 describes experiments using femoral arteries isolated from male and female systemic protease-activated receptor 2 (PAR2KO) mice (n=31; 21 – 39 weeks of age) using tcLIGRLO and the G_q -inhibitor, YM-254890 (YM). Contractions produced by tcLIGRLO did not differ by sex but decreased as age increased. YM inhibited tcLIGRLO-induced contractions. Chapter 3 describes preliminary work to identify a human GPCR for tcLIGRLO, other than PAR2, using the TANGO assay to screen four candidates. We identified a potential human GPCR target that warrants additional study. In conclusion, tcLIGRLO activates a novel mechanism involving a G_q -coupled receptor. This novel mechanism may have potential significance in vascular biology.

Keywords

tcLIGRLO, G-protein coupled receptor, G_q , calcium signalling, smooth muscle contraction, YM-254890, orphan receptor, protease-activated receptor 2, TANGO assay

Summary for Lay Audience

We have a test compound called tcLIGRLO that causes smooth muscle contraction in a mouse artery. We do not know how the compound works but we believe it is a novel receptor for which no drugs have yet been designed to target. We used a compound called YM to block the pathways for a common type of receptor called G-protein coupled receptors or GPCRs. We found YM blocked our test compound. We also screened some candidate human GPCRs as targets of tcLIGRLO. We found some evidence that one of these receptors was activated by tcLIGRLO. In summary, we discovered more details about a novel mechanism found in mouse blood vessels and a potential human receptor that could have relevance to human vascular pathophysiology.

Co-authorship statement

Joselia Carlos conducted all experiments, data collection, and analyses unless otherwise noted below.

Dr. John McGuire conceived the research projects outlined in this thesis, advised, and supervised JC on experimental design, conducting experiments, analyses and interpretations of data, the presentation of results and the writing, editing, revising of drafts of this entire thesis.

Chapter 1.2 is a piece of writing by JC from early drafts of a systematic review on YM submitted for scientific publication and currently, is in revision.

The authorship details of this manuscript are : Joselia Carlos, Haleh Zabihi, Andrea N. Wang, and John J. McGuire. Discovering G protein coupled receptor signals: a review of the $G\alpha_{q/11}$ inhibitor YM-254890. 51 pages. 160 references.

Experiments with ecPAR2KO mice (Chapter 2.3.2) were conducted in concert with Haleh Zabihi, but only the work completed by JC is reported.

Dr. Rithwik Ramachandran was instrumental in the design, execution, analyses, and interpretation of Ca^{2+} signalling studies (Chapter 2) and the TANGO assay (Chapter 3).

Under Dr. Ramachandran's supervision Victor Mirka (grad student) provided technical assistance to JC for conducting experiments, and preliminary data analyses in Chapters 2.3.4 and 3.3.1.

Acknowledgments

This research was a Discovery Grant awarded to Dr. McGuire (principal investigator) by the Natural Sciences and Engineering Research Council (NSERC). Joselia Carlos received a Western Graduate Research Scholarship.

This thesis would not have been possible without the contribution and support of several people. Firstly, I would like to thank my supervisor, Dr. John McGuire, for your continuous guidance. Thank you for introducing me to the field of cardiovascular pharmacology. Your ambitiousness and perseverance are truly admirable.

Thank you to my committee members—Dr. Jefferson Frisbee, Dr. Krishna Singh, and Dr. Rithwik Ramachandran. Thank you all for your input and guidance. Thank you, Jeff, for your “life advice” from our occasional chats. I enjoyed our brief chats because I always gained some novel insight on not just in science, but also in life. Thank you, Krishna, for your expertise on molecular biology techniques. Your work ethic and humility are commendable. Thank you, Rithwik, for basically welcoming me as an additional member in your laboratory during this masters. Your expertise on cell work and patience are highly appreciated. I really did enjoy getting to know the members of your lab.

I would like to thank my fellow lab members—Cheng Lim, Qing Zong, Ryan Singer, Haleh Zabihi, Caroline Marszal, and Andrea Wang—for creating a positive lab environment. Thank you, Cheng and Qing, for teaching me wire myography. Thank you, Ryan, Haleh, and Andrea, for your assistance in data collection. As well, thank you Haleh for co-writing the YM review article with me. Most importantly, thank you, Andrea, for being my confidant during my graduate studies. As the only two graduate students in the lab, we faced a lot of obstacles together—one of them being completing two-thirds of our masters in the middle of a global pandemic. I am thankful for our friendship.

Thank you, Victor Mirka, for helping me to troubleshoot and optimize my TANGO experiments in addition to your own thesis work. While the TANGO experiments took a lot longer than expected, I will always appreciate your unwavering support.

Thank you, David Michels and Dr Lyn Wang, for helping out with genotyping. Thank you, Mariola, for managing our mice and promptly having the mice ready for us every morning on the day of experiments.

Thank you to my parents for supporting me emotionally and financially as I embarked on this thesis. Lastly, thank you, Cullen, for your emotional support and for being my encourager throughout this whole process.

Table of Contents

Abstract.....	ii
Summary for Lay Audience	iii
Co-authorship statement.....	iv
Acknowledgments	v
Table of Contents	vii
Abbreviation and Glossary	xi
List of Tables	xiii
List of Figures.....	xiv
Chapter 1	1
1 Introduction.....	1
1.1 tcLIGRLO: a PAR2-activating peptide	3
1.2 YM: a tool for investigating GPCR signals.....	8
1.2.1 Introduction to YM.....	8
1.2.2 GPCRs and heteromeric G proteins	8
1.2.3 Investigating PAR2 with YM.....	9
1.2.4 Uses of YM to study vascular smooth muscle contraction	10
1.2.5 Refining characteristics of GPCRs and discovering novel G _q -mediated signalling mechanisms.....	14
1.3 Orphan receptors: a class of GPCRs whose ligands remain unknown.....	14
1.3.1 Introduction to orphan receptors	14
1.3.2 Techniques for de-orphanization	15
1.3.2.1 Reverse pharmacology	15
1.3.2.2 TANGO and PRESTO-TANGO assay	16
1.3.3 Lesser known and uncharacterized receptors: SUCNR1, CCRL2, GPR15, and GPR135.....	19

1.3.3.1	SUCNR1: a de-orphanized receptor.....	19
1.3.3.2	The remaining orphans: CCRL2, GPR15, and GPR135.....	20
1.4	Thesis statement, hypothesis, objectives, rationale	23
Chapter 2	25
2	Role of G _q in tcLIGRLO-induced contractions of mouse vascular smooth muscle.....	25
2.1	Introduction	25
2.2	Materials and methods.....	25
2.2.1	Chemical reagents and drug solutions.....	25
2.2.2	Animals.....	26
2.2.2.1	Ethics Statement on the care and use of animals in research.....	26
2.2.2.2	Mice.....	26
2.2.3	Wire Myograph Experiments	27
2.2.3.1	Isolation of femoral arteries	27
2.2.3.2	DMT myographs	27
2.2.3.3	Normalization of baseline tension for femoral arteries.....	27
2.2.3.4	Vascular smooth muscle contraction and relaxation bioassay protocols.....	28
Substudy 1:	Sex and age in PAR2KO mice	28
Substudy 2:	Effects of YM on femoral arteries from PAR2KOs.....	29
Substudy 2.1.	tcLIGRLO and YM.....	29
Substudy 2.2.	Phenylephrine and YM	29
Substudy 2.3.	KCl and YM.....	29
Substudy 3:	ecPAR2KO.....	29
Substudy 3.1.	tcLIGRLO dose-response curves	29

Substudy 3.2. Ach and SNP relaxation.....	29
2.2.4 Cell lines	30
2.2.5 Ca ²⁺ signalling	30
2.2.6 Data analysis and statistics.	31
2.3 Results	34
2.3.1 Effects of sex and age on tcLIGRLO-induced contractions.....	34
2.3.2. Effects of the G _q inhibitor YM on femoral arteries	42
2.3.2 tcLIGRLO effects in ecPAR2KO mice	47
2.3.3 Effects of the G _q inhibitor YM on Ca ²⁺ signals in PAR2WT HEK293 cells	51
2.4 Discussion.....	55
2.4.1 Age-related effects on tcLIGRLO-mediated contractions.....	55
2.4.2 tcLIGRLO-mediated contractions are G _q -dependent	57
2.4.3 YM inhibition of PAR2 Ca ²⁺ signalling pathway	57
Chapter 3	59
3 Assessing for GPCR activation with the TANGO assay.....	59
3.1 Introduction	59
3.2 Materials and Methods	60
3.2.1 Chemical reagents and drug solutions	60
3.2.2 Cloning and transfection.....	61
3.2.3 Luciferase reporter assay	61
3.2.4 Data and statistical analyses	62
3.3 Results	63
3.3.1 PAR2 activation with tcLIGRLO, SLIGRL, 2fLIGRLO	63
3.3.2 Effects of tcLIGRLO on CCRL2, GPR15, GPR135, and SUCNR1 expressing HTLA cells in TANGO assay	66

3.4 Discussion.....	68
3.4.1 PAR2 activation with SLIGRL, 2fLIGRLO, and tcLIGRLO with the TANGO assay	68
3.4.2 β -arrestin activity with CCRL2, GPR135, GPR15, and SUCNR1.....	68
Chapter 4	69
4 Overall discussion and conclusions	69
4.1 Overall discussion	69
4.1.1 tcLIGRLO-smooth muscle contractions.....	69
4.1.2 <i>In vivo</i> studies with tcLIGRLO and YM	69
4.1.3 tcLIGRLO as a potential ligand for GPR135	70
4.1.4 Future directions	71
4.2 Conclusions	72
References	73
Appendices	89
Curriculum Vitae	90

Abbreviation and Glossary

Ach	Acetylcholine
ANOVA	Analysis of variance
cAMP	Cyclic adenosine monophosphate
Ca ²⁺	Calcium ion
CCRL2	C-C chemokine receptor-like 2, a type of GPCR
CRC	Concentration response curve; in this thesis, is used synonymously with dose-response curve
DAG	diacylglycerol
ecPAR2KO	Endothelial cell-specific protease-activated receptor 2 knockout
EC ₅₀	Molar concentration of drug or activator producing 50% of E _{max}
E _{max}	Maximum effect produced by an activator or agonist
eNOS	Endothelial nitric oxide synthase; encoded by <i>nos3</i>
ERK	Extracellular signal-regulated kinase
GDP	Guanine diphosphate
GPCR	G-protein coupled receptor; in this thesis, is specific to the 7 transmembrane receptor form
GTP	Guanine triphosphate
HBSS	Hank's Balanced Salt Solution
HEK293	Human embryonic kidney 293 cells
HTLA	HEK293 cells stably expressing a tetracycline transactivator-dependent luciferase, reporter, and a β -arrestin-2-Tobacco Etch Virus fusion gene
IC ₁	Internal circumference of blood vessel at resting tension and is equal to 90% of IC ₁₀₀ (see abbreviation below)
IC ₅₀	Concentration of inhibitor that produces 50% of E _{max}
IC ₁₀₀	100% internal circumference of blood vessel under pre-determined target transmural pressure 13.3kPa (100mmHg)

IP ₃	Inositol triphosphate
KO	Knockout; referring to targeted gene deletion
PAR	Protease-activated receptor
PAR1	Protease-activated receptor 1
PAR2	Protease-activated receptor 2; encoded by <i>par2</i> (<i>F2rl1</i>) gene
PAR2AP	PAR2-activating peptide, all peptide sequences are amides unless otherwise noted
PBS	Phosphate buffer saline
PKC	Protein kinase C
PIP ₂	Phosphatidylinositol 4,5-bisphosphate
PRESTO	Parallel receptor-ome expression and screening via transcriptional output
RhoA	Ras homolog family member A
ROCK	Rho-associated protein kinase
SNP	Sodium nitroprusside
SLIGRL	serine-leucine-isoleucine-glycine-arginine-leucine
S.E.	Standard error of the mean
SUCNR1	Succinate receptor 1, a family of GPCRs
TANGO	transcriptional activation following arrestin translocation
tcLIGRLO	trans-cinnamoyl-leucine-isoleucine-glycine-arginine-leucine-ornithine
WT	Wildtype, also refers to the control strain
2fLIGRLO	2-furoyl-leucine-isoleucine-glycine-arginine-leucine-ornithine
YM	YM-254890; (R)-1-((3S,6S,9S,12S,18R,21S,22R)-21-acetamido-18-benzyl-3-((R)-1-methoxyethyl)-4,9,10,12,16,22-hexamethyl-15-methylene-2,5,8,11,14,17,20-hepta-oxo-1,19-dioxo-4,7,10,13,16-pentaazacyclodocosan-6-yl)-2-methylpropyl (2S,3R)-2-acetamido-3-hydroxy-4-methylpentanoate

List of Tables

Table 1. Comparison of pEC ₅₀ values for PAR2-mediated signalling with PAR2-activating peptides tcLIGRLO, SLIGRL, and 2-fLIGRLO in intracellular Ca ²⁺ signalling and blood vessel relaxation assays.	6
Table 2. List of agents, their respective targets, and effects on 50μM tcLIGRLO-mediated contractions.....	7
Table 3. Summary of pIC ₅₀ values for YM inhibition of G protein couple receptors and ligands signalling in vascular smooth muscle contraction.	12
Table 4. Summary table providing tissue distribution profile, G-protein signalling, putative ligands, and reported physiological roles of CCRL2, GPR15, SUCNR1, and GPR135.....	21
Table 5. A summary table of physical characteristics of mice (weight and age) and femoral arteries (length and diameter) and sample size.....	32
Table 6. A summary table of pEC ₅₀ , E _{max} , and sample size values of tcLIGRLO and phenylephrine drug treatments in PAR2KO mice.....	39
Table 7. E _{max} values of tcLIGRLO-mediated contractions of male PAR2KO femoral arteries from three different age groups	41
Table 8. E _{max} and pEC ₅₀ values of tcLIGRLO- and phenylephrine-induced contractions following YM treatments in femoral arteries from male PAR2KO mice.	45
Table 9. pEC ₅₀ and E _{max} values of Ach- and SNP-induced relaxation in femoral arteries from ecPAR2KO and WT mice following pre-contraction to 3μM phenylephrine.	50
Table 10. E _{max} and pEC ₅₀ values of PAR2 activation with PAR2-APs in PAR2-transfected HTLA cells in the TANGO assay	65

List of Figures

Figure 1. Schematic of tcLIGRLO mechanisms of action in mouse blood vessels.	2
Figure 2. Schematic representation of the TANGO assay.	18
Figure 3. tcLIGRLO-induced contractions of femoral arteries from male PAR2KO mice.	35
Figure 4. tcLIGRLO-response curves in male vs female PAR2KO femoral arteries.	36
Figure 5. Phenylephrine CRCs in male vs female PAR2KO femoral arteries.	37
Figure 6. Ach and SNP relaxation response curves in femoral arteries from male PAR2KO mice.	38
Figure 7. Effect of age on tcLIGRLO contractions of male PAR2KO femoral arteries.	40
Figure 8. YM inhibition of tcLIGRLO-mediated contractions in femoral arteries of PAR2KO male mice.	43
Figure 9. YM inhibition of phenylephrine-mediated contractions in femoral arteries of PAR2KO male mice.	44
Figure 10. K ⁺ contractions in the presence and absence of YM.	46
Figure 11. tcLIGRLO-mediated contractions in ecPAR2KO and PAR2WT femoral arteries.	48
Figure 12. Ach- and SNP CRCs in ecPAR2KO and PAR2WT femoral arteries.	49
Figure 13. tcLIGRLO-mediated Ca ²⁺ signalling in PAR2KO and PAR2WT HEK293 cells.	52
Figure 14. YM inhibition of PAR2-activated Ca ²⁺ signalling for tcLIGRLO-treated PAR2WT HEK293 cells.	53
Figure 15. tcLIGRLO-mediated Ca ²⁺ signalling in PAR2WT HEK293 cells.	54

Figure 16. PAR2 activation with SLIGRL, 2fLIGRLO, and tcLIGRLO in PAR2-transfected HTLA cells using the TANGO assay.....	64
Figure 17. TANGO luminescence of tcLIGRLO treated HTLA cells-expressing PAR2, SUCNR1, GPR135, GPR15, or CCRL2.	67

Chapter 1

1 Introduction

The seven transmembrane domain G-protein coupled receptors (GPCRs) are highly druggable targets, with over 700 approved drugs targeting this protein superfamily (Sriram & Insel, 2018). Over 800 genes encode GPCRs, whose known ligands consist of hormones, neurotransmitters, chemokines, ions, odourants, and physical stimuli (Pierce et al., 2002). There are also about 100 GPCRs, which are referred here as orphan GPCRs, having no ligands identified yet. Protease-activated receptor 2 belongs to the protease-activated receptors (PARs) family whose endogenous activators are serine proteases (Barrios et al., 2003; Coughlin et al., 1992; Feld et al., 2013; Vergnolle et al., 1998a). PAR2 is expressed in many tissues, but its particular expression on the endothelium, and its many effects on endothelium functions highlight the interest in its role in cardiovascular health and disease (Kagota et al., 2016; J. McGuire, 2004; Vergnolle et al., 2001). The PAR2-activating peptide (PAR2AP) trans-cinnamoyl-LIGRLO-NH₂ (tcLIGRLO) is one of several synthetic ligands, which were developed to mimic the tethered ligand mechanism of activation of PAR2 by proteases. Nevertheless, tcLIGRLO exhibits biological activities that cannot be explained by PAR2 activation (McGuire et al., 2002; Stenton et al., 2002; Vergnolle et al., 1998a). In particular, McGuire et al.(2002) discovered tcLIGRLO produced smooth muscle contraction in mouse femoral arteries (Figure 1).The two overlapping goals of this thesis is to further delineate the mechanism of contractions *ex vivo* and identify a human GPCR target of tcLIGRLO, other than PAR2. We anticipate the outcomes of this thesis will lead to further exploration of a novel mechanism, potentially involved with vascular health and receptors in human diseases.

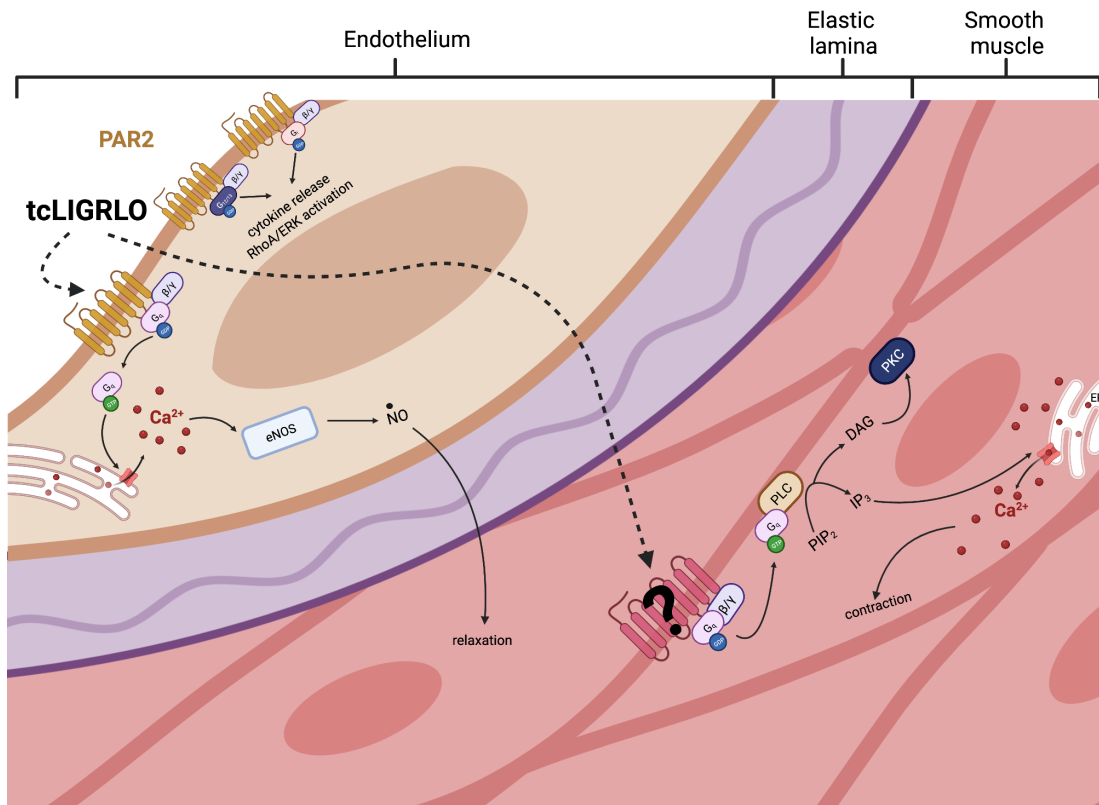


Figure 1. Schematic of tcLIGRLO mechanisms of action in mouse blood vessels.

PAR2 activates G_q, G_{12/13} and G_i signals in endothelial cells. PAR2-G_{12/13} and PAR2-G_i signalling are associated with downstream signalling pathways that involve cytokine release and RhoA and ERK activation (Avet et al., 2020; Suzuki et al., 2009). tcLIGRLO activates PAR2 which results in processes associated with pathophysiological functions of the endothelium. tcLIGRLO also activates an unidentified receptor that directly causes smooth muscle contraction via a mechanism of contraction dependent on intracellular Ca²⁺ stores. Our working hypothesis for this research is the receptor is a G_q-coupled GPCR. Figure created by JC using BioRender.

Abbreviations: eNOS, endothelial nitric oxide synthase; ERK, extracellular signal-regulated kinase; GDP, guanosine diphosphate; GTP, guanosine triphosphate; Ca²⁺, calcium; DAG, diacylglycerol; IP₃, inositol triphosphate; PKC, protein kinase C; PLC, phospholipase C; PAR2; protease-activated receptor 2; PIP₂, phosphatidylinositol 4,5-bisphosphate; RhoA, Ras homolog family member A; tcLIGRLO, trans-cinnamoyl-LIGRLO

1.1 tcLIGRLO: a PAR2-activating peptide

tcLIGRLO is a second generation PAR2AP. During physiological PAR2 signalling, endogenous proteases such as the serine protease prototype, trypsin, cleave the N-terminus of PAR2 to reveal a tethered ligand sequence that binds to extracellular loop 2 of the receptor (Hollenberg et al., 2014; McGuire, 2004). High concentration of thrombin (100 – 500nM) can also activate PAR2 (Mihara et al., 2016; Ramachandran et al., 2012). tcLIGRLO activates PAR2 by mimicking the tethered ligand sequence that interacts with extracellular loop 2. Seeing how extracellular loop 2 is an important point of contact, altering the amino acid sequence of extracellular loop 2 affects the binding specificity of PAR2 agonists (Al-Ani et al., 1999). For instance, changing phenylalanine to serine at residue 40 of extracellular loop 2 induced calcium (Ca^{2+}) signals that were 4 times higher than the wildtype (WT) receptor (Compton et al., 2000). It was speculated that the single point mutation allowed the trans-cinnamoyl group of tcLIGRLO to dock more efficiently due to the removal of the aromatic chain (Compton et al., 2000). In addition to the interaction with PAR2, the trans-cinnamoyl group addition to a PAR1AP was reported to produce an antagonist response (Bernatowicz et al., 1996), which suggests this particular functional group as a site for interaction with GPCRs.

tcLIGRLO is equipotent to the PAR2AP SLIGRL (serine-leucine-isoleucine-glycine-arginine-leucine) for Ca^{2+} signalling in PAR2-transfected cell lines and rat aortic relaxation. 2-furoyl-leucine-isoleucine-glycine-arginine-leucine-ornithine (2fLIGRLO) is the most potent out of these three PAR2APs (Table 1). Amongst these PAR2APs, the rank order potencies for Ca^{2+} signals correlate with endothelium-dependent blood vessel relaxations. However, the relative potencies of tcLIGRLO and SLIGRL for inducing rat jejunal chloride transport differed greatly (Vergnolle et al., 1998b). The difference in rank order potencies for tcLIGRLO and SLIGRL in the intestinal assay compared with the Ca^{2+} signalling and blood vessel relaxation assays suggested potential for an unidentified receptor distinct from PAR2 in the rat jejunum that regulates intestinal transport via a prostanoid-sensitive mechanism (Vergnolle et al., 1998b). Likewise, a

subsequent study showed PAR2 mRNA expression in rat peritoneal mast cells, but tcLIGRLO stimulated the secretion of β -hexosaminidase via a PAR2-independent pathway (Stenton et al., 2002). tcLIGRLO activation of PAR2 leads to the release of cytokines and expression levels of cell-adhesion molecules on neutrophil cell surfaces (Han et al., 2003; Niu et al., 2008; Shpacovitch et al., 2004, 2007; Wang & He, 2006). Indomethacin reduced tcLIGRLO-induced edema in rat paws (Vergnolle et al., 1999), demonstrating the involvement of prostanoid-sensitive mechanisms in PAR2-mediated edema.

Similar to studies using rat aortas, tcLIGRLO and SLIGRL caused comparable relaxation to each other in mouse femoral arteries from C57BL/6J (WT) mice (Table 1). In the same study, McGuire et al. (2002) also found that tcLIGRLO caused contraction in femoral arteries by a non-PAR2 mechanism (Figure 1). The threshold tcLIGRLO concentration was 10 μ M, which is \sim 10-times higher than its EC₅₀ for relaxation and 3 times higher than the maximal effective dose for relaxation. Thus, in the presence of PAR2, tcLIGRLO produces biphasic relaxation-contraction responses in normal mouse blood vessels. More interestingly, tcLIGRLO contracted endothelium-denuded arteries from WT mice, whereas SLIGRL did not. Further study of this response found that tcLIGRLO caused contraction of endothelium-intact femoral arteries from endothelial nitric oxide synthase (eNOS) gene knockout and *par2* gene knockout (PAR2KO) mice. Pre-treatment of mouse femoral arteries with pharmacological compounds to inhibit known GPCRs (Table 3) did not inhibit tcLIGRLO responses in the mouse PAR2KO blood vessels. However, the selective depletion of intracellular Ca²⁺ stores (Table 3) resulted in complete inhibition of the contractions by tcLIGRLO. The study concluded that tcLIGRLO contraction was a novel mechanism and warranted further work to identify the receptor. We are not aware of any further characterization of the novel mechanism of tcLIGRLO in mouse femoral arteries in scientific literature.

Figure 1 provides a summary of the mechanism of action of tcLIGRLO in mouse blood vessels and the background rationale for this thesis research. As shown in Figure 1,

tcLIGRLO is not only an endothelial cell PAR2 agonist, but also activates another receptor aside from PAR2 that mediates release of Ca^{2+} from intracellular stores in the smooth muscle of mouse femoral arteries. Our working hypothesis for this research is the receptor is a G_q -coupled GPCR (Figure 1). We will test this hypothesis using a G_q selective pharmacological inhibitor which is described in Section 2. We will also look at GPCRs whose ligands have not been well defined as potential GPCR candidates of tcLIGRLO. This class of GPCRs is referred to as orphan GPCRs and described in Section 3.

Table 1. Comparison of pEC₅₀ values for PAR2-mediated signalling with PAR2-activating peptides tcLIGRLO, SLIGRL, and 2-fLIGRLO in intracellular Ca²⁺ signalling and blood vessel relaxation assays.

Study	PAR2AP	Ca ²⁺ pEC ₅₀	Blood vessel relaxation pEC ₅₀	Reference
1	tcLIGRLO	5.09 ^a		(Saifeddine et al., 1998)
	SLIGRL	5.09 ^a		
2	tcLIGRLO	6.10 ^a		(Vergnolle et al., 1998b)
	tcLIGRLO		6.00 ^b	
	SLIGRL	6.10 ^a		
	SLIGRL		6.00 ^b	
3	tcLIGRLO		5.80 ^c	(McGuire et al., 2002)
	SLIGRL		5.80 ^c	
4	SLIGRL	4.60 – 5.50 ^a	5.60 – 5.70 ^{b, c}	(McGuire et al., 2004)
	2fLIGRLO	5.50 – 7.00 ^a	6.50 – 7.70 ^{b, c}	
5	tcLIGRLO		6.00 ^b	(Hollenberg et al., 2008)
	SLIGRL		5.74 ^b	
	2fLIGRLO		6.47 ^b	

a, human PAR2 transfected into rat kidney cells; b, endothelium-intact aortas from male Sprague Dawley rats; c, endothelium-intact C57BL/6J mouse femoral arteries

Table 2. List of agents, their respective targets, and effects on 50 μ M tcLIGRLO-mediated contractions.

Target	Agent	Inhibition of contractions
Angiotensin II receptor type 1	Losartan	No effect
α 1-adrenoreceptor	prazosin	No effect
Cyclooxygenase 1/2	Indomethacin	No effect
Calcium-sensitive internal stores	Cyclopiazonic acid	Reduced contractions
	Caffeine	
endothelin- receptor 1A	BQ123	No effect
Histamine receptor 1/2	chlorpheniramine	No effect
Muscarinic receptors	Atropine	No effect
Neurokinin 1 receptor	SR140333	No effect
Neurokinin 2 receptor	SR48986	No effect
CdCl ₂	Non-specific cation channels	No effect
Protease-activated receptor 4	AYPGKF-NH ₂	No effect
Thromboxane A2 receptor	SQ29548	No effect
Voltage-gated calcium channels	Nifedipine	No effect

Results of compounds tested are from (McGuire et al., 2002).

1.2 YM: a tool for investigating GPCR signals

1.2.1 Introduction to YM

YM-254890 (YM) is a cyclodepsipeptide and a selective inhibitor of G_q signalling by seven transmembrane GPCRs (Hermes et al., 2021; Kaur et al., 2015). YM is used to dissect, characterize, and discover novel GPCR signalling, pharmacology, and pathophysiology. Researchers recognize this utility of YM for studies developing novel drugs targeting known and lesser characterized GPCRs, and novel therapeutics targeting human disease, including chronic pulmonary disease, cardiovascular disease, and certain types of cancer (Kamoto et al., 2015, 2017; Kaur et al., 2015; Touge et al., 2007; Zhang et al., 2020). Given that 35% of human GPCRs are targets of prescribed drugs, tools to allow researchers to selectively target G_q signalling and apply them in appropriate *in vivo* models of human disease are essential (Sriram & Insel, 2018).

1.2.2 GPCRs and heteromeric G proteins

The combination of GPCR subtype and ligand determines the selectivity for the profile of G protein signalling. Generally, activated GPCRs catalyze the exchange of guanine triphosphate (GTP) with guanine diphosphate (GDP) bound to the $G\alpha$ subunit of the heterotrimeric G proteins, which leads to $G\alpha$ dissociation from $G\beta\gamma$ and activation of downstream second messenger pathways (Campbell & Smrcka, 2018). Second messenger pathways are selective for the isoforms of the $G\alpha$ subtypes (e.g. G_s , $G_{i/o}$, G_q , and $G_{12/13}$) (Campbell & Smrcka, 2018; Mizuno & Itoh, 2009) and $\beta\gamma$ -complexes. The specific effectors are also dependent on the cell type and can vary with disease and environmental cues. Targeting the inhibition of the heterotrimeric G proteins is an ongoing approach to developing therapeutics, particularly in cases where mutations produce constitutive activity (Campbell & Smrcka, 2018; Kostenis et al., 2020; Li et al., 2020), but there are obvious caveats to this approach given the ubiquitous expression of heteromeric G proteins.

Downstream of the ligand binding that stabilize the molecular conformations of activated GPCRs, YM targets the G_q subtypes $G\alpha_q$, $G\alpha_{11}$, $G\alpha_{14}$, and $G\alpha_{15/16}$ (in mice and humans, respectively), which normally stimulate phospholipase C (PLC) β (Campbell & Smrcka, 2018; Kamato et al., 2017). PLC β hydrolyses membrane-bound phosphatidylinositol-4,5-bisphosphate (PIP₂) to produce diacylglycerol (DAG) and inositol trisphosphate (IP₃) which activate the classical (α , β , and γ) and novel isoforms (δ , ϵ , θ , and η) of protein kinase C (PKC) (Bhavanasi et al., 2011; Bynagari et al., 2009; Nagy et al., 2009; Uchiyama et al., 2009), and IP₃ receptors, respectively. Thus, pharmacological inhibition of GPCR-mediated intracellular Ca²⁺ release from intracellular stores (i.e. via IP₃ receptors) is a characteristic of selective inhibitors of G_q and therefore, YM and YM analogues (Campbell & Smrcka, 2018; Kamato et al., 2017).

1.2.3 Investigating PAR2 with YM

YM has been used to examine differences between PAR1 and PAR2, prior to the availability of effective antagonists for PAR1 and PAR2. In endothelial cells, the regulation of eNOS activity by PAR2, but not by PAR1, was sensitive to inhibition by YM, which highlighted separate roles played by the PARs in vascular biology (Suzuki et al., 2009). The most common pharmacological tools for PAR2 are trypsin, which is used as a protease activator, and selective PAR2APs (examples mentioned in Table 1 in Section 1.1.1). Differences have been noted in the PAR2 signalling when using these PAR2 agonists. Again, YM has been used to look at these differences between PAR2 activators. YM inhibited β -arrestin recruitment following PAR2APs but not trypsin. This evidence suggests that the tethered ligand mechanism of PAR2, as demonstrated with trypsin, stimulates β -arrestin signalling independent of G_q (Thibeault & Ramachandran, 2020). K-14585 is a synthetic peptide that is described as a partial PAR2 agonist. YM inhibits both IP₃ accumulation and p38 mitogen-activated protein kinase stimulated by 30 μ M K-14585 (Goh et al., 2009). As shown in Figure 1, PAR2 is reported to also activate $G_{12/13}$ and G_i (Avet et al., 2020). Common to GPCRs, there is crosstalk in signalling. For instance, PAR2 activation of both G_q and G_i signalling includes

downstream extracellular signal-regulate kinase (ERK) activation (Avet et al., 2020; Suzuki et al., 2009). However, YM failed to inhibit Ras homolog family member A (RhoA) activation following trypsin- and PAR2AP SLIGRL, and yet, YM inhibited these same responses in cells lacking $G_{12/13}$ (Avet et al., 2020). These results indicate that G_q is sufficient for activating RhoA, but this signalling mechanism is minimized in the presence of $G_{12/13}$. The studies mentioned here are part of a growing body of evidence supporting the development of PAR2 ligands with selective biased signalling.

1.2.4 Uses of YM to study vascular smooth muscle contraction

YM inhibits vasoconstrictions, and vascular smooth muscle contractions by multiple GPCR ligands in different vascular preparations across species. In these cases, YM is administered prior to the GPCR ligands. Uemura et al. (2006) reported that YM caused direct relaxation of vascular smooth muscle in rat aortic rings, which had been pretreated with either thrombin, phenylephrine, serotonin, or endothelin-1, with or without an intact endothelium (pIC_{50} 7.0 – 9.0; Table 3). In addition to its inhibition of GPCR ligands, YM is reported to inhibit the intrinsic properties of vascular smooth muscle that results in an increased myogenic tone in response to increased active stretching (Björling et al., 2018). This so-called myogenic tone is a key function that helps maintains constant perfusion over the normal physiological range of blood pressures to critically important organs such as the brain, heart, and kidneys. With preparations of larger arteries (e.g., rat aorta and rabbit basilar arteries), YM inhibited the myogenic tone induced by GPCR agonists (i.e. phenylephrine, thrombin, and endothelin-1) (pIC_{50} 7.0 – 9.0; Table 3) (Kikkawa et al., 2010b; Meleka et al., 2019). Likewise, YM reduced spontaneous myogenic tone development in small resistance arteries i.e., mouse mesenteric arteries (Björling et al., 2018). These results provide evidence of distinct G_q signalling in mechanotransduction and initiation of contraction by endogenous ligands. Specific GPCRs such as angiotensin II type 1 receptor and cysteinyl leukotriene receptor 1 have been proposed as mechanosensors that transmit biophysical stimuli, such as stretch of smooth muscle and shear stress on endothelial cells (Schnitzler et al., 2016; Storch et al., 2015). YM inhibition of shear stress-induced endothelial cell signalling has not yet been reported.

The effects of YM on vascular smooth muscle contraction were linked partly via G_q to inhibition of L-type Ca^{2+} channels (Meleka et al., 2019). Suppression of L-type Ca^{2+} channel activity in cardiomyocytes leads to decreased heart rate, contractility, and cardiac output *in vivo* (Xu & Brink, 2016). As reported by Kawasaki et al. (2003), in preclinical studies evaluating the use of YM for platelet aggregation and anti-thrombosis, the putative therapeutic doses fall within the range of those reported to cause hypotension. Accordingly, their suggestion is that YM be used as local agent rather than a systemic agent (Kawasaki et al., 2003). However, based on the evidence reviewed by us, there is lack of evidence to support the use of YM as either a local or systemic agent on the circulation and platelets given the many GPCR expressed on the endothelium, and its role in both vascular tone and hemostasis.

Table 3. Summary of pIC₅₀ values for YM inhibition of G protein couple receptors and ligands signalling in vascular smooth muscle contraction.

Study	Receptor	Ligand	Assay	pIC ₅₀	Model	Study
1	Endothelin receptor type A	Endothelin-1	Isometric contraction	7.16	Rabbit basilar artery with subarachnoid hemorrhage	(Kikkawa et al., 2010a)
	Protease-activated receptor 1	thrombin	Isometric contraction	7.16	Rabbit basilar artery with subarachnoid hemorrhage	
	α_1 -adrenoceptor	phenylephrine	Isometric contraction	7.07	Rabbit basilar artery with subarachnoid hemorrhage	
2	Endothelin receptor type A	Endothelin-1	Isometric contraction	7.74	Rat aorta	(Uemura, Takamatsu, et al., 2006a)
	α_1 -adrenoceptor	phenylephrine	Isometric contraction	8.80	Rat aorta with intact endothelium	

α_1 - adrenoceptor	phenylephrine	Isometric contraction	8.96	Rat aorta with denuded endotheli um
5-HT ^a receptor (not specified)	serotonin	Isometric contraction	8.07	Rat aorta

The tabulated data are derived from all studies where pIC₅₀ values were determined.

^a, 5-hydroxytryptamine (i.e., serotonin)

1.2.5 Refining characteristics of GPCRs and discovering novel G_q-mediated signalling mechanisms

The refinement of well characterized GPCR signalling is not the sole use for YM. The signal transduction profiles of lesser known G_q-coupled receptors have been expanded using this tool. For example, YM inhibited MAS1 receptor-induced upregulation of angiotensin II type 1 receptor (Canals et al., 2006). The use of YM revealed a novel G_q-mediated pathway mechanism of action for 02F04, a steroid alkaloid derivative, which leads to activation of Rho-associated protein kinase (ROCK) and ERK during the production of thymic stromal lymphopoietin in mouse keratinocytes (Mizuno et al., 2017; Weng et al., 2019). Thymic stromal lymphopoietin production is associated with severe allergy pathologies. Similarly, the identification of the GPCR mediating cholecystokinin secretion in enteroendocrine cells remains undetermined, but its inhibition by YM links it to a G_q-coupled signalling mechanism (Hira et al., 2009). Of course, studies have also used the resistance to inhibition by YM to exclude G_q as a requisite for cellular events. For example, YM failed to inhibit activation of apelin receptor ligand apelin-13 signalling involving ERK and early growth response factor-1 expression (Liu et al., 2015). Treatment of cells with YM had no effect on primary neurite outgrowth that was stimulated by palmitoyl-lysophosphatidylethanolamine, but did inhibit the stimulation by stearoyl-lysophosphatidylethanolamine (Hisano et al., 2021). In primary cultured rat cortical astrocytes, lysophosphatidic acid stimulates the G_i-coupled receptors lysophosphatidic acid receptor 1 and lysophosphatidic acid receptor 3 to induce thrombospondin-1 production, which may contribute to normal brain function, and in other cases, neurological disorders (Hisaoka-Nakashima et al., 2020).

1.3 Orphan receptors: a class of GPCRs whose ligands remain unknown

1.3.1 Introduction to orphan receptors

Within the GPCR superfamily, there is a class of receptors whose endogenous and synthetic ligands are undetermined yet; these GPCRs are formally recognized as “orphan

receptors” (Pierce et al., 2002; Sriram & Insel, 2018). Ligand binding is not always a requisite to initiate GPCR signalling e.g., in cases where receptors remain constitutively active (Kjelsberg et al., 1992; Samama et al., 1993) or dimerize prior to activation (Nelson et al., 2002). For these cases, identifying synthetic ligands is useful for revealing the signalling profile of GPCRs whose method of activation typically occurs in a ligand-independent manner. Since the downstream signalling repertoire of G protein signalling cascades depends on the receptor type and ligand (Kobilka et al., 1988; O’Dowd et al., 1988; Ostrowski et al., 1992), discovering both endogenous and synthetic ligands (i.e., de-orphanization) of the remaining ~150 orphan receptors would reveal their pharmacology and function, as well as pinpoint de-orphanized receptors as novel GPCR drug targets (Fredriksson et al., 2003; Hauser et al., 2017; Ngo et al., 2016).

1.3.2 Techniques for de-orphanization

1.3.2.1 Reverse pharmacology

Reverse pharmacology contributed towards the de-orphanization of orphan GPCRs. In general, reverse pharmacology involves identifying prospective ligands of orphan receptors, followed by an investigation of the pharmacological and physiological context via gene KO or overexpression of candidate orphan receptors (Kotarsky & Nilsson, 2004). There are three different strategies associated with reverse pharmacology in regards to de-orphanization (Kotarsky & Nilsson, 2004). The first method involves screening an extensive library of potential ligands against an orphan receptor library (Brown et al., 2003; Kotarsky & Nilsson, 2004). This technique screened a bank of prospective ligands in yeast and identified short chain fatty acids as agonists for orphans GPR41 and GPR43, both de-orphanized as free fatty acid receptor 3 and 2, respectively (Brown et al., 2003). Exposing cells that heterologously express candidate orphan receptors to fractionated tissue extracts containing prospective ligands is a defining characteristic of the second strategy i.e., “the orphan receptor strategy,” which led to the discovery of the neuropeptide orphanin FQ or nociceptin (Kotarsky & Nilsson, 2004; Lin & Civelli, 2004; Reinscheid et al., 1995). Lastly, the information based-approach , which

involves assessing activation by few prospective ligands from a previous database screening in a small subset of orphan GPCRs, contributed towards the identification of niacin receptor 2 in adipose tissues (Kotarsky & Nilsson, 2004; Tunaru et al., 2003).

Traditional de-orphanization strategies of reverse pharmacology were successful in proposing orphan receptors as novel GPCR drug targets, but with the caveat of detecting changes on the second messenger level (Tang et al., 2012). Examples of second messenger assays include cytosolic G_q/Ca^{2+} transients, GTP γ binding or radioligand binding of $G_{12/13}$, and modulation of cyclic adenosine monophosphate (cAMP) levels following G_i or G_s stimulation (Cerione et al., 1984; Lorenz et al., 1990; Stiles et al., 1984). However, some GPCR signalling pathways can occur independently of G proteins (Heuss et al., 1999; Tang et al., 2012). Therefore, more sufficient screening methods that detect “orphan receptor hits” via a G protein-independent approach are needed.

1.3.2.2 TANGO and PRESTO-TANGO assay

The recruitment of β -arrestin to the plasma membrane and co-localization with a ligand bound-receptor is characteristic of most GPCRs. In general, β -arrestin proteins (i.e., arrestin-1 – 4) bind to a phosphorylated GPCR, which leads to receptor desensitization and signalling attenuation (Shukla et al., 2011). The receptor-arrestin complex promotes GPCR internalization via clathrin-coated pit endocytosis and also acts as a scaffold to relay signals from the GPCR to another receptor or intracellular molecules (Luttrell et al., 1999; Shukla et al., 2011). Measuring β -arrestin recruitment is one way of detecting GPCR activation, and therefore, orphan receptor hits independent of G protein coupling.

The *transcriptional activation following arrestin translocation* (TANGO) assay depends on the binding of β -arrestin-2 (also known as arrestin-3) to the activated GPCR following ligand binding (Barnea et al., 2008). This assay involves the fusion of a GPCR with a transcriptional activator, which are separated by a cleavage site for a highly specific viral protease that is fused with β -arrestin (Figure 2) (Barnea et al., 2008). Ligand binding recruits β -arrestin-2 fused with the viral protease to the cleavage site, thereby allowing

the transcriptional activator to enter the nucleus to activate the luciferase reporter gene (Figure 2) (Barnea et al., 2008). The TANGO assay is advantageous when testing for potential ligands of orphan receptors whose second messenger signalling profiles remain unknown or weak. For instance, the structural similarity between chemokine like receptor 1 (i.e., a leukocyte chemoattractant receptor) and the orphan receptor GPR1 led to the hypothesis that GPR1 responds to the leukocyte chemoattractant chemerin i.e., an endogenous ligand of chemokine-like receptor 1 (Barnea et al., 2008; Meder et al., 2003; Wittamer et al., 2003). In the TANGO assay, GPR1 responded to chemerin with EC₅₀ 240pM compared with 3nM for chemokine like receptor 1, whereas chemerin-treatment to cells expressing GPR1 resulted in only intracellular Ca²⁺ levels 30% of that observed in cells expressing chemokine like receptor 1 (Barnea et al., 2008). While independent of second messenger pathways, the TANGO assay is limited to screening GPCRs “one target at a time” and is unable to probe hundreds of GPCRs in a simultaneous fashion (Kroeze et al., 2015). An improved version of the TANGO assay is known as the, “Parallel Receptor-ome Expression and Screening via Transcriptional Output (PRESTO)-TANGO assay,” which facilitates the parallel and simultaneous profiling of prospective ligands across more than 300 human GPCRs (Kroeze et al., 2015).

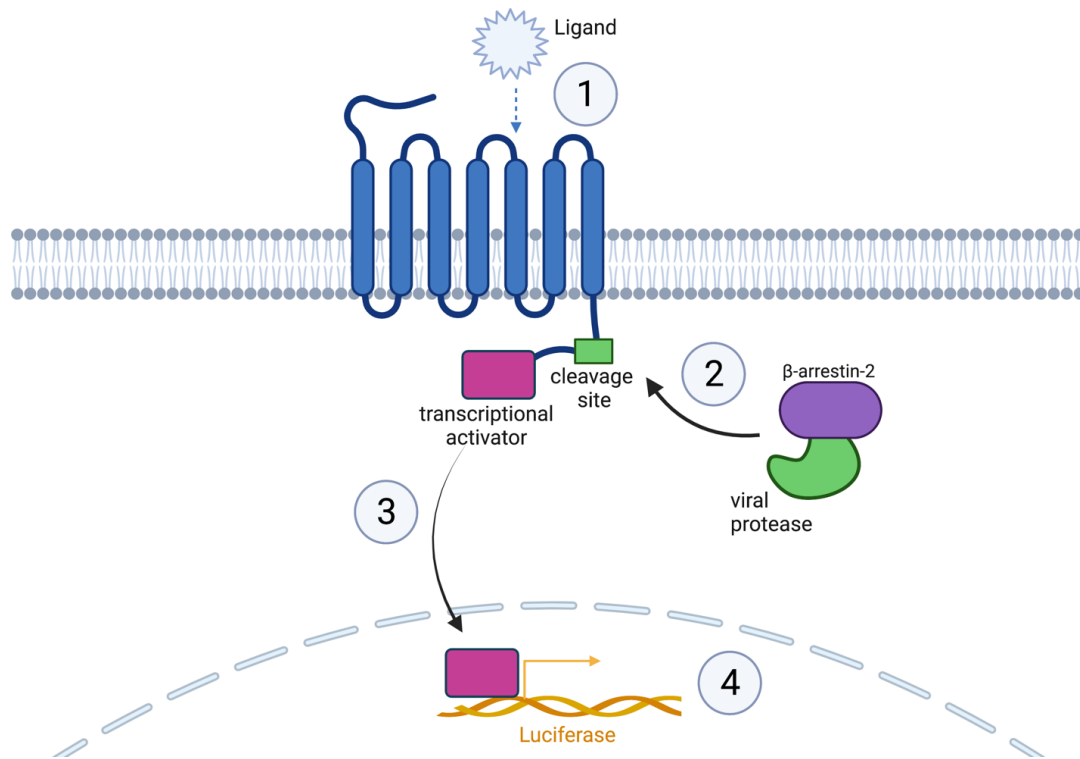


Figure 2. Schematic representation of the TANGO assay.

Upon ligand binding to the GPCR fused with a transcriptional activator at the cytoplasmic tail (1), β -arrestin-2, with a viral protease attached, translocates to the cleavage site (2). This releases the transcriptional activator (3) to enter the nucleus to upregulate expression of the luciferase reporter gene (4). Figure created by JC with BioRender.

1.3.3 Lesser known and uncharacterized receptors: SUCNR1, CCRL2, GPR15, and GPR135

Pharmacological interventions and assays mentioned in previous chapters (i.e., treatment with the highly selective G_q inhibitor YM or assessing for GPCR activation with the TANGO assay) are current methods that are used to further define the signalling profiles of lesser characterized and orphan GPCRs. Table 4 provides a list of four GPCRs—C-C chemokine receptor-like 2 (CCRL2), GPR15, succinate receptor 1 SUCNR1 (previously known as GPR91), and GPR135—and summarizes their tissue distribution profile, G-proteins they couple to, any putative and confirmed ligands, and physiological roles. These four GPCRs were selected as candidates for the tcLIGRLO-activated receptor from a pilot survey (unpublished data, Dr. McGuire) screen of >70 orphan GPCRs using the human orphan GPCR PathHunter® (DiscoverX, San Francisco, CA) assay contract service.

1.3.3.1 SUCNR1: a de-orphanized receptor

Out of the four receptors in Table 4, SUCNR1 is the only de-orphanized receptor, with succinate as its only identified endogenous ligand to date (He et al., 2004). As well, it is the only receptor to have evidence of coupling to G_i and G_q (He et al., 2004; Robben et al., 2009). Blockade of the G_q pathway with YM resulted in reduced Ca^{2+} signalling in canine kidney cells following SUCNR1 stimulation by succinate (Robben et al., 2009). Similarly, treatment of human embryonic kidney 293 cells (HEK293) with a G_i inhibitor led to reduced Ca^{2+} signalling and inositol phosphate accumulation (He et al., 2004). In the study by He et al. (2004), intravenous injection of succinate into rats produced increased plasma levels of renin, which is an enzyme in the renin-angiotensin system that is responsible for regulating blood pressure. The association of SUCNR1 with blood pressure regulation proposes its role in modulating metabolic diseases (e.g., obesity, Type 2 diabetes mellitus, etc.). Thus, identifying another ligand in addition to succinate would provide a new avenue for investigating the downstream pathways following SUCNR1 activation.

1.3.3.2 The remaining orphans: CCRL2, GPR15, and GPR135

CCRL2, GPR15, and GPR135, are still classified as orphan GPCRs. Studies have identified ligands for CCRL2 and GPR15; however, these ligands are merely putative (Biber et al., 2003; Hartmann et al., 2008; Pan et al., 2017; Suply et al., 2017). The pending name for CCRL2 is, “atypical chemoattractant receptor 5,” due to its supposed role in scavenging and internalizing chemokine ligands via a G_i -sensitive pathway in leukocytes (Biber et al., 2003; Leick et al., 2010). However, its additional role as a chemerin-presenting protein for chemokine receptor 1 via a G_i -independent mechanism challenges its presumed classification as the fifth member of the atypical chemoattractant receptor family (Hartmann et al., 2008).

GPR15, which is differentially expressed in T-cell subtypes in humans (helper T cell) and mice (regulatory T cells and helper T cell 17), is reported to bind to GPR15L (i.e., a natural protein ligand expressed in skin and colon epithelium) to activate G_i -signalling networks when homing T-cells to the colon (Suply et al., 2017). GPR15 is also reported to bind thrombomodulin. This interaction promotes angiogenesis by preventing the expression of apoptotic proteins in vascular endothelial cells (Pan et al., 2017). The thrombomodulin-activated GPR15 G-protein signalling is undetermined yet.

In comparison to CCRL2 and GPR15, GPR135 remains the most obscure out of the three orphan GPCRs. GPR135 is considered a prominent hypermethylation site in lung and ovarian cancers (Cardenas et al., 2014; Kettunen et al., 2017), but to date, it has no evidence of G-protein coupling or prospective ligand binding. GPR135 does heterodimerize with melatonin receptor 2 in a ligand-independent fashion (Watkins & Orlandi, 2020). Having no known endogenous ligand that readily activates GPR135, discovering potential synthetic ligands would reveal its downstream signalling network. In summary, prospective ligands for these four receptors—SUCNR1, CCRL2, GPR15, and GPR135—would advance understanding about their G protein signalling profiles, as well as propose novel roles for these four receptors during physical and disease processes.

Table 4. Summary table providing tissue distribution profile, G-protein signalling, putative ligands, and reported physiological roles of CCRL2, GPR15, SUCNR1, and GPR135

Receptor	Tissue distribution	G-protein signalling	Putative ligands	Physiological roles
CCRL2	Leukocytes (Migeotte et al., 2002; Otero et al., 2010; Yoshimura & Oppenheim, 2011)	G _i (Biber et al., 2003)	Chemokine ligand 2,7,8,5, 19 (Biber et al., 2003)	Scavenge and internalize chemokine ligands (Leick et al., 2010)
		G _i -insensitive (Hartmann et al., 2008)	Chemerin (Hartmann et al., 2008)	Chemerin-presenting protein for chemokine receptor 1 (Hartmann et al., 2008)
GPR15	T-cell subsets in humans (helper T cell 12) and mice (regulatory T cells and helper T cell 17) (Nguyen et al., 2015)	G _i (Suply et al., 2017)	GPR15L (Suply et al., 2017)	T-cell homing to colon (Suply et al., 2017)
		Not reported	Thrombomodulin (Pan et al., 2017)	Endothelial cytoprotective function and

		(Pan et al., 2017)		angiogenesis (Pan et al., 2017)
SUCNR1	Kidney, liver, spleen, immune cells, white adipose, retina (Toma et al., 2008)	G _i or G _q (He et al., 2004; Sundström et al., 2013)	Succinate (He et al., 2004)	Mediates metabolic conditions (e.g., hypertension, Type 2 diabetes mellitus, obesity, etc.) via renin-angiotensin system (He et al., 2004; Robben et al., 2009; Toma et al., 2008)
GPR135	Pituitary gland, eye, brain, stomach, testis (Fredriksson et al., 2003; Vanti et al., 2003)	Not reported	Heterodimerize with melatonin receptor 2 in a ligand-independent manner to mediate melatonin signalling (Watkins & Orlandi, 2020)	Hypermethylation target in cancers (e.g., lung and ovarian) (Cardenas et al., 2014; Kettunen et al., 2017)

1.4 Thesis statement, hypothesis, objectives, rationale

The working hypothesis for this thesis research is tcLIGRLO activates a GPCR G_q -coupled signalling network to cause contraction of vascular smooth muscle in mouse femoral arteries (Figure 1).

The first aim of this thesis was:

1. To determine the effects of the G_q inhibitor YM on tcLIGRLO-induced contractions. Experiments associated with this research objective employed wire myography to measure the functional response (i.e., contraction) of femoral arteries to tcLIGRLO. Considerations of the potential for sex- and age-related differences in tcLIGRLO responses were not explored in previous studies. Optimal conditions for such studies and effective inhibitor concentrations of YM needed to be determined for these assays. Therefore, we divided this research objective into two further sub-objectives:
 - A. To assess the effect of sex and age on tcLIGRLO-induced contractions, which would help refine our choice of animal model and further optimize the assays of tcLIGRLO-elicited contractions.
 - B. To determine the effects of the G_q inhibitor YM on tcLIGRLO-induced contractions. We treated mouse femoral arteries *ex vivo* with YM using a range of concentrations based on published studies. We also tested the effects of YM on non- G_q contractions stimulated by high extracellular K^+ and the known G_q -coupled α_1 -adrenoreceptor type 1 using phenylephrine. We anticipated that YM would inhibit tcLIGRLO-mediated contractions. In separate studies, we conducted experiments *in vitro* to confirm YM inhibition of G_q - Ca^{2+} signalling *in vitro* using tcLIGRLO and other PAR2APs with HEK293 cells expressing human PAR2.

The second aim was:

2. To assess the feasibility of using the TANGO assay to screen human GPCRs for potential tcLIGRLO targets.

- A. To use tcLIGRLO and the other PAR2APs SLIGRL and 2fLIGRLO in the TANGO assay with cells expressing human PAR2. We expected to find that tcLIGRLO and the other PAR2APs would activate PAR2 in the assay.
- B. To test tcLIGRLO in the TANGO assay with cells expressing other human GPCRs. A pilot survey of over 70 orphan GPCRs (McGuire, unpublished data) using a single dose of tcLIGRLO had identified several candidates. We used four candidate GPCRs (CCRL2, GPR15, SUCNR1, and GPR135) with available plasmid constructs for use in the PRESTO-TANGO kit. Amongst this selection, SUCNR1 is known to activate G_q signalling whereas less is known about G protein signalling by the other three GPCRs

Chapter 2

2 Role of G_q in tcLIGRLO-induced contractions of mouse vascular smooth muscle

2.1 Introduction

The PAR2AP tcLIGRLO activates PAR2 and one or more other receptors. These receptors remain unidentified (Chapter 1.3.3). tcLIGRLO causes vasoconstriction of mouse femoral arteries by stimulating a smooth muscle cell receptor that is distinct from PAR2 (Chapter 1.1). This contraction is dependent on the transient release of Ca^{2+} from internal stores (Chapter 1.1). GPCR G_q signalling pathways, including Ca^{2+} transients, cause vascular smooth muscle contraction (Chapter 1.1). To date, the cyclodepsipeptide, YM, is one of the only known selective inhibitors of G_q signalling (Chapter 1.2).

Inhibition of GPCR contraction of aortic ring preparations by treatments with YM has been used to demonstrate the critical role of G_q in signalling by specific GPCRs (Table 3; Chapter 1.2.4).

We hypothesize that tcLIGRLO activates G_q - Ca^{2+} signalling to contract mouse femoral arteries. The purpose of this study was to determine the effects of G_q inhibition on tcLIGRLO-mediated contractions. We also tested the effects of YM on contractions mediated by the known G_q -coupled α_1 -adrenoreceptor type 1 with phenylephrine, and PAR2/ Ca^{2+} signalling stimulated by tcLIGRLO in HEK293 cells. The effects of subjects' sex and age were also determined on baseline tcLIGRLO responses of mouse femoral arteries. The main finding of this study is tcLIGRLO contractions are mediated via G_q .

2.2 Materials and methods

2.2.1 Chemical reagents and drug solutions

Chemicals used to make Krebs buffer solutions were purchased from Bio Basic Inc. (Markham, ON) and Thermo Fisher Scientific (Mississauga, ON). YM (1mg) was purchased from Focus Biomolecules (Plymouth Meeting, PA) and was dissolved in

dimethyl sulfoxide to create stock solution of 2mM. The peptide tcLIGRLO was purchased from GenScript (Piscataway, NJ) and prepared as a 10 mM stock solution using 25mM HEPES buffer (pH 7.4). Phenylephrine was purchased from Bio Basic Inc. and was dissolved in double-distilled water. Acetylcholine (Ach) and sodium nitroprusside (SNP) were purchased from Sigma-Aldrich. Stock solutions were stored at -20 °C. Dilutions of stock solutions were prepared on the day of experiments.

2.2.2 Animals

2.2.2.1 Ethics Statement on the care and use of animals in research

All procedures for the care and use of animals in this study were approved by Western's Institutional Animal Care Committee in accordance with the guidelines of the Canadian Council for Animal Care.

2.2.2.2 Mice

We used 31 systemic PAR2KO in substudy 1 and 2. For substudy 3, we used mice having homozygous floxed PAR2 alleles and a single copy Cre recombinase with expression regulated by the promoter for VE-cadherin. These mice are referred to as endothelial cell-specific PAR2 knockout (ecPAR2KO; n = 5). We used littermates (n=5) having genotypes that do not knockout PAR2 in endothelial cells as the controls, which are referred to as WT.

All the mice are from local colonies maintained and housed in the West Valley Barrier Facility at Western University. For the PAR2KO, the original breeders (Stock 4993) were three pairs of homozygous *par2* KOs obtained from the Jackson Laboratory (Bar Harbor, ME) (Schmidlin et al., 2002). ecPAR2KO and WT strains were created at Western by Dr. McGuire lab with collaborators (Dr. Singh, Dr. Ramachandran).

2.2.3 Wire Myograph Experiments

Wire myography experiments using mouse femoral arteries were performed as described previously (McGuire et al., 2002). Procedures and protocols are outlined briefly in following section.

2.2.3.1 Isolation of femoral arteries

Mice were euthanized by cervical dislocation. Femoral arteries were isolated from hindlimb region of mice. Arterial ring preparations of mouse femoral arteries (two to four per mouse, 1.25 – 1.96mm in length, 231 – 382 μ m in diameter) were suspended by two stainless steel coated tungsten wires (40- μ m diameter) between a micropositioner and force transducer in separate chambers of 620M Danish Myo Technology Multi Wire Myograph Systems (Hinnerup, DK). Each temperature (37°C) controlled chamber contained 5mL Krebs buffer (pH 7.4) and was bubbled continuously with 95% O₂/5% CO₂ gas mixture. Krebs buffer was composed of (in mM): 118 NaCl, 4.7 KCl, 0.87 MgSO₄, 0.86 KH₂PO₄, 2.5 CaCl₂, 10 D-glucose, 25 NaHCO₃, and 25 HEPES.

2.2.3.2 DMT myographs

DMT force transducers were frequently calibrated according to manufacturer's instructions. During each experiment, isometric tension measurements were recorded continuously using a computer (Microsoft Windows operating system) with the LabChart software (AD Instruments; Dunedin, NZ).

2.2.3.3 Normalization of baseline tension for femoral arteries

A resting baseline tension was set by stretching each arterial ring along their short-axis (radii) to an optimized internal diameter under isometric tension conditions. In brief, we used the normalization protocol for setting resting tension of small arteries described by (Mulvany & Halpern, 1976). From a starting point with no tension applied, the small arterial rings were stretched to an internal circumference IC₁, which is a fraction (normalization factor) of the internal circumference (IC₁₀₀) that is estimated from length-

tension measurements to produce a target transmural pressure. The normalization parameters used in the calculations for the mouse femoral arteries in this study were: target transmural pressure = 13.3kPa; $IC_1/IC_{100}= 0.9$ (Normalization factor). Calculations of IC_1 and IC_{100} were determined using the DMT Normalization plug-in for LabChart software (AD Instruments; Dunedin, NZ), which interpolates the IC_{100} from a curve fit of length (diameter)-tension (mN/wall length) relationship data using equations derived from the Law of LaPlace. The formulas are modified to account for the elliptical circumference of the mounted vessels and the diameter of the mounting wires. The long axis of the mounted vessels was measured at 40X magnification using a calibrated ocular eyepiece (2mm/number ocular divisions) in a binocular dissection microscope (wall length = 2 x artery long axis length). For each arterial ring, length-tension relationships were determined by step wise moving the distance between the mounting wires and recording the tension for 90s. Sufficient data points to interpolate the IC_{100} value from a curve fit of the data were acquired. Femoral arteries were equilibrated at the optimized resting tension for 30 – 40 min prior to the bioassay protocols.

2.2.3.4 Vascular smooth muscle contraction and relaxation bioassay protocols

Arterial rings were exposed to KCl (30, 60, 90 mM) to test viability. Tissues producing <1.5mN were excluded from this study. Arteries were exposed to a 20 – 30-min washout period before conducting further studies. Table 5 is organized according to substudies 1 – 3 and provides a list of physical characteristics of mice, blood vessel dimensions, and sample size of the different treatments.

Substudy 1: Sex and age in PAR2KO mice

tcLIGRLO dose-response curves (10, 20, 30 μ M) were constructed with PAR2KO mice. Mice were grouped by sex (males n=18; females n=3). Data from male mice were binned by age groups 20-25, 30-35, and 35-40 weeks. We assessed endothelium-dependent relaxation with Ach (0.001 – 30 μ M) and endothelium-independent relaxation with SNP (0.001 – 30 μ M) in vessels from male mice after their vessels were pre-contracted with

3 μ M phenylephrine. Phenylephrine (0.001 – 10 μ M) was added to femoral arteries from male and female mice. Tissues were exposed to a 30-min washout period between each dose-response curve.

Substudy 2: Effects of YM on femoral arteries from PAR2KOs

Substudy 2.1. tcLIGRLO and YM

An additional tcLIGRLO dose-response curve (0.5 – 50 μ M) was performed with femoral arteries from male mice (n=4). Following a 30-min washout period, different concentrations of YM (10, 30, 100 nM) were added to each channel. YM was incubated with the tissues in each channel for 15 min prior to repeating the tcLIGRLO dose-response curve.

Substudy 2.2. Phenylephrine and YM

In a separate study, phenylephrine dose-response curves (0.001 – 10 μ M) in combination with YM was performed with male mice using the same protocol from substudy 2.1.

Substudy 2.3. KCl and YM

With the mice cohort from substudy 1, after a 30-min washout period, different concentrations of YM (control, 10, 30, 100nM) were added to each channel 15 min prior to treating tissues with 90mM KCl.

Substudy 3: ecPAR2KO

Substudy 3.1. tcLIGRLO dose-response curves

tcLIGRLO dose-response curves (10, 20, 30 μ M) were performed with ecPAR2KO (n=5) and PAR2WT mice (n=5).

Substudy 3.2. Ach and SNP relaxation

After a 30-min washout period following treatment of vessels with tcLIGRLO, endothelium-dependent and -independent relaxation were assessed with Ach (0.001 –

30 μ M) and SNP (0.001 – 30 μ M), respectively. A 30-min washout period was performed between each dose-response curve.

2.2.4 Cell lines

Cell lines and cell culture reagents were purchased from Thermo Fisher Scientific. PAR2KO HEK293 were generated using CRISPR/Cas9 targeting as described (Sanjana et al., 2014; Shalem et al., 2014; Thibeault & Ramachandran, 2020). Normal HEK293 were referred to as PAR2WT cells. The PAR2 gene sequence (CCCCAGCAGCCACGCCGCGC) was cloned into the lentiCRISPR v2 plasmid (Addgene plasmid no. 52961). Approximately 48h after transfection, PAR2-deficient cells were selected in media containing puromycin (5 μ g/mL). PAR2WT HEK293 and PAR2KO HEK293 were maintained in Dulbecco's modified Eagle's medium supplemented with 10% fetal bovine serum, 1% sodium pyruvate, and penicillin streptomycin solution (50 000 units penicillin, 50 000 μ g streptomycin). Since trypsin activates PAR2, cells were routinely subcultured with enzyme-free isotonic phosphate-buffered saline (PBS) containing EDTA (1mM).

2.2.5 Ca²⁺ signalling

We measured whole cell Ca²⁺ transients in PAR2WT HEK293 and PAR2KO HEK293 cell suspensions using a Photon Technology International QuantaMaster 800 spectrophotometer (Birmingham, NJ) as described (Thibeault & Ramachandran, 2020). Once cells reached 70-80% confluency in a T-25 flask, they were detached in enzyme-free cell dissociation buffer, centrifuged with EppendorfTM 5804R with a S-4-72 rotor (1000 rpm, 5 min), to attain a pellet and re-suspended in 1mL of Fluo-4 no wash Ca²⁺ indicator dye (Thermo Fisher Scientific) for 30 min at room temperature. 2mL of cell suspension was added to each cuvette and intracellular dye fluorescence (excitation, 488nm; emission, 506 nm) was monitored before and after the addition of tcLIGRLO to PAR2WT HEK293 (1-100 μ M tcLIGRLO) and PAR2KO HEK293 (30 μ M tcLIGRLO) at room temperature (20°C). YM (0.03 – 1 μ M) was added to cuvettes containing cells 10

min prior to adding tcLIGRLO (30 μ M) in PAR2WT cells at room temperature. Each cuvette was read for 2 min before changing to the next cuvette.

2.2.6 Data analysis and statistics.

Data are reported as mean \pm standard error of mean (S.E.; error bars) in graphs and Tables. n indicates number of mice per group or number of independent experiments with cells. Arterial ring contractions produced by cumulative concentrations of tcLIGRLO and phenylephrine are reported as a percentage of 90mM KCl contractions. The maximum effect (E_{\max}) for each agonist was determined from the concentration (dose)-response curves (CRCs) for each treatment and mouse. YM inhibition of agonist responses were calculated from agonist responses prior to and after pretreatment with YM. Ach and SNP-induced relaxations (Relaxation (%)) were determined by the reversal of the tone produced by 3 μ M phenylephrine. EC_{50} values (concentration producing 50% of E_{\max}) for agonists were estimated from best-fit sigmoidal dose response curves based on nonlinear regression of the group mean data. pEC_{50} is $-\log_{10} EC_{50}$ (M). Ca^{2+} -dye fluorescence changes to agonists were normalized to an internal control, the Ca^{2+} ionophore A23187 (3 μ M; Sigma-Aldrich).

Statistical analyses were performed in GraphPad Prism v.9.2.0. Correlation between tcLIGRLO responses and age was tested using linear regression test. F-test was used to compare the slope to non-zero value. E_{\max} were compared between groups by unpaired Student's *t*-test or one-way analysis of variance calculations (ANOVA) followed by Bonferroni post hoc. F-test was used to compare the curves for differences in EC_{50} or IC_{50} as applicable. tcLIGRLO dose-response data from ecPAR2KO and WT mice were compared by two-way ANOVA followed by Bonferroni post hoc. * $p < 0.05$ was considered significant for all comparisons.

Table 5. A summary table of physical characteristics of mice (weight and age) and femoral arteries (length and diameter) and sample size

Treatment	Weight^c (g)	Age^c (weeks)	Tissue length^c (mm)	Diameter^c (μm)	Sex (n)
Substudy 1: Sex and age in PAR2KO mice					
tcLIGRLO^a	30.7 \pm 0.9	32.0 \pm 2.8	1.55 \pm 0.01	310 \pm 9	Males (18)
	25.3 \pm 3.8	31.8 \pm 5.3	1.57 \pm 0.09	318 \pm 25	Females (3)
Ach^b	30.8 \pm 2.9	37.7 \pm 1.3	1.63 \pm 0.16	317 \pm 14	Males (4)
SNP^c	30.4 \pm 3.1	36.9 \pm 1.7	1.50 \pm 0.30	327 \pm 34	Males (7)
Phenylephrine^b	23.8 \pm 0.4	32.4 \pm 1.7	1.66 \pm 0.20	310 \pm 7	Males (3)
	27.8 \pm 2.2	21.4 \pm 2.8	1.47 \pm 0.06	270 \pm 28	Females (3)
Substudy 2: YM inhibition in PAR2KO mice					
tcLIGRLO^d	30.0 \pm 0.6	22.6 \pm 0.3	1.60 \pm 0.10	280 \pm 8	Males (4)
Phenylephrine^c	29.9 \pm 3.7	32.5 \pm 7.3	1.53 \pm 0.14	317 \pm 48	Males (12)
90mM KCl	30.3 \pm 3.1	31.5 \pm 3.8	1.57 \pm 0.13	317 \pm 32	Males (10)

Substudy 3: ecPAR2KO

tcLIGRLO^a, Ach^b/SNP^c in ecPAR2KO mice	25.1±1.2	19.4±1.2	1.57±0.09	306±9	Males ^f (2), Females (3)
tcLIGRLO^a, Ach^b/SNP^c in PAR2WT mice	25.1±1.7	19.0±0.7	1.48±0.07	260±28	Males (4), Females ^{f(1)}

No differences were detected for weight, age, tissue length, and diameter between sex ($p>0.05$; unpaired Student's *t*-test) and treatment groups ($p>0.05$; One-way ANOVA)

a, 10 – 30 μ M; b, 0.001 – 10 μ M; c, 0.001 – 30 μ M; d, 0.5 – 50 μ M; e, mean±SD; f, was pooled with matched sex because sample size was <3

2.3 Results

2.3.1 Effects of sex and age on tcLIGRLO-induced contractions

tcLIGRLO produced concentration-dependent contractions of femoral arteries from male PAR2KO (Figure 3, Table 6). tcLIGRLO dose-response curves did not differ between males and females (Figure 4, Table 6). K^+ -induced contractions, which were used to normalize the tcLIGRLO data between experiments, did not differ between sexes (inset Figure 4B). Phenylephrine was more potent in femoral arteries of female versus male PAR2KO, as demonstrated by a leftward shift of the curve for females and a 10-fold difference in EC_{50} values (Figure 5, Table 6). Phenylephrine produced larger E_{max} contractions in male than female PAR2KO arteries by nearly 30% (Figure 5, Table 6). K^+ -induced contractions prior to phenylephrine-treatments did not differ between sexes (inset Figure 5B). tcLIGRLO-induced contractions exhibited a significant negative linear correlation to age despite its low r^2 value 0.20 (inset Figure 7C). When data were binned according to age categories of approximate equal sizes, we found the magnitude of contractions were larger in arteries from the youngest age group mice (20 – 25 weeks, Figure 7A, Table 7) by $\geq 50\%$ from the 30 – 35 weeks and nearly 30% from the 35 – 40 weeks age group. Baseline contractions to K^+ prior to tcLIGRLO contractions did not differ between age groups (Figure 7B). Figure 6 shows the endothelium-dependent and -independent relaxation of femoral arteries from PAR2KO mice. (Figure 4, Table 6).

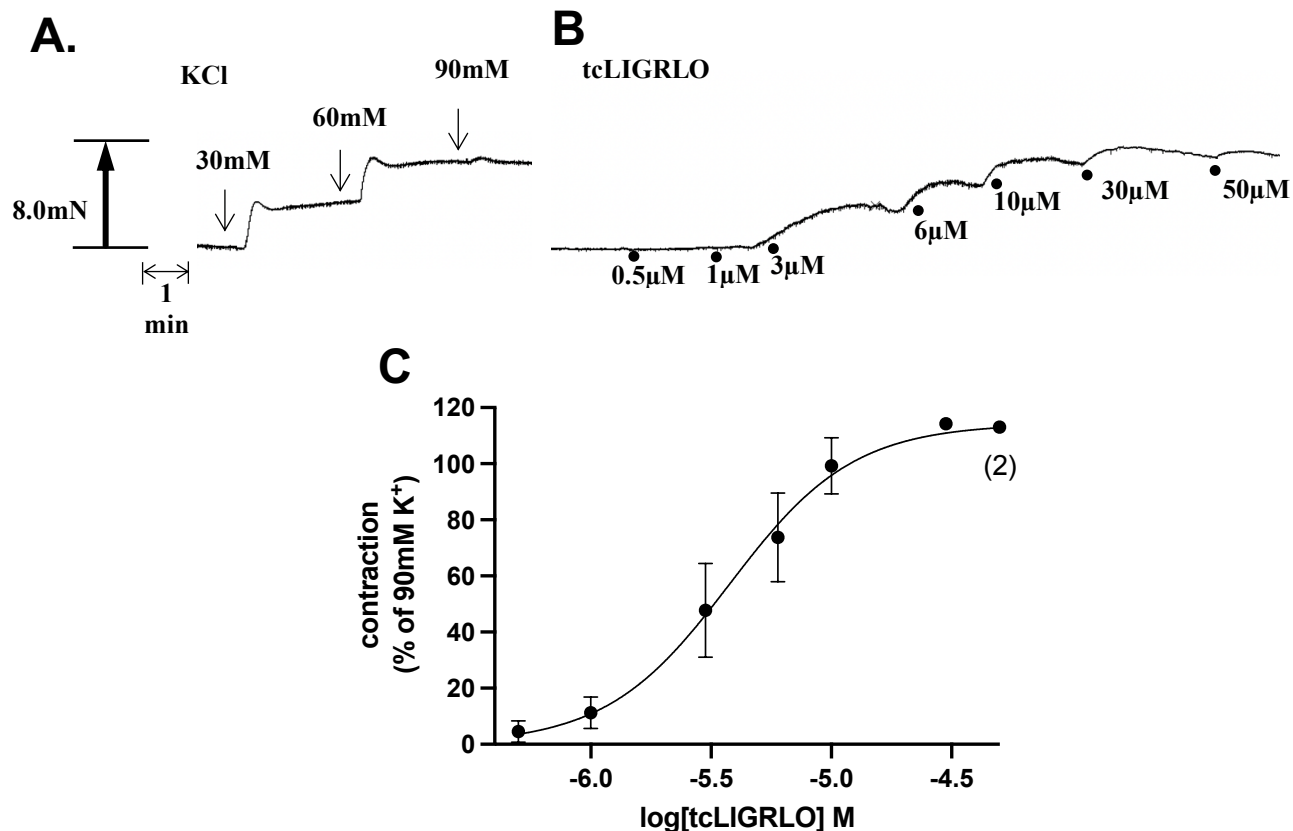


Figure 3. tcLIGRLO-induced contractions of femoral arteries from male PAR2KO mice.

Femoral arteries were given 0.5μM – 50μM of tcLIGRLO to produce contractions, which were normalized by 90mM KCl-treatment. A representative recording of isometric tension experiment showing contractions produced by the addition of KCl (*A*) and tcLIGRLO (*B*) is provided. *C.* E_{\max} and pEC_{50} are provided in Table 6. Nonlinear regression curve fit is shown as mean \pm S.E. (error bars) for subjects ($n=4$). *N.B.* the response to the highest dose of tcLIGRLO (50 μM) was determined in two samples, as indicated by parentheses.

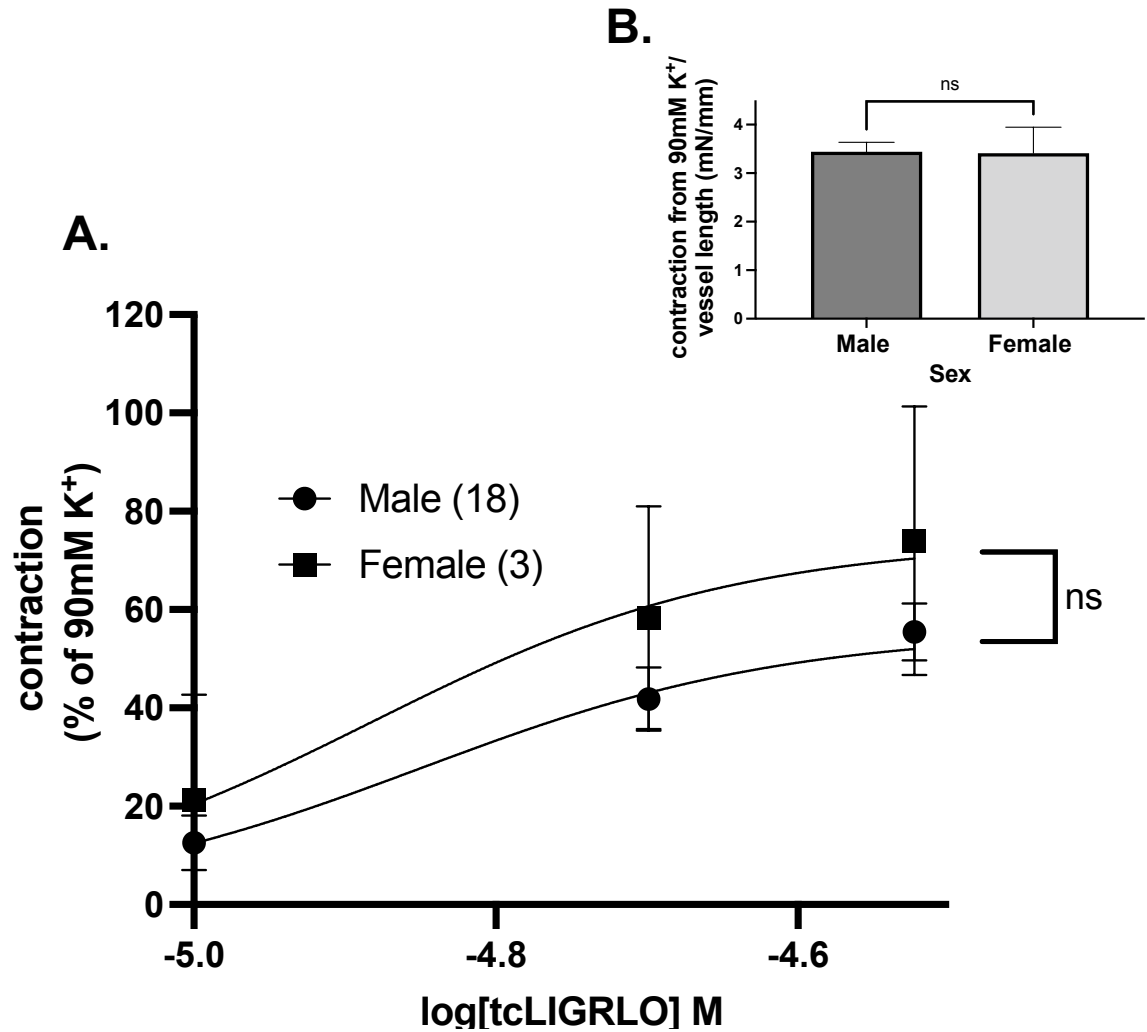


Figure 4. tcLIGRLO-response curves in male vs female PAR2KO femoral arteries.

Femoral arteries from both sexes were treated with 10, 20, and 30 μ M tcLIGRLO to produce contractions, which were normalized against baseline contraction values from 90mM K⁺-treatment. *A.* E_{\max} and pEC_{50} are provided in Table 6. There were no differences between means of E_{\max} ($p>0.05$; Unpaired Student's *t*-test) and EC_{50} values ($p>0.05$; F-test). Nonlinear regression curve fit is shown as mean \pm S.E. *N.B.* Sample size for females was a lot smaller due to limited availability of mice during breeding.

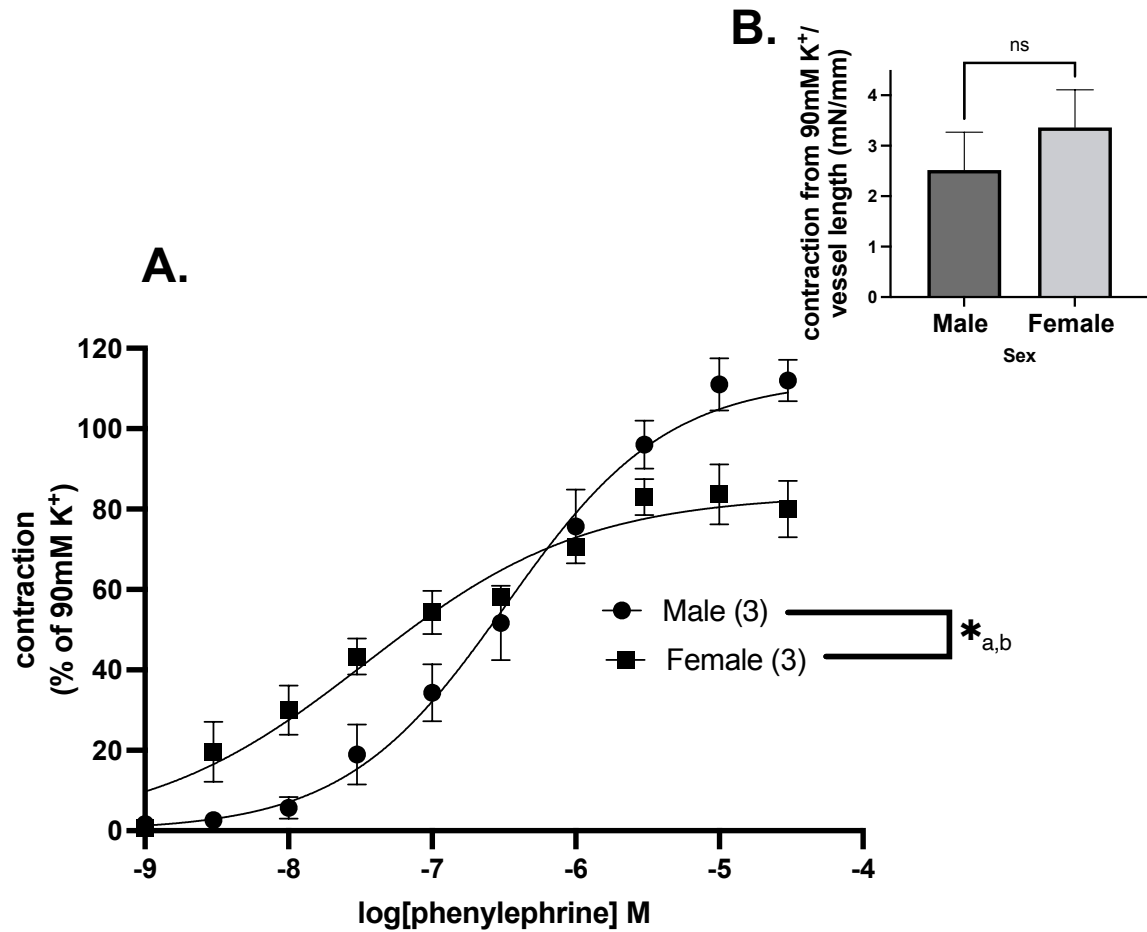


Figure 5. Phenylephrine CRCs in male vs female PAR2KO femoral arteries.

Femoral arteries from both sexes were treated with 0.01 – 10 μ M of phenylephrine to produce contractions, which were normalized against baseline contraction values from 90mM K⁺-treatment. *A.* E_{\max}^a (* p <0.05; Unpaired Student's t -test) and pEC_{50}^b (* p <0.05; F-test) are provided in Table 6. *Inset B.* Contractions to 90mM K⁺-treatment between male and female mice were not significantly different from each other (p >0.05; Unpaired Student's t -test).

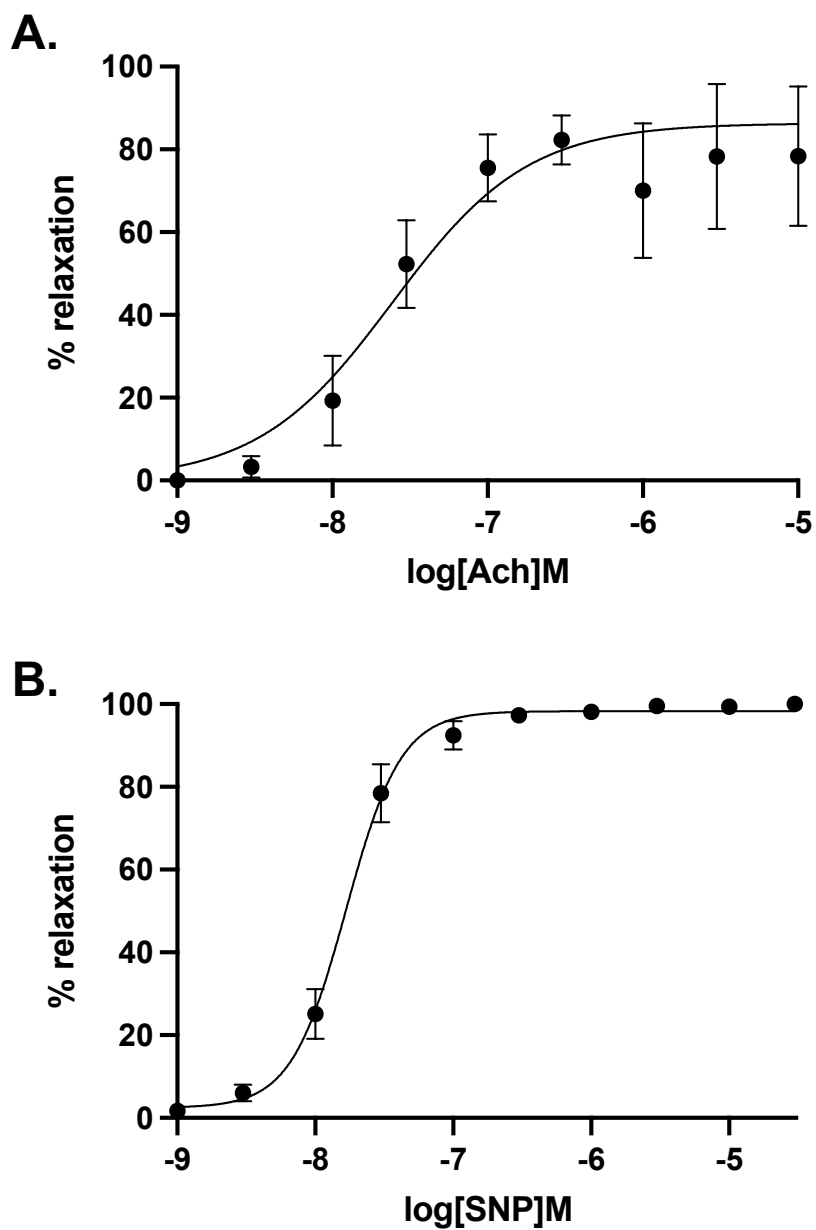


Figure 6. Ach and SNP-relaxation response curves in femoral arteries from male PAR2KO mice.

Relaxation responses to 3 μ M phenylephrine using 0.001 – 10 μ M Ach (A; n=4) and 0.001 – 30 μ M SNP (B; n=7) were performed following tcLIGRLO-treatment. Nonlinear regression curve fit is shown as mean \pm S.E. (error bars).

Table 6. A summary table of pEC₅₀, E_{max}, and sample size values of tcLIGRLO and phenylephrine drug treatments in PAR2KO mice.

Treatment	pEC₅₀ (M)	E_{max}(M)	Sex (n)
tcLIGRLO^a	5.41±0.02	114±1	Males (4)
tcLIGRLO^b	4.85±0.03	56±6	Males (18)
	4.88±0.02	74±27	Females (3)
Ach^c	7.61±0.10	78±17	Males (4)
SNP^d	7.78±0.02	100±0	Males (7)
Phenylephrine^c	6.49±0.04	113±6	Males (3)
	7.45±0.09*	84±7*	Females (3)

*p<0.05 with F-test (pEC₅₀) and unpaired Student's *t*-test (E_{max}), males vs. females.

a, 0.5 – 50μM; b, 10 – 30μM; c, 0.001 – 10μM; d, 0.001 – 30μM

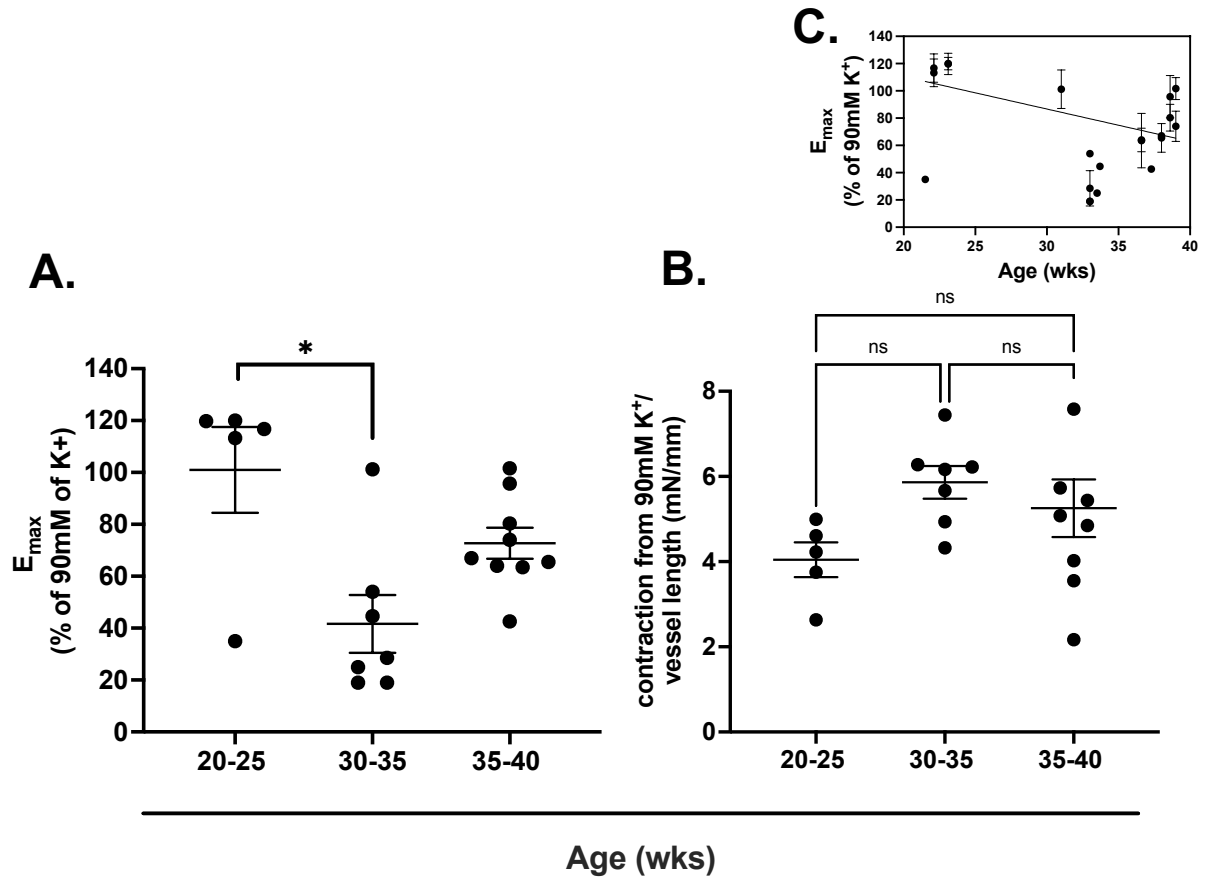


Figure 7. Effect of age on tcLIGRLO contractions of male PAR2KO femoral arteries.

E_{\max} of tcLIGRLO-induced contractions were normalized relative to baseline contractions values at 90mM K^+ -treatment. Mice were grouped into three different age groups—20 – 25 weeks ($n=5$), 30 – 35 weeks ($n=7$), and 35 – 40 weeks ($n=9$). Data are reported as mean \pm S.E. (error bars). *A.* A summary table of mean E_{\max} values of the three different age groups is shown in Table 7. Significance ($*p<0.05$) was determined by one-way ANOVA followed by Bonferroni post hoc. *B.* Contractions to 90mM K^+ -treatment between age groups were not significantly different from each other ($p>0.05$; One-way ANOVA). *Inset C.* Equation for linear graph is $y=-2.4x + 158.0$. Slope of E_{\max} demonstrates a significant negative correlation to age ($*p<0.05$; F-test) with $r^2=0.20$.

Table 7. E_{\max} values of tcLIGRLO-mediated contractions of male PAR2KO femoral arteries from three age groups

Age group (weeks)	n	E_{\max}^a (%)
20-25	5	101 ± 16*
30-35	7	42 ± 11
35-40	9	73 ± 6

E_{\max} values of tcLIGRLO-mediated contractions were recorded at 30 μ M tcLIGRLO.

*p<0.05, compared to 30 – 35 weeks; One-way ANOVA followed by Bonferroni post hoc

a, mean±SEM

2.3.2. Effects of the G_q inhibitor YM on femoral arteries

To determine the role of G_q in tcLIGRLO-induced contractions, we incubated femoral arteries with YM for 15 min before adding tcLIGRLO (Figure 8, Table 8). We found that 10 and 30nM of YM did not inhibit tcLIGRLO-mediated contractions, while 100nM YM abolished contractions. Similarly, in pilot experiments where we pre-treated mouse femoral arteries with YM for 30 min (n=2), 10 and 30 nM of YM also did not induce inhibition, while 100nM YM completely inhibited tcLIGRLO-mediated contractions. We also tested the effect of YM on phenylephrine CRCs (Figure 9, Table 8). We found that all doses of YM inhibited phenylephrine-induced contractions, with complete abolishment of contractions at 100nM YM. K⁺ contractions of YM-treated arteries did not differ from untreated arteries (Figure 10).

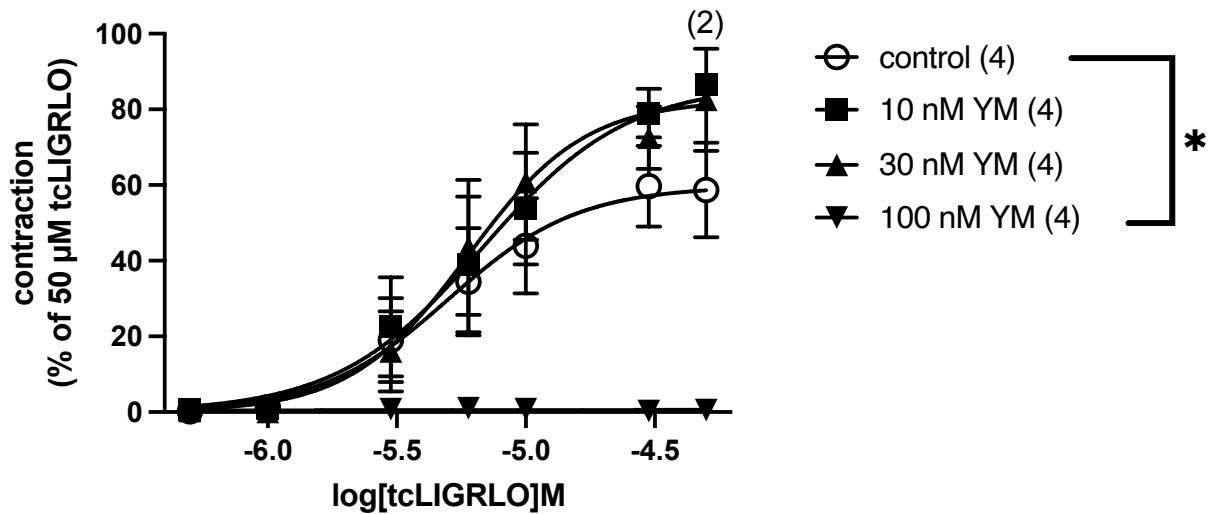


Figure 8. YM inhibition of tcLIGRLO-mediated contractions in femoral arteries of PAR2KO male mice.

Contractions to 0.5 – 50 μ M tcLIGRLO were normalized relative to the maximum contractions at 50 μ M tcLIGRLO prior to 15-min pre-treatment of YM. Table 8 provides E_{\max} and pEC_{50} values of tcLIGRLO-mediated contractions. 100nM YM completely abolished tcLIGRLO-mediated contractions as compared with untreated arteries (* $p < 0.05$; F-test). E_{\max} values did not differ between groups in both data sets in control vs. 10nM YM and control vs. 30nM YM ($p > 0.05$; One-way ANOVA). 10nM and 30nM YM failed to inhibit tcLIGRLO-mediated contractions as compared with control ($p > 0.05$; F-test). Nonlinear regression curve fit is shown as mean \pm S.E. (error bars). *N.B.* only two mice were done for the highest dose of tcLIGRLO (50 μ M), as indicated by parentheses. Numbers within parentheses beside respective group indicate number of animals used.

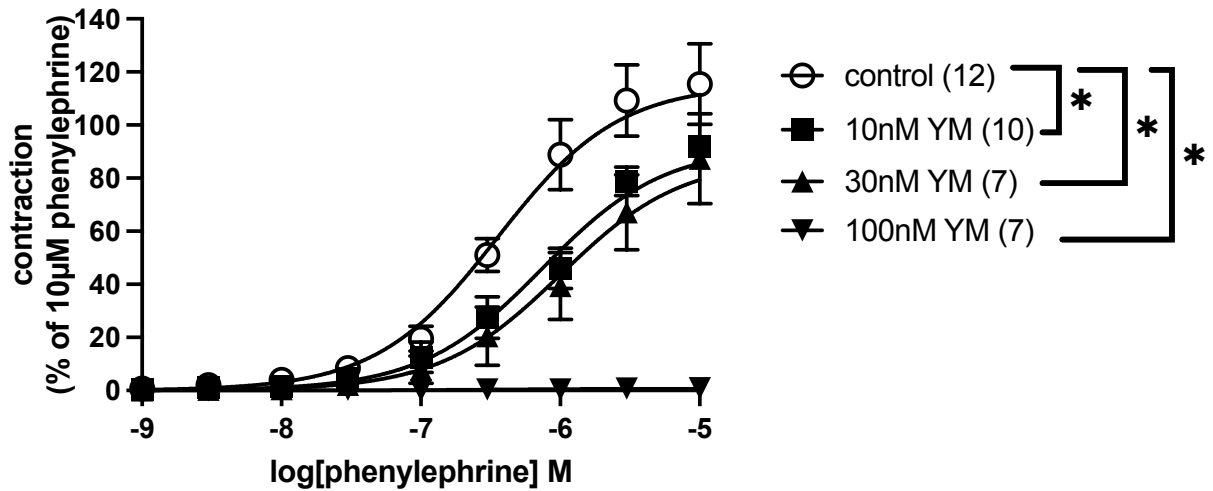


Figure 9. YM inhibition of phenylephrine-mediated contractions in femoral arteries of PAR2KO male mice.

Contractions to 0.001 – 10µM phenylephrine were normalized relative to the maximum contractions at 10µM phenylephrine prior to 15-min pre-treatment of YM. Table 8 provides E_{\max} and pEC_{50} values of contractions. 100nM YM completely abolished phenylephrine-mediated contractions as compared with untreated arteries (* $p < 0.05$; F-test). Both 10nM and 30nM YM inhibited phenylephrine-induced contractions, as demonstrated by significant rightward shift in EC_{50} values in comparison to control (* $p < 0.05$; F-test). Nonlinear regression curve fit is shown as mean \pm S.E. (error bars).

Table 8. E_{\max} and pEC_{50} values of tcLIGRLO- and phenylephrine-induced contractions following YM treatments in femoral arteries from male PAR2KO mice.

control ^{a,b}		YM		
		10nM ^{a,c}	30nM ^{a,d}	100nM ^{a,d}
tcLIGRLO ^e				
E_{max} ^f (%)	60±11	87±1	83±14	0*
pEC₅₀ ^f (M)	5.30±0.02	5.17±0.02	5.22±0.03	--
Phenylephrine ^g				
E_{max} ^f (%)	115±15	92±3	87±17	0*
pEC₅₀ ^f (M)	6.45±0.02	6.13±0.05*	6.00±0.04*	--

Femoral arteries were treated with tcLIGRLO and phenylephrine to determine effects of YM inhibition. *p<0.05, treatment compared to control; F-test

a, tcLIGRLO-treatment n=4; b, phenylephrine-treatment n=12; c, phenylephrine-treatment n=10; d, phenylephrine-treatment n=7; e, 0.5 – 50μM; f, mean±SEM ; g, 0.001 – 10μM

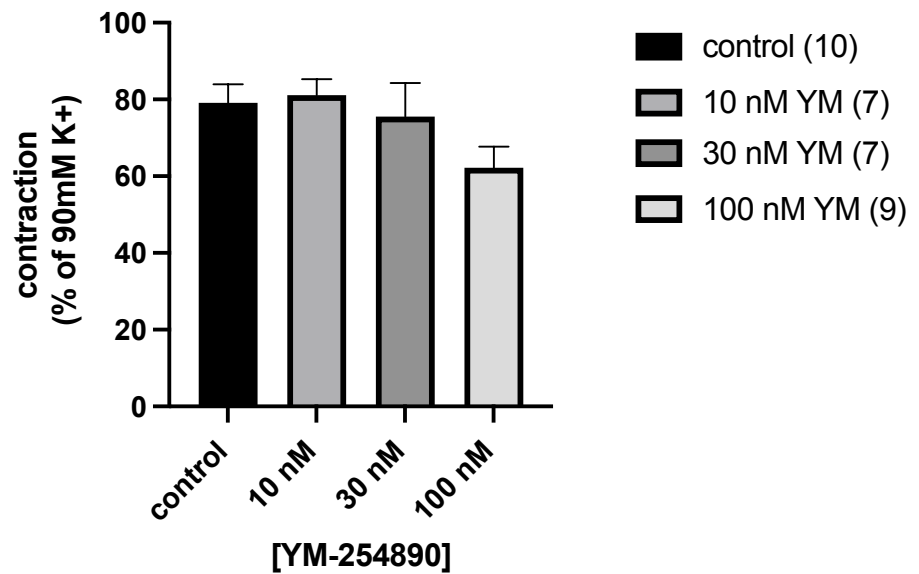


Figure 10. K⁺ contractions in the presence and absence of YM.

Contractions to 90mM K⁺ of arteries treated with 0 (control), 10, 30, and 100nM YM were normalized to 90mM K⁺ determined by a K⁺ dose-response curve for each artery. Data are reported as mean \pm S.E. (error bars). K⁺ contractions of YM treated arteries did not significantly differ from untreated arteries ($p > 0.05$, one-way ANOVA). Numbers within parentheses beside respective group indicate number of animals used.

2.3.2 tcLIGRLO effects in ecPAR2KO mice

tcLIGRLO- and K^+ -induced contractions of femoral arteries in ecPAR2KO did not differ from WT (Figure 11A and Inset B). Endothelium-dependent and -independent relaxations of femoral arteries did not differ between ecPAR2KO and WT (Figure 12A and B, Table 9).

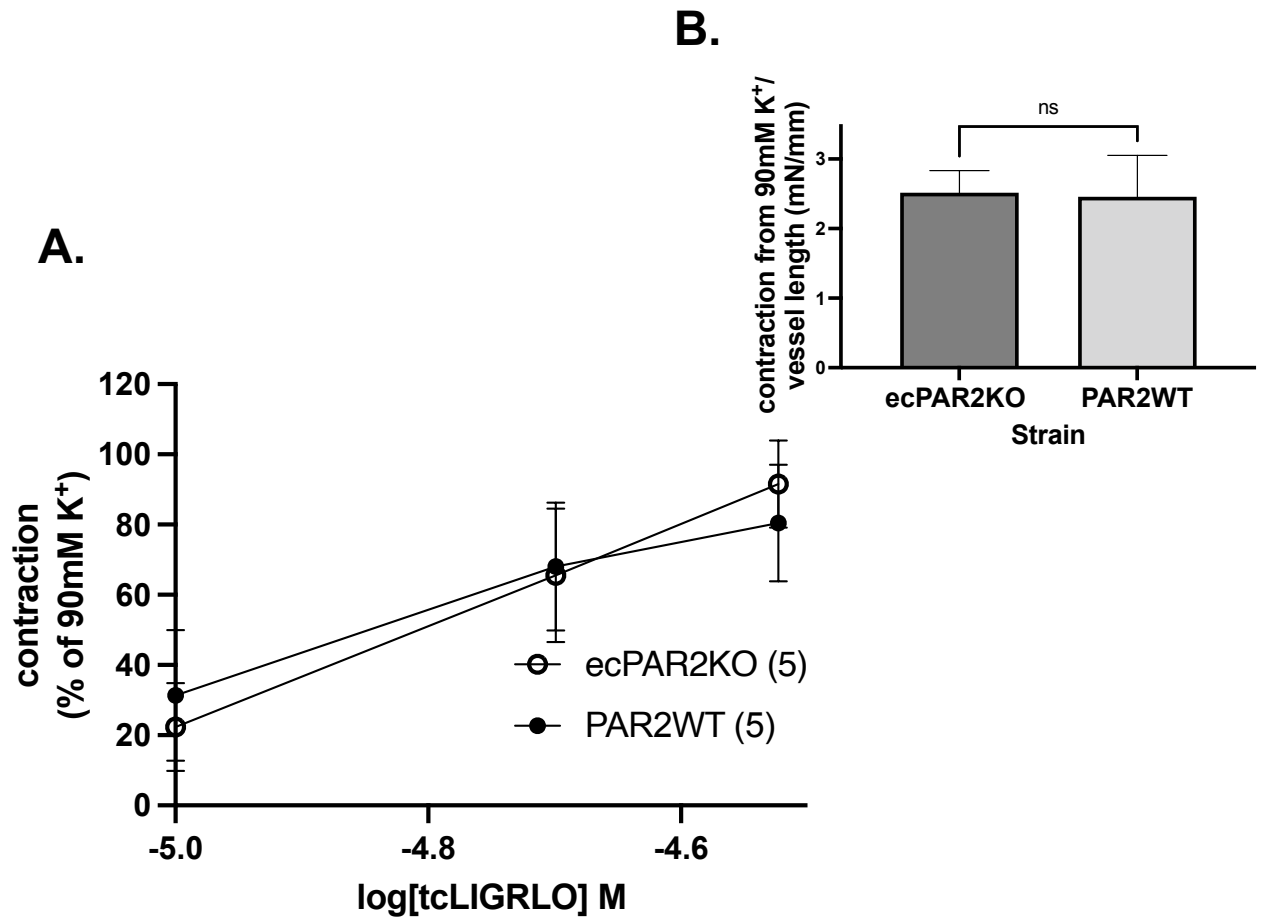


Figure 11. tcLIGRLO-mediated contractions in ecPAR2KO and PAR2WT femoral arteries.

A. Under baseline conditions, arteries were treated with 10, 20, and 30 μ M tcLIGRLO. Data points are the tcLIGRLO contractions normalized to 90 mM K⁺ contractions (*Inset B*). tcLIGRLO-induced contractions did not significantly differ between strains ($p > 0.05$; two-way ANOVA). Contractions to 90mM K⁺-treatment also did not significantly differ between strains ($p > 0.05$; unpaired Student's *t*-test). E_{\max} and pEC_{50} values are given by Table 9. Nonlinear regression curve fits were done via F-test. Data points are mean \pm S.E. (error bars). Numbers within parentheses indicate the sample size (number of animals) for each group.

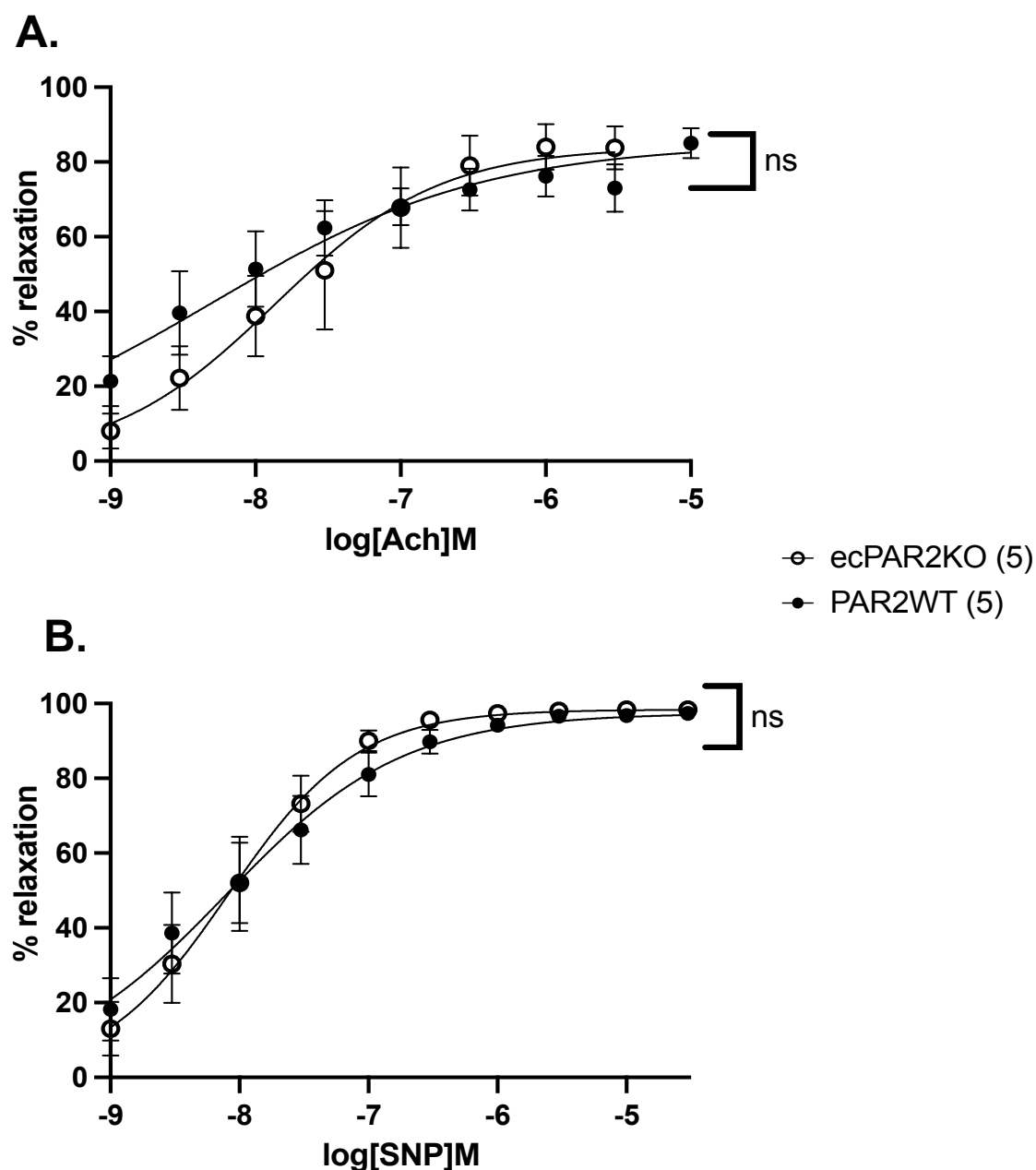


Figure 12. Ach- and SNP CRCs in ecPAR2KO and PAR2WT femoral arteries.

Relaxation responses to 0.001 – 10 μ M Ach (A) and 0.001 – 30 μ M SNP (B) induced by 3 μ M phenylephrine pretreatment are provided. E_{\max} and pEC_{50} values are given by Table 8. Nonlinear regression curve fits were performed via F-test. Data points are mean \pm S.E. (error bars). Numbers within parentheses indicate the sample size (number of animals) for each group.

Table 9. pEC₅₀ and E_{max} values of Ach- and SNP-induced relaxation in femoral arteries from ecPAR2KO and WT mice following pre-contraction to 3μM phenylephrine.

	Ach^a	
	ecPAR2KO^b	WT^c
E_{max}^d (%)	84±6	85±4
pEC₅₀^d (M)	7.86±0.12	8.29±0.16
	SNP^e	
E_{max}^d (%)	98.4±0.5	97±2
pEC₅₀^d (M)	8.08±0.07	8.11±0.10

Ach CRCs were conducted following a 30-min washout period subsequent to tcLIGRLO contractions. After another 30-min washout period, SNP CRCs were performed. There were no differences in E_{max} (p>0.05; unpaired Student's *t*-test) and pEC₅₀ values (p>0.05; F-test) between strains.

a, 0.001 – 10μM; b, n=5; c, n=5; d, mean±SEM; e, 0.001 – 30μM

2.3.3 Effects of the G_q inhibitor YM on Ca²⁺ signals in PAR2WT HEK293 cells

To confirm inhibition of G_q-coupled Ca²⁺ signals by YM, we first assessed Ca²⁺ signalling with 30μM tcLIGRLO using PAR2WT HEK293 (Figure 13B and C). Following that, we assessed tcLIGRLO-induced Ca²⁺ signals at four different incubation periods with YM (0, 5, 20, 30 min; Figure 14). We found that 1μM YM abolished tcLIGRLO-mediated Ca²⁺ signals at 20 min. The incubation time of 30 min also abolished Ca²⁺ signals, but we noted that one of the replicates showed less inhibition. 30μM tcLIGRLO did not activate Ca²⁺ signals in PAR2KO HEK293 cells (Figure 13A). This result validated the specificity of tcLIGRLO for PAR2 *in vitro* (Figure 13A and C). Thrombin elicited a Ca²⁺ signal in PAR2KO HEK293 which shows the cells were viable and responsive to other GPCR, specifically PAR1 in these cells, activations. After treating cells with increasing concentrations of YM for 10 min, YM inhibited tcLIGRLO-induced PAR2-Ca²⁺ signalling, with a pIC₅₀ value of 6.85±0.08M (Figure 15).

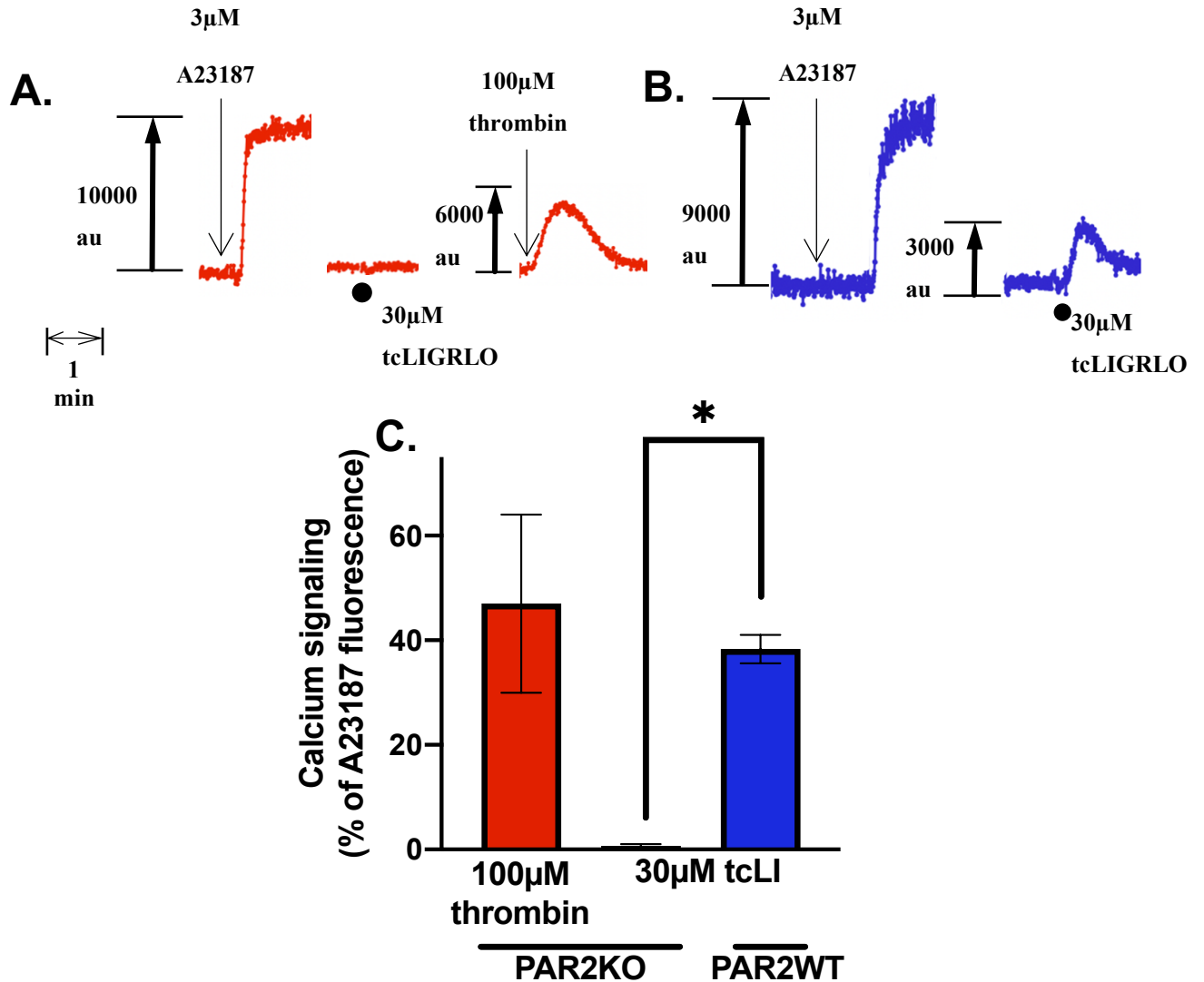


Figure 13. tcLIGRLO-mediated Ca²⁺ signalling in PAR2KO and PAR2WT HEK293 cells.

Representative data recordings of 30μM tcLIGRLO-mediated Ca²⁺ signalling in PAR2KO (A) and PAR2WT HEK293 cells (B) are provided. C. Ca²⁺ signalling in response to drugs (thrombin, tcLIGRLO, and YM) was normalized to Ca²⁺ response to ionophore (3μM; A23187). A. Thrombin (100μM) was added to ensure the presence of PAR1 in PAR2KO HEK293 cells. C. When treating PAR2KO cells (n=3) with 100μM thrombin, this resulted in 47±17% Ca²⁺ signalling, while 30μM tcLIGRLO failed to induce any response. Treatment of HEK293 cells (n=3) with 30μM tcLIGRLO resulted in a 42±3% Ca²⁺ response. Significance (*p<0.05) was determined via unpaired Student's *t*-test. Data are reported as mean ± S.E. (error bars).

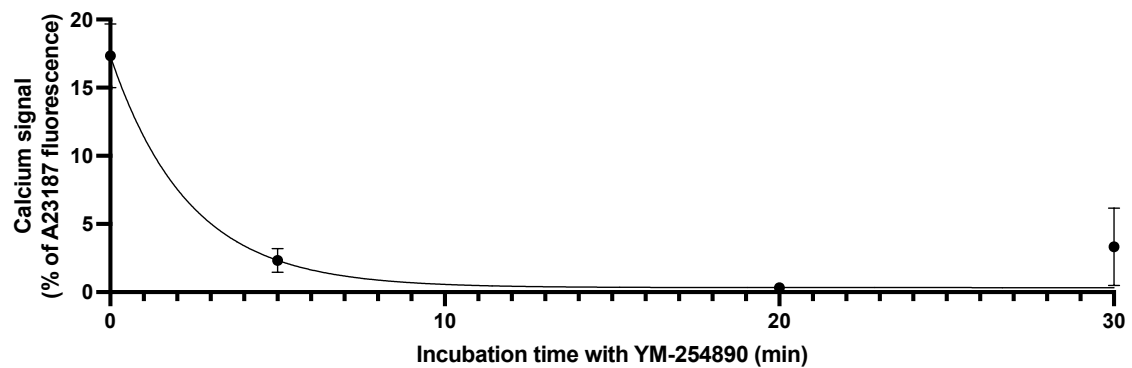


Figure 14. YM inhibition of PAR2-activated Ca^{2+} signalling for tcLIGRLO-treated PAR2WT HEK293 cells.

HEK293 cells ($n=3$) were incubated with $1\mu\text{M}$ YM at different incubation time points (0, 5, 20, and 30 min) prior to tcLIGRLO-treatment. Data are reported as mean \pm S.E. (error bars). Nonlinear regression curve fit is shown as mean \pm S.E. (error bars).

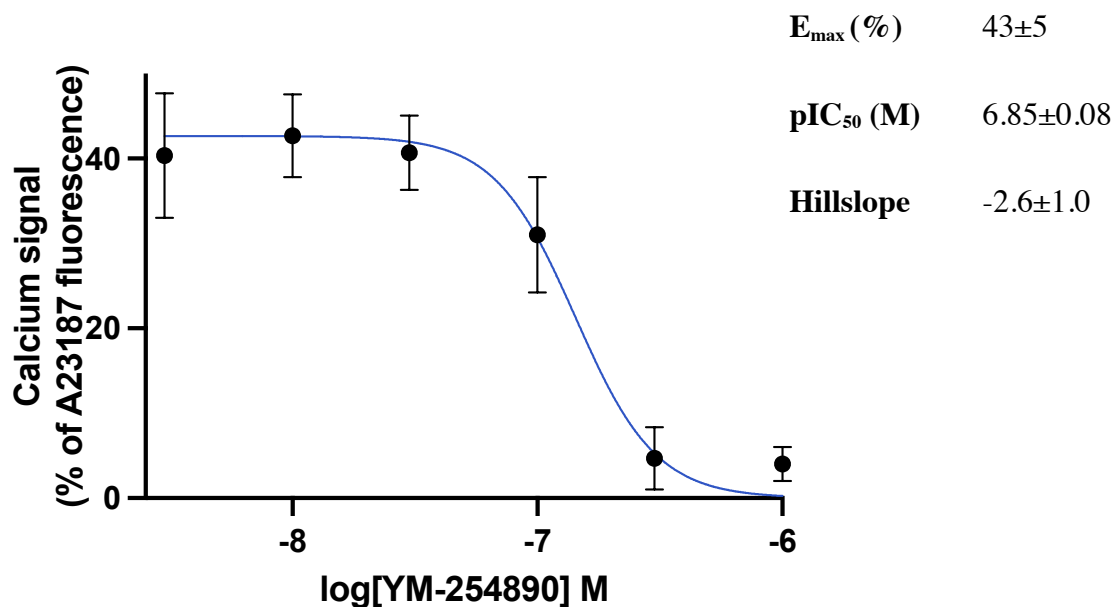


Figure 15. tcLIGRLO-mediated Ca^{2+} signalling in PAR2WT HEK293 cells.

Inhibitory dose response curve with 10 min pre-treatment of 0.003 – 1 μ M YM of 30 μ M tcLIGRLO-mediated Ca^{2+} signalling in PAR2WT HEK293 (n=3) cells is shown. E_{\max} signal for tcLIGRLO relative to A23187 and pIC_{50} value for YM inhibition of tcLIGRLO signal are reported as mean \pm SEM. Nonlinear regression curve fit is shown as mean \pm S.E. (error bars).

2.4 Discussion

The main finding of this study are age-related effects and a link to G_q -coupling in tcLIGRLO-mediated contractions in mouse femoral arteries. Results from this study will contribute towards the further delineation of the signal transduction profile that mediate contractions elicited by tcLIGRLO.

2.4.1 Age-related effects on tcLIGRLO-mediated contractions

Risk factors that compromise vascular health on the morphological and structural level of arteries include age and sex. In particular, the human ageing process is marked by an imbalance of vasoconstrictor and vasodilator molecules (e.g., nitric oxide) in the endothelium (i.e., endothelial dysfunction) (Brandes et al., 2005; Herrera et al., 2010), as well as an increased ratio of collagen to elastin in the extracellular matrix due to elastin fragmentation (Duca et al., 2016; Greenwald, 2007; Sehgel et al., 2015). Here, we looked at age as a factor that affects tcLIGRLO-induced contractions in mouse femoral arteries and discovered a novel G_q -mediated vasoconstrictor mechanism.

The tcLIGRLO-activated receptor is reported to be in the smooth muscle of mouse femoral arteries (McGuire et al., 2002). We found that the magnitude of tcLIGRLO-induced contractions exhibited a negative linear correlation to increasing age (Figure 8). There was a significant reduction in tcLIGRLO-induced contractions following 25 weeks, specifically between the age groups 20-25 weeks and 30-35 weeks. However, we note a gap in data covering the age range from 25-30 weeks and overall a more narrow age range (20-40 weeks) than studies by Seawright et al. (2016, 2018). In those studies using 16 and 96 weeks of age rats, various GPCR ligands including norepinephrine, phenylephrine, and angiotensin II were tested and their contractions of soleus muscle feed arteries were reduced in the older rats. Interestingly, age-related effects in smooth muscle contractions induced by norepinephrine disappeared upon endothelium denudation, whereas reduced vasoconstrictor responses to phenylephrine and angiotensin II were still apparent in aged vessels (Seawright et al., 2018). Preserved contractions to

norepinephrine in denuded vessels suggest that decreased norepinephrine-induced constrictions in aged, intact arteries are due to endothelial dysfunction. In contrast, age-induced decline in constrictions stimulated by phenylephrine and angiotensin II in both intact and denuded arteries are predominantly due to reduced vascular smooth muscle function from ageing effects.

Studies have pointed to increased vascular stiffness during the ageing process as one of the reasons for diminished vasoconstrictor responses (Duca et al., 2016; Greenwald, 2007; Seawright et al., 2018; Sehgel et al., 2015). More specifically, a heightened vascular stiffness is attributed to an increased expression of adhesion molecules such as $\alpha 1\beta 1$ (Seawright et al., 2018; Sehgel et al., 2015) in compensation for reduced proteins essential for smooth muscle contractions (e.g. vinculin and pFAK397) in old versus young vessels (Seawright et al., 2018). Additional experiments involving endothelium denudation are needed to comment on the interplay between the endothelium and smooth muscle in tcLIGRLO-mediated contractions.

We did not detect sex differences in tcLIGRLO-mediated contractions of femoral arteries in PAR2KO. In our experiments using phenylephrine with PAR2KO femoral arteries, arteries from females were initially more sensitive to $\alpha 1$ adrenergic receptor activation in comparison to male arteries, as demonstrated by the leftward shift in EC_{50} values experienced by female arteries by nearly 10 folds (Table 6). As shown by their E_{max} values, arteries from male mice managed to surpass contractions experienced by female arteries by almost 30% at higher concentrations ($>0.3\mu M$; Table 6). Younger human males are reported to initially exhibit higher levels of $\alpha 1$ adrenergic reactivity, while human females experience an increased sensitivity to phenylephrine later on in life (Aloysius et al., 2012; Keung et al., 2005; Turner et al., 1999). Considering the age difference in the male and female PAR2KO mice (21 ± 3 weeks vs. 32 ± 2 weeks), there is potential for an interaction between sex and age to influence contractions due to declining levels of estrogen with increasing age in our mouse models (McNeill et al., 2002; Novella et al., 2012; Turner et al., 1999). Estrogen is known as a protective agent against

cardiovascular disease by promoting the expression of eNOS, thus increasing nitric oxide production levels (McNeill et al., 2002; Novensà et al., 2011). Novensà et al. (2011) found that an increased estrogen receptor β to α ratio in aged female mice may be linked to oxidative stress, which likely contributes to higher vasoreactivity in older females. Altogether, tcLIGRLO-mediated contractions did not differ between sexes, but did decrease with increasing age of mice.

2.4.2 tcLIGRLO-mediated contractions are G_q -dependent

tcLIGRLO-mediated contractions are dependent on the transient release of Ca^{2+} from internal stores (Chapter 1.1), leading us to test the role of G_q . In our experiments with tcLIGRLO and PAR2KO femoral artery contractions, 100nM of YM, a highly specific G_q -inhibitor (Chapter 1.2), abolished tcLIGRLO-mediated contractions (Figure 1; Chapter 1). The specificity of YM's effect on G_q -coupled contractions was confirmed by its inhibitory effect on phenylephrine (Figure 9) and lack of effect on K^+ contractions (Figure 10). These data are consistent with the reported inhibition by YM of rat aortas contractions by other GPCRs which are known to involve G_q (Table 3; Chapter 1.2.4). We also found that the concentration of YM used in the *ex vivo* studies was effective for inhibition of tcLIGRLO activation of PAR2- Ca^{2+} signal in HEK293 (Figure 13B and C). These data demonstrate that tcLIGRLO-induced contractions are mediated by a G_q pathway, providing evidence of an unidentified GPCR as the target of tcLIGRLO in mouse femoral arteries.

2.4.3 YM inhibition of PAR2 Ca^{2+} signalling pathway

We found that YM's use displayed an all-or-none inhibitory response, resulting in a steep Hill coefficient (>1) estimated in the Ca^{2+} signal assay to tcLIGRLO in PAR2WT cells following YM pre-treatment (2.6 ± 1.0 ; Figure 15). We found a 5 min incubation threshold for inhibition of PAR2 Ca^{2+} signal by YM ($1\mu M$) and complete inhibition after 10 min. A small reduction in effectiveness of YM ($1\mu M$) after 30 min incubation, potentially due to decreased peptide stability, was observed in a single replicate. This decreased peptide stability of YM after a prolonged period has not been reported by previous studies. To

date, there are few studies that investigate the effects of YM inhibition on PARs signalling, and in particular, PAR2 signalling. In the study by Thibeault & Ramachandran (2020), where they measured β -arrestin recruitment in HEK293 cells following the addition of SLIGRL, 100nM of YM resulted in reduced EC_{50} values in β -arrestin-1 and -2 recruitment in comparison to untreated cells by nearly 1.5 – 2 folds. We are not aware of any studies that have reported a pIC_{50} value for the effects of YM on PAR2- Ca^{2+} signalling stimulated by tcLIGRLO in HEK293 cells.

Chapter 3

3 Assessing for GPCR activation with the TANGO assay

3.1 Introduction

Of the 800 human GPCRs, over 150 of these receptors are classified as orphan receptors (i.e., GPCRs whose endogenous and synthetic ligands remain undetermined) (Pierce et al., 2002; Stockert & Devi, 2015). A limit to traditional high throughput screening methods for potential orphan receptor hits with GPCR ligands is they rely on assays of second messengers (e.g., Ca^{2+} , cAMP) mediated by the different $\text{G}\alpha$ proteins— G_s , G_i , $\text{G}_{12/13}$, or G_q . (Chapter 1.3.2). The rate of de-orphanization has decreased from its peak during the 1990s – early 2000s, at around 10 de-orphanized GPCRs per year (Hauser et al., 2017, 2020). While GPCRs interact with the heterotrimeric G-protein complex formed by $\text{G}\alpha$ and $\text{G}\beta/\gamma$, this does not preclude GPCR signalling via G-protein independent pathways (Heuss et al., 1999; Tang et al., 2012). For example, β -arrestin recruitment assays provide another avenue for measuring GPCR activation independent of G-protein signalling. The TANGO assay applies the knowledge that most GPCRs interact with β -arrestin-1 and/or -2 (Chapter 1.3.2.2). Specifically, the TANGO assay uses GPCR constructs containing modified C-terminus fused with a transcriptional activator that is separated by a cleavage site, where β -arrestin-2 binds to following external ligand binding to the receptor (Figure 2; Chapter 1.3.2.2). Following receptor activation from ligand binding, this allows the transcriptional activator to enter the nucleus to upregulate the luciferase reporter gene, which gives off a luminescence signal (Figure 2; Chapter 1.3.2.2). Several GPCRs have been deorphanized using the TANGO assay since the time of its introduction almost 20 years ago (Barnea et al., 2008; Kroeze et al., 2015; Meder et al., 2003; Wittamer et al., 2003). The advantage of this approach is that the ligand screening is independent of the $\text{G}\alpha$ subtype protein that is coupled to the native receptor and is independent of specific second messenger signalling.

In chapter 2, we showed that tcLIGRLO activates G_q -dependent contractions of mouse femoral arteries. The GPCR linking tcLIGRLO to contraction is undetermined in PAR2KO femoral arteries. In this study, we proposed to use the TANGO assay to identify potential human orphan GPCRs as targets. tcLIGRLO is a known PAR2 activator, but has not been tested in the TANGO system. First, we compared tcLIGRLO to other known PAR2APs in PAR2 expressing cells using the TANGO assay. Next, we used tcLIGRLO in cells expressing CCRL2, GPR15, SUCNR1, and GPR135 using the TANGO assay. These candidate receptors were selected based on a pilot study (unpublished data, Dr. McGuire) screen of >70 orphan GPCRs using the human orphan GPCR PathHunter® assay contract service screen. Expression of the mouse orthologues for these receptors have been confirmed in mouse blood vessels, including the mouse femoral artery of PAR2KO (unpublished data, Dr. McGuire). By the time of this study, the orphan receptor GPR91 was de-orphanized and renamed as SUCNR1, with succinate as its only confirmed endogenous ligand to date (He et al., 2004). GPR15 and CCRL2 have their prospective ligands GPR15L/thrombomodulin and chemokines/chemerin, respectively (Biber et al., 2003; Hartmann et al., 2008; Pan et al., 2017; Suply et al., 2017), whereas ligands for GPR135 remain undetermined (Watkins & Orlandi, 2020). In this chapter, our goal was to validate the TANGO assay for PAR2 activation by tcLIGRLO, in concurrence to the assessment for GPCR activation with the four receptors. Here, we confirmed tcLIGRLO activated PAR2, but had less activity compared with the PAR2APs SLIGRL and 2fLIGRLO.

3.2 Materials and Methods

3.2.1 Chemical reagents and drug solutions

Chemical reagents and buffer solutions were purchased from Thermo Fisher Scientific (Mississauga, ON). PAR2APs SLIGRL, tcLIGRLO, and 2fLIGRLO were synthesized as amides (GenScript). Stock solution of SLIGRL, tcLIGRLO, and 2fLIGRLO were made in 25mM HEPES buffer, pH 7.4. Dilutions of synthetic peptides were made at room temperature in 1x Hank's Balanced Salt Solution (HBSS) containing Ca^{2+} (1.3mM),

magnesium (0.9mM), and glucose (5.6mM). D-luciferin, sodium salt for Glo reagent was purchased from GoldBio (St. Louis, MO), and 15mg/mL stock solution was made in double-distilled H₂O according to manufacturer's protocol.

3.2.2 Cloning and transfection

The plasmid constructs of CCRL2, GPR15, GPR135, SUCNR1, and PAR2 were purchased from Addgene, which distributes these constructs designed by the Roth lab as part of the PRESTO-TANGO kit. Plasmid DNA purification was performed with HiSpeed Plasmid Midi Kit from Qiagen (Germantown, MD). Cell culture reagents were purchased from Thermo Fisher Scientific. HTLA cells (a HEK293 cell line stably expressing a tetracycline transactivator-dependent luciferase, reporter, and β -arrestin-2-Tobacco Etch Virus fusion gene) were provided to Dr. Rithwik Ramachandran by the Barnea lab (Brown University, Providence, RI) and maintained in Dulbecco's modified Eagle's medium supplemented with 10% fetal bovine serum, 1% sodium pyruvate, penicillin streptomycin solution (50 000 units penicillin, 50 000 μ g streptomycin), 200 μ g/mL hydromycin B, 500 μ g/mL G418, and 5 μ g/mL puromycin at 37°C, 5%CO₂. XtremeGene 9 DNA Transfection Reagent Transfection was purchased from Roche (Basel, Switzerland) and was diluted with Opti-MEM Reduced Serum Medium, without Phenol Red containing L-glutamine and HEPES (Thermo Fisher Scientific) to a concentration of 3 μ L reagent/ 100 μ L medium. On day 1, at 70-80% confluency, cells were sub-cultured with 0.25% trypsin-EDTA (1X) and seeded on a 9.5cm² 6-well plate at a density of 0.7 x 10⁶ cells/mL. Approximately 1 μ g of DNA was incubated in 100 μ L of diluted XtremeGENE 9 DNA Transfection Reagent for 20 min. In a dropwise manner, the transfection complex was added to cells, which were then incubated for 24h at 37°C, 5% CO₂.

3.2.3 Luciferase reporter assay

On day 2, cell media was switched with serum-free media to stop cells from dividing. Cells were then re-plated on a 96-well polystyrene microplate and left alone for at least 20 min at 37°C, 5% CO₂ prior to drug treatment. Diluted drug solutions containing

tcLIGRLO, SLIGRL, and 2fLIGRLO were added to wells according to a 1:1 (volume) ratio of drug to cell solution. HBSS without drug was used as control treatment. Cells were incubated with PAR2AP or control for 24h. The concentrations of PAR2APs were chosen according to published studies (Table 1; Chapter 1.1) with these PAR2APs in HEK293 (SLIGRL, 0.3 – 300 μ M; 2fLIGRLO and tcLIGRLO, 0.1 – 100 μ M). Experiments were conducted to determine that a 24h-incubation time was sufficient to detect a drug response for PAR2. On day 3, the drug-cell media mixture was aspirated from wells and replaced with 20 μ L Glo reagent containing 108mM Tris-HCl, 42mM Tris-Base, 75mM NaCl, 3mM MgCl₂, 5mM dithiothreitol, 0.14 mg/mL D-luciferin, 1.1mM ATP, and 0.25% v/v Triton X-100 as described (Laroche & Giguère, 2019). After incubating cells with Glo reagent for 30 min at room temperature in the dark, the luciferase-generated luminescence was recorded using the Mithras LB 940 Multimode Microplate Reader (Berthold Technologies GmbH and Co. KG; Bad Wildbad, DE). Plates were read at room temperature (20°C). The dwell time on each well was 20s. Each 96-well plate contained 12 columns x 8 rows of wells. Columns contained replicate doses for drugs (up to three) and rows contained different concentrations of drug or vehicle. The sequence of measurements started with the first row and first column, then continued to the next row. The first sample read was the well containing cells treated with the highest concentration of each drug. The last sample in each row contained the control (0 drug; HBSS Ca²⁺) treated cells

3.2.4 Data and statistical analyses

Luciferase luminescence data are reported in Figures as the average luminescence of drug-treated cells relative to baseline. For each replicate sample, this calculation is: luminescence value in well divided by baseline value. The baseline for each replicate is the luminescence of cells treated with HBSS containing Ca²⁺ from the same sample as the column. Data are reported as mean \pm S.E. (error bars) for n=number of independent experiments with triplicate samples in each experiment. E_{max} values were compared by Kriskal-Wallis test followed by Dunn's post hoc. Nonlinear regression curve fits were

determined using the mean data from each group. Curves were compared between groups using F-test. * $p < 0.05$ were considered significant.

3.3 Results

3.3.1 PAR2 activation with tcLIGRLO, SLIGRL, 2fLIGRLO

We detected PAR2 activation by tcLIGRLO in the TANGO assay (Figure 16). In a pilot experiment ($n=1$), the average response of cells to $300\mu\text{M}$ SLIGRL at 12h (ratio of signal to baseline: 5 ± 1 for 3 replicates, mean \pm SD) was similar to effects shown at 24h (Figure 16; 3.1 ± 0.6 for $n=3$ with 3 replicates, mean \pm SEM). In the 24h-treatment of cells with PAR2APs SLIGRL ($n=3$), 2fLIGRLO ($n=3$), and tcLIGRLO ($n=7$) in the TANGO assay, E_{max} values did not differ between PAR2APs (Figure 16, Table 10). The rank order of potency according to EC_{50} values was: 2fLIGRLO > tcLIGRLO > SLIGRL.

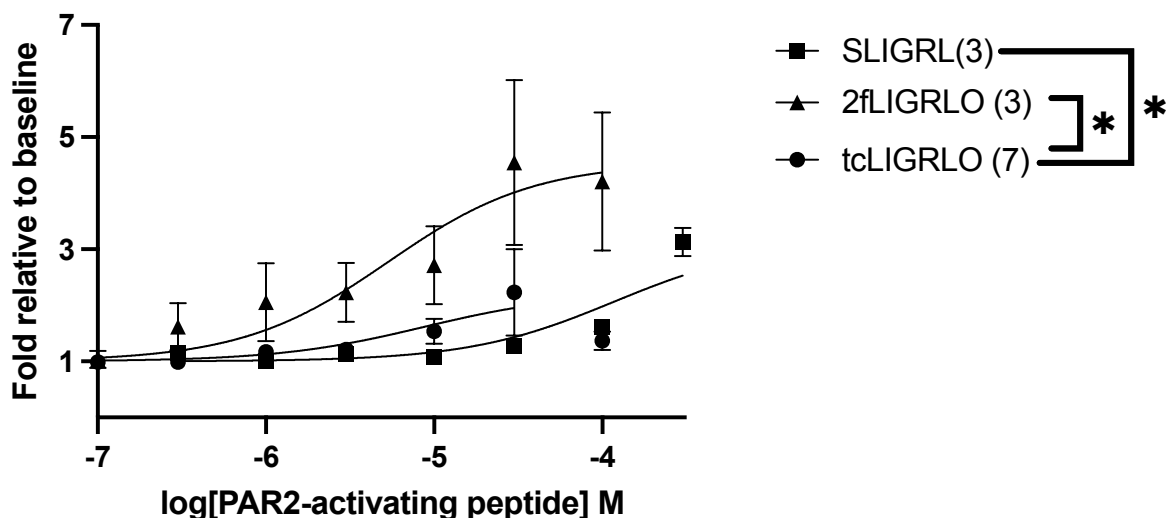


Figure 16. PAR2 activation with SLIGRL, 2fLIGRLO, and tcLIGRLO in PAR2-transfected HTLA cells using the TANGO assay.

Luminescence values to 24h-treatment with drugs were normalized against baseline luminescence values (i.e., cells treated with 1x HBSS) to get fold increase over baseline values. Nonlinear regression curve fit is shown as mean \pm S.E. (error bars). E_{\max} and pEC_{50} are provided in Table 10. E_{\max} values did not significantly differ between the three peptides ($p > 0.05$; Kriskal-Wallis). The peptide 2fLIGRLO demonstrated the highest potency, followed by a significant rightward shift by tcLIGRLO and SLIGRL (* $p < 0.05$; F-test). Numbers within parentheses beside peptide indicate number of independent experiments that were done with respective peptide.

Table 10. E_{\max} and pEC_{50} values of PAR2 activation with PAR2APs in PAR2-transfected HTLA cells in the TANGO assay

	SLIGRL ^a	2fLIGRLO ^a	tcLIGRLO ^b
$E_{\max}^{c,d}$ (%)	3.13±0.46	4.55±2.43	2.13±0.94
pEC_{50}^c (M)	3.92±0.08*	5.27±0.14*	5.06±0.14

CRCs were performed with 0.3 – 300 μ M SLIGRL and 0.1 – 100 μ M 2fLIGRLO and tcLIGRLO. n=number of independent experiments with 3 replicates each; *p<0.05 compared to tcLIGRLO, F-test.

a, n=3; b, n=7; c, mean±SEM; d, E_{\max} is maximum agonist signal relative to baseline signal (1x HBSS)

3.3.2 Effects of tcLIGRLO on CCRL2, GPR15, GPR135, and SUCNR1 expressing HTLA cells in TANGO assay

Treatment of GPR135 expressing HTLA cells with 0.3 μ M tcLIGRLO generated a two-fold increase in luminescence relative to baseline (Figure 17; * $p < 0.05$, 0.3 μ M tcLIGRLO for GPR135 vs. PAR2). This same treatment did not result in a detectable luminescence signal in PAR2 expressing HTLA cells. (Figure 17). We did not detect activation of CCRL2, GPR15, and SUCNR1 by tcLIGRLO under the conditions of the TANGO assay ($p > 0.05$).

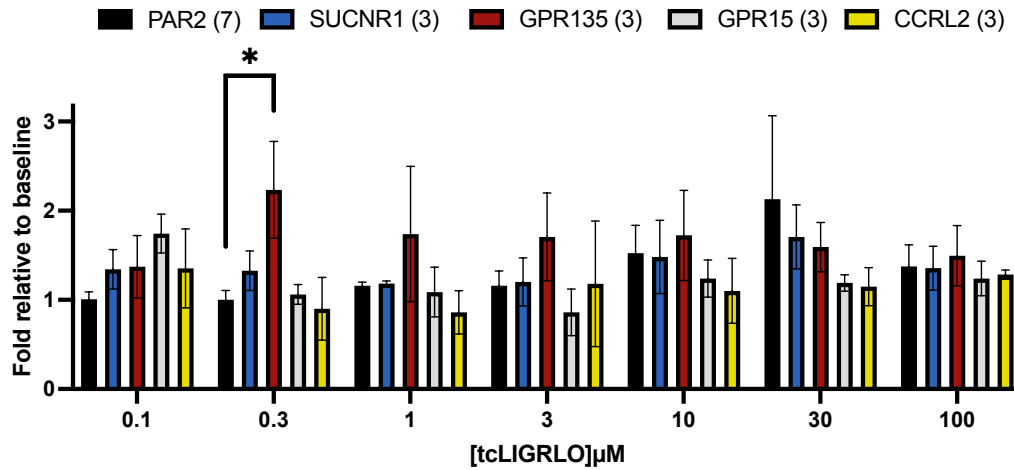


Figure 17. TANGO luminescence of tcLIGRLO treated HTLA cells-expressing PAR2, SUCNR1, GPR135, GPR15, or CCRL2.

HTLA cells expressing specific GPCR constructs as listed above, were incubated for 24h with 1x HBSS, or different doses of tcLIGRLO. Bars show the luminescence signal generated in presence of substrate (n.b. added after 24 h) relative to baseline (HBSS) as described in Methods. * $p < 0.05$; 0.3 μ M tcLIGRLO, PAR2 vs. GPR135 by one-way ANOVA and Bonferroni post hoc. Data are shown as mean \pm S.E. (error bars). Numbers within parentheses beside receptor indicate number of independent experiments that were conducted with respective receptor.

3.4 Discussion

The main finding of this study is that we detected activation of PAR2 and human GPR135 by tcLIGRLO using the TANGO assay. The results from this study will be used to explore the mechanism of vascular smooth muscle contraction by tcLIGRLO.

3.4.1 PAR2 activation with SLIGRL, 2fLIGRLO, and tcLIGRLO with the TANGO assay

Similar to the study by Thibeault & Ramachandran (2020), who found different mechanisms regulating β -arrestin interaction with PAR2 following tethered ligand (by protease) and synthetic ligand peptide-mediated activation, there may be differences in β -arrestin recruitment between the three PAR2APs. This would account for the differences exhibited by the three PAR2APs in the TANGO assay. In comparison to tcLIGRLO and SLIGRL, 2fLIGRLO is the most potent agonist out of the three peptides, with an EC_{50} value that is approximately 8 folds higher in magnitude than SLIGRL and tcLIGRLO (Table 10 and Table 1 from Chapter 1.1). We found that there was reduced luminescence signalling at $100\mu\text{M}$ tcLIGRLO, possibly due to desensitization effects (Figure 10). Hence, we showed the curve fit for tcLIGRLO as constrained within the concentration range $0.1 - 30\mu\text{M}$. Since the TANGO assay was effective for detecting PAR2 activation with ligands, testing non-peptide PAR2 ligands that have become available would be useful to exploring the structure activity relationships of PAR2 ligands in the TANGO assay.

3.4.2 β -arrestin activity with CCRL2, GPR135, GPR15, and SUCNR1

At $0.3\mu\text{M}$ tcLIGRLO, a concentration that did not activate PAR2, we detected a 2-fold increase in luminescence signal with GPR135 cells (Figure 17). We interpret this result as evidence of GPR135 as a target of tcLIGRLO. We speculate that GPR135 is the target of tcLIGRLO in vascular smooth muscle of mouse femoral arteries. In chapter 4, we expand upon these discussion points.

Chapter 4

4 Overall discussion and conclusions

4.1 Overall discussion

4.1.1 tcLIGRLO-smooth muscle contractions

YM inhibition of tcLIGRLO-induced contractions indicates a novel G_q -signalling in vascular smooth muscle of mouse femoral arteries. Discovering this novel receptor that mediates smooth muscle contractions provides another avenue for investigating smooth muscle function during the ageing process. To supplement our findings, it is suggested to look at the expression profiles of proteins mentioned in Chapter 2.4.1 following tcLIGRLO-treatment in vascular smooth muscle from aged and young mice. For instance, since there was a decreased expression of smooth muscle contraction proteins vinculin and phospho-focal-adhesion kinase 397 in aged versus young vessels from rats (Chapter 2.4.1), we can see if this interaction is present in response to tcLIGRLO in vascular smooth muscle cells from aged and young mice.

While we did not find any sex differences, establishing age as a factor that contributes to differences in tcLIGRLO-induced contractions prompts for further investigation of potential sex differences in young versus older mice. Additionally, the expression profile of this tcLIGRLO-activated receptor is not known in other tissues such as gastrointestinal- or cardiac smooth muscle. Potential expression of this tcLIGRLO-activated receptor in other tissues would imply novel roles for this receptor such as a regulator of gastric motility in the gastrointestinal tract or of ventricular contractions in the heart.

4.1.2 *In vivo* studies with tcLIGRLO and YM

A potential extension of this current work is to pursue *in vivo* studies, which could include dosing mice with tcLIGRLO and YM while measuring their effects on variables such as blood pressure and heart rate. Such *in vivo* studies would be useful to determining

the potential for tcLIGRLO and YM as potential therapeutic agents for blood vessel function. Indeed, previous studies have looked at the effects of YM *in vivo*, where they administered YM as an antithrombotic agent in rats, mice, and cynomolgus monkeys (Kawasaki et al., 2003, 2005; Uemura, Kawasaki, et al., 2006; Uemura, Takamatsu, et al., 2006b). It is important to note that while YM dose-dependently inhibited thrombus formation in all studies, there was an adverse effect of prolonged bleeding. This issue of prolonged bleeding is something to monitor in future *in vivo* studies involving tcLIGRLO and YM. In terms of YM, our study was one of the first studies to test the effects of YM inhibition on PAR2-Ca²⁺ signalling stimulated by tcLIGRLO. Previous studies, which we summarized in Chapter 1.2.3, thus far have used YM to further delineate the signalling networks of PAR2.

4.1.3 tcLIGRLO as a potential ligand for GPR135

In a ligand-independent fashion, GPR135 forms a heterodimer with melatonin receptor 2 as a method of activation (Chapter 1.3.3.2). Melatonin signalling via receptors such as melatonin receptor 2 elicits vasoconstriction in pig coronary arteries, whereas it induces vasorelaxation in pig pulmonary arteries *ex vivo* (Weekley, 1993). Melatonin does not bind to GPR135 (Oishi et al., 2017), but its function in heterodimerizing with melatonin receptor 2 presents a potential role for GPR135 in regulating vascular tone. Currently, the only known physiological role of GPR135 is it is a prominent hypermethylation site in lung and ovarian cancers (Chapter 1.3.3.2). Potentially, the absence of GPR135 activation via hypermethylation leads to aberrant melatonin signalling in certain cancers.

Considering how GPR135's only known method of activation is forming a heterodimer with melatonin receptor 2, identifying a new ligand for GPR135 would be a useful tool in delineating GPR135's role in cancer.

Based on results of screening with the TANGO assay, tcLIGRLO was a ligand for GPR135. We speculate that GPR135 is a potential target for tcLIGRLO at lower concentrations. tcLIGRLO would not be unique among ligands that activate GPCR families. Fluoxetine binds to additional receptors (e.g., SSTR3 somatostatin receptor and

σ_1 -receptor) in addition to its primary target (i.e., the serotonin receptors) (Keiser et al., 2009; Kroeze et al., 2015). We also detected luminescence signal, indicating GPCR activation by ligands using SLIGRL and 2fLIGRLO at various incubation times in PAR2-transfected HTLA cells. Similar to Kroeze et al. (2015), we found that the length of exposure to agonists in the TANGO luminescence assay affected the signalling response. Our pilot study (n=1) for SLIGRL indicated that the 12h-treatment was similar in effects to the 24h-treatment. Exposing our cells to 24h with SLIGRL and 2fLIGRLO ensured detectable signal when running assays with the two PAR2APs at the same time. Luminescence signals to these two PAR2APs were used as positive controls to compare our TANGO signal to tcLIGRLO.

4.1.4 Future directions

To further validate our findings from the TANGO assay, we recommend testing for GPR135 activation with tcLIGRLO via another method such as the bioluminescence resonance energy transfer (BRET) assay. In the BRET assay, upon β -arrestin recruitment, the donor probe attached to β -arrestin transfers energy to the acceptor probe that is fused with the receptor (Rajagopal et al., 2010; Ramachandran et al., 2009). This energy transfer results in luminescence signalling, which signifies GPCR activation (Rajagopal et al., 2010; Ramachandran et al., 2009). The difference between the TANGO and BRET assay is the TANGO assay relies on the reporter-gene expression of luciferase following the release of the transcriptional activator from the receptor, while BRET experiments rely on the receptor to β -arrestin interaction in real-time for a signal response (Rajagopal et al., 2010; Ramachandran et al., 2009). Additionally, the TANGO assay involves testing activation of non-native receptors, while BRET experiments allow for the measurement of β -arrestin recruitment to receptors in their natural cell systems. Expression of receptors in their unnatural cell environment may change properties in their downstream signalling pathways.

Another follow-up study is to investigate the potential effects of GPR135 activation on G_q/Ca^{2+} signalling. We suggest assessing for Ca^{2+} signals following tcLIGRLO-treatment

in both mouse vascular smooth muscle cells (GPR135WTs) and GPR135KOs. Absence of Ca^{2+} signalling in GPR135KO cells would provide more evidence for GPR135 as a candidate for the tcLIGRLO-activated receptor.

4.2 Conclusions

In conclusion, mouse femoral contractions elicited by tcLIGRLO did not differ by sex and present age-related effects. The downstream pathways mediating these tcLIGRLO-induced contractions involve G_q signalling. tcLIGRLO activated human PAR2 and human GPR135 in the TANGO assay. Further study of this novel G_q signalling mechanism and the identification of the tcLIGRLO-activated receptor will provide novel insight on human health and diseases in the field of vascular biology.

References

- Al-Ani, B., Saifeddine, M., Kawabata, A., & Hollenberg, M. D. (1999). Proteinase activated receptor 2: Role of extracellular loop 2 for ligand-mediated activation. *British Journal of Pharmacology*, 128(5), 1105–1113. <https://doi.org/10.1038/sj.bjp.0702834>
- Aloysius, U. I., Achike, F. I., & Mustafa, M. R. (2012). Mechanisms underlining gender differences in Phenylephrine contraction of normoglycaemic and short-term Streptozotocin-induced diabetic WKY rat aorta. *Vascular Pharmacology*, 57(2–4), 81–90. <https://doi.org/10.1016/j.vph.2011.11.009>
- Avet, C., Sturino, C., Grastilleur, S., Gouill, C. L., Semache, M., Gross, F., Gendron, L., Bennani, Y., Mancini, J. A., Sayegh, C. E., & Bouvier, M. (2020). The PAR2 inhibitor I-287 selectively targets Gα q and Gα 12/13 signaling and has anti-inflammatory effects. *Communications Biology*, 3(1), 1–13. <https://doi.org/10.1038/s42003-020-01453-8>
- Barnea, G., Strapps, W., Herrada, G., Berman, Y., Ong, J., Kloss, B., Axel, R., & Lee, K. J. (2008). The genetic design of signaling cascades to record receptor activation. *Proceedings of the National Academy of Sciences*, 105(1), 64–69. <https://doi.org/10.1073/pnas.0710487105>
- Barrios, V. E., Jarosinski, M. A., & Wright, C. D. (2003). Proteinase-activated receptor-2 mediates hyperresponsiveness in isolated guinea pig bronchi. *Biochemical Pharmacology*, 66(3), 519–525. [https://doi.org/10.1016/S0006-2952\(03\)00292-2](https://doi.org/10.1016/S0006-2952(03)00292-2)
- Bernatowicz, M. S., Klimas, C. E., Hartl, K. S., Peluso, M., Allegretto, N. J., & Seiler, S. M. (1996). Development of Potent Thrombin Receptor Antagonist Peptides. *Journal of Medicinal Chemistry*, 39(25), 4879–4887. <https://doi.org/10.1021/jm960455s>
- Bhavanasi, D., Kim, S., Goldfinger, L. E., & Kunapuli, S. P. (2011). Protein Kinase Cδ mediates the activation of Protein Kinase D2 in Platelets. *Biochemical Pharmacology*, 82(7), 720–727. <https://doi.org/10.1016/j.bcp.2011.06.032>
- Biber, K., Zuurman, M. W., Homan, H., & Boddeke, H. W. G. M. (2003). Expression of L-CCR in HEK 293 cells reveals functional responses to CCL2, CCL5, CCL7, and CCL8. *Journal of Leukocyte Biology*, 74(2), 243–251. <https://doi.org/10.1189/jlb.0802415>
- Björling, K., Joseph, P. D., Egebjerg, K., Salomonsson, M., Hansen, J. L., Ludvigsen, T. P., & Jensen, L. J. (2018). Role of age, Rho-kinase 2 expression, and G protein-mediated signaling in the myogenic response in mouse small mesenteric arteries. *Physiological Reports*, 6(17), e13863. <https://doi.org/10.14814/phy2.13863>

- Brandes, R. P., Fleming, I., & Busse, R. (2005). Endothelial aging. *Cardiovascular Research*, 66(2), 286–294. <https://doi.org/10.1016/j.cardiores.2004.12.027>
- Brown, A. J., Goldsworthy, S. M., Barnes, A. A., Eilert, M. M., Tcheang, L., Daniels, D., Muir, A. I., Wigglesworth, M. J., Kinghorn, I., Fraser, N. J., Pike, N. B., Strum, J. C., Steplewski, K. M., Murdock, P. R., Holder, J. C., Marshall, F. H., Szekeres, P. G., Wilson, S., Ignar, D. M., ... Dowell, S. J. (2003). The Orphan G Protein-coupled Receptors GPR41 and GPR43 Are Activated by Propionate and Other Short Chain Carboxylic Acids. *Journal of Biological Chemistry*, 278(13), 11312–11319. <https://doi.org/10.1074/jbc.M211609200>
- Bynagari, Y. S., Nagy, B., Tuluc, F., Bhavaraju, K., Kim, S., Vijayan, K. V., & Kunapuli, S. P. (2009). Mechanism of Activation and Functional Role of Protein Kinase C η in Human Platelets. *The Journal of Biological Chemistry*, 284(20), 13413–13421. <https://doi.org/10.1074/jbc.M808970200>
- Campbell, A. P., & Smrcka, A. V. (2018). Targeting G protein-coupled receptor signalling by blocking G proteins. *Nature Reviews. Drug Discovery*, 17(11), 789–803. <https://doi.org/10.1038/nrd.2018.135>
- Canals, M., Jenkins, L., Kellett, E., & Milligan, G. (2006). Up-regulation of the Angiotensin II Type 1 Receptor by the MAS Proto-oncogene Is Due to Constitutive Activation of Gq/G11 by MAS. *Journal of Biological Chemistry*, 281(24), 16757–16767. <https://doi.org/10.1074/jbc.M601121200>
- Cardenas, H., Vieth, E., Lee, J., Segar, M., Liu, Y., Nephew, K. P., & Matei, D. (2014). TGF- β induces global changes in DNA methylation during the epithelial-to-mesenchymal transition in ovarian cancer cells. *Epigenetics*, 9(11), 1461. <https://doi.org/10.4161/15592294.2014.971608>
- Cerione, R. A., Sibley, D. R., Codina, J., Benovic, J. L., Winslow, J., Neer, E. J., Birnbaumer, L., Caron, M. G., & Lefkowitz, R. J. (1984). Reconstitution of a hormone-sensitive adenylate cyclase system. The pure beta-adrenergic receptor and guanine nucleotide regulatory protein confer hormone responsiveness on the resolved catalytic unit. *Journal of Biological Chemistry*, 259(16), 9979–9982. [https://doi.org/10.1016/S0021-9258\(18\)90913-0](https://doi.org/10.1016/S0021-9258(18)90913-0)
- Compton, S. J., Cairns, J. A., Palmer, K.-J., Al-Ani, B., Hollenberg, M. D., & Walls, A. F. (2000). A Polymorphic Protease-activated Receptor 2 (PAR2) Displaying Reduced Sensitivity to Trypsin and Differential Responses to PAR Agonists. *Journal of Biological Chemistry*, 275(50), 39207–39212. <https://doi.org/10.1074/jbc.M007215200>

- Coughlin, S. R., Vu, T. K., Hung, D. T., & Wheaton, V. I. (1992). Characterization of a functional thrombin receptor. Issues and opportunities. *Journal of Clinical Investigation*, 89(2), 351–355.
- Duca, L., Blaise, S., Romier, B., Laffargue, M., Gayral, S., El Btaouri, H., Kawecki, C., Guillot, A., Martiny, L., Debelle, L., & Maurice, P. (2016). Matrix ageing and vascular impacts: Focus on elastin fragmentation. *Cardiovascular Research*, 110(3), 298–308. <https://doi.org/10.1093/cvr/cvw061>
- Feld, M., Shpacovitch, V., Ehrhardt, C., Fastrich, M., Goerge, T., Ludwig, S., & Steinhoff, M. (2013). Proteinase-Activated Receptor-2 Agonist Activates Anti-Influenza Mechanisms and Modulates IFN γ -Induced Antiviral Pathways in Human Neutrophils. *BioMed Research International*, 2013, 879080. <https://doi.org/10.1155/2013/879080>
- Fredriksson, R., Lagerström, M. C., Lundin, L.-G., & Schiöth, H. B. (2003). The G-Protein-Coupled Receptors in the Human Genome Form Five Main Families. Phylogenetic Analysis, Paralogon Groups, and Fingerprints. *Molecular Pharmacology*, 63(6), 1256–1272. <https://doi.org/10.1124/mol.63.6.1256>
- Goh, F. G., Ng, P. Y., Nilsson, M., Kanke, T., & Plevin, R. (2009). Dual effect of the novel peptide antagonist K-14585 on proteinase-activated receptor-2-mediated signalling. *British Journal of Pharmacology*, 158(7), 1695–1704. <https://doi.org/10.1111/j.1476-5381.2009.00415.x>
- Greenwald, S. E. (2007). Ageing of the conduit arteries. *The Journal of Pathology*, 211(2), 157–172. <https://doi.org/10.1002/path.2101>
- Han, S.-W., Tae, J., Kim, J.-A., Kim, D.-K., Seo, G.-S., Yun, K.-J., Choi, S.-C., Kim, T.-H., Nah, Y.-H., & Lee, Y.-M. (2003). The aqueous extract of *Solanum melongena* inhibits PAR2 agonist-induced inflammation. *Clinica Chimica Acta*, 328(1–2), 39–44. [https://doi.org/10.1016/S0009-8981\(02\)00377-7](https://doi.org/10.1016/S0009-8981(02)00377-7)
- Hartmann, T. N., Leick, M., Ewers, S., Diefenbacher, A., Schraufstatter, I., Honczarenko, M., & Burger, M. (2008). Human B cells express the orphan chemokine receptor CCR4-1 in a maturation-stage-dependent and CCR5-modulated manner. *Immunology*, 125(2), 252–262. <https://doi.org/10.1111/j.1365-2567.2008.02836.x>
- Hauser, A. S., Attwood, M. M., Rask-Andersen, M., Schiöth, H. B., & Gloriam, D. E. (2017). Trends in GPCR drug discovery: New agents, targets and indications. *Nature Reviews Drug Discovery*, 16(12), 829–842. <https://doi.org/10.1038/nrd.2017.178>

- Hauser, A. S., Gloriam, D. E., Bräuner-Osborne, H., & Foster, S. R. (2020). Novel approaches leading towards peptide GPCR de-orphanisation. *British Journal of Pharmacology*, 177(5), 961–968. <https://doi.org/10.1111/bph.14950>
- He, W., Miao, F. J.-P., Lin, D. C.-H., Schwandner, R. T., Wang, Z., Gao, J., Chen, J.-L., Tian, H., & Ling, L. (2004). Citric acid cycle intermediates as ligands for orphan G-protein-coupled receptors. *Nature*, 429(6988), 188–193. <https://doi.org/10.1038/nature02488>
- Hermes, C., König, G. M., & Crüsemann, M. (2021). The chromodepsins – chemistry, biology and biosynthesis of a selective Gq inhibitor natural product family. *Natural Product Reports*, 10.1039/D1NP00005E. <https://doi.org/10.1039/D1NP00005E>
- Herrera, M. D., Mingorance, C., Rodríguez-Rodríguez, R., & Alvarez de Sotomayor, M. (2010). Endothelial dysfunction and aging: An update. *Ageing Research Reviews*, 9(2), 142–152. <https://doi.org/10.1016/j.arr.2009.07.002>
- Heuss, C., Scanziani, M., Gähwiler, B. H., & Gerber, U. (1999). G-protein-independent signaling mediated by metabotropic glutamate receptors. *Nature Neuroscience*, 2(12), 1070–1077. <https://doi.org/10.1038/15996>
- Hira, T., Maekawa, T., Asano, K., & Hara, H. (2009). Cholecystokinin secretion induced by β -conglycinin peptone depends on G α_q -mediated pathways in enteroendocrine cells. *European Journal of Nutrition*, 48(2), 124–127. <https://doi.org/10.1007/s00394-008-0764-1>
- Hisano, K., Kawase, S., Mimura, T., Yoshida, H., Yamada, H., Haniu, H., Tsukahara, T., Kurihara, T., Matsuda, Y., Saito, N., & Uemura, T. (2021). Structurally different lysophosphatidylethanolamine species stimulate neurite outgrowth in cultured cortical neurons via distinct G-protein-coupled receptors and signaling cascades. *Biochemical and Biophysical Research Communications*, 534, 179–185. <https://doi.org/10.1016/j.bbrc.2020.11.119>
- Hisaoka-Nakashima, K., Yokoe, T., Watanabe, S., Nakamura, Y., Kajitani, N., Okada-Tsuchioka, M., Takebayashi, M., Nakata, Y., & Morioka, N. (2020). Lysophosphatidic acid induces thrombospondin-1 production in primary cultured rat cortical astrocytes. *Journal of Neurochemistry*, n/a(n/a), 1–16. <https://doi.org/10.1111/jnc.15227>
- Hollenberg, M. D., Mihara, K., Polley, D., Suen, J. Y., Han, A., Fairlie, D. P., & Ramachandran, R. (2014). Biased signalling and proteinase-activated receptors (PARs): Targeting inflammatory disease. *British Journal of Pharmacology*, 171(5), 1180–1194. <https://doi.org/10.1111/bph.12544>

- Hollenberg, M. D., Renaux, B., Hyun, E., Houle, S., Vergnolle, N., Saifeddine, M., & Ramachandran, R. (2008). Derivatized 2-Furoyl-LIGRLO-amide, a Versatile and Selective Probe for Proteinase-Activated Receptor 2: Binding and Visualization. *Journal of Pharmacology and Experimental Therapeutics*, 326(2), 453–462. <https://doi.org/10.1124/jpet.108.136432>
- Kagota, S., Maruyama, K., & McGuire, J. J. (2016). Characterization and Functions of Protease-Activated Receptor 2 in Obesity, Diabetes, and Metabolic Syndrome: A Systematic Review. *BioMed Research International*, 2016, e3130496. <https://doi.org/10.1155/2016/3130496>
- Kamato, D., Mitra, P., Davis, F., Osman, N., Chaplin, R., Cabot, P. J., Afroz, R., Thomas, W., Zheng, W., Kaur, H., Brimble, M., & Little, P. J. (2017). Gq proteins: Molecular pharmacology and therapeutic potential. *Cellular and Molecular Life Sciences*, 74(8), 1379–1390. <https://doi.org/10.1007/s00018-016-2405-9>
- Kamato, D., Thach, L., Bernard, R., Chan, V., Zheng, W., Kaur, H., Brimble, M., Osman, N., & Little, P. J. (2015). Structure, Function, Pharmacology, and Therapeutic Potential of the G Protein, Gα/q,11. *Frontiers in Cardiovascular Medicine*, 2, 14. <https://doi.org/10.3389/fcvm.2015.00014>
- Kaur, H., Harris, P. W. R., Little, P. J., & Brimble, M. A. (2015). Total Synthesis of the Cyclic Dipeptide YM-280193, a Platelet Aggregation Inhibitor. *Organic Letters*, 17(3), 492–495. <https://doi.org/10.1021/ol503507g>
- Kawasaki, T., Taniguchi, M., Moritani, Y., Hayashi, K., Saito, T., Takasaki, J., Nagai, K., Inagaki, O., & Shikama, H. (2003). Antithrombotic and thrombolytic efficacy of YM-254890, a Gq/11 inhibitor, in a rat model of arterial thrombosis. *Thrombosis and Haemostasis*, 90(09), 406–413. <https://doi.org/10.1160/TH03-02-0115>
- Kawasaki, T., Taniguchi, M., Moritani, Y., Uemura, T., Shigenaga, T., Takamatsu, H., Hayashi, K., Takasaki, J., Saito, T., & Nagai, K. (2005). Pharmacological properties of YM-254890, a specific Gαq/11 inhibitor, on thrombosis and neointima formation in mice. *Thrombosis and Haemostasis*, 94(07), 184–192. <https://doi.org/10.1160/TH04-09-0635>
- Keiser, M. J., Setola, V., Irwin, J. J., Laggner, C., Abbas, A. I., Hufeisen, S. J., Jensen, N. H., Kuijter, M. B., Matos, R. C., Tran, T. B., Whaley, R., Glennon, R. A., Hert, J., Thomas, K. L. H., Edwards, D. D., Shoichet, B. K., & Roth, B. L. (2009). Predicting new molecular targets for known drugs. *Nature*, 462(7270), 175–181. <https://doi.org/10.1038/nature08506>
- Kettunen, E., Hernandez-Vargas, H., Cros, M.-P., Durand, G., Calvez-Kelm, F. L., Stuoelyte, K., Jarmalaite, S., Salmenkivi, K., Anttila, S., Wolff, H., Herceg, Z., & Husgafvel-Pursiainen, K. (2017). Asbestos-associated genome-wide DNA

- methylation changes in lung cancer. *International Journal of Cancer*, 141(10), 2014–2029. <https://doi.org/10.1002/ijc.30897>
- Keung, W., Vanhoutte, P. M., & Man, R. Y. K. (2005). Nongenomic responses to 17 β -estradiol in male rat mesenteric arteries abolish intrinsic gender differences in vascular responses. *British Journal of Pharmacology*, 146(8), 1148–1155. <https://doi.org/10.1038/sj.bjp.0706422>
- Kikkawa, Y., Kameda, K., Hirano, M., Sasaki, T., & Hirano, K. (2010a). Impaired feedback regulation of the receptor activity and the myofilament Ca²⁺ sensitivity contributes to increased vascular reactivity after subarachnoid hemorrhage. *Journal of Cerebral Blood Flow and Metabolism*, 30(9), 1637–1650. <https://doi.org/10.1038/jcbfm.2010.35>
- Kikkawa, Y., Kameda, K., Hirano, M., Sasaki, T., & Hirano, K. (2010b). Impaired feedback regulation of the receptor activity and the myofilament Ca²⁺ sensitivity contributes to increased vascular reactivity after subarachnoid hemorrhage. *Journal of Cerebral Blood Flow and Metabolism: Official Journal of the International Society of Cerebral Blood Flow and Metabolism*, 30(9), 1637–1650. <https://doi.org/10.1038/jcbfm.2010.35>
- Kjelsberg, M. A., Cotecchia, S., Ostrowski, J., Caron, M. G., & Lefkowitz, R. J. (1992). Constitutive activation of the alpha 1B-adrenergic receptor by all amino acid substitutions at a single site. Evidence for a region which constrains receptor activation. *Journal of Biological Chemistry*, 267(3), 1430–1433. [https://doi.org/10.1016/S0021-9258\(18\)45962-5](https://doi.org/10.1016/S0021-9258(18)45962-5)
- Kobilka, B. K., Kobilka, T. S., Daniel, K., Regan, J. W., Caron, M. G., & Lefkowitz, R. J. (1988). Chimeric alpha 2-,beta 2-adrenergic receptors: Delineation of domains involved in effector coupling and ligand binding specificity. *Science*, 240(4857), 1310–1316. <https://doi.org/10.1126/science.2836950>
- Kostenis, E., Pfeil, E. M., & Annala, S. (2020). Heterotrimeric Gq proteins as therapeutic targets? *The Journal of Biological Chemistry*, 295(16), 5206–5215. <https://doi.org/10.1074/jbc.REV119.007061>
- Kotarsky, K., & Nilsson, N. E. (2004). Reverse pharmacology and the de-orphanization of 7TM receptors. *Drug Discovery Today: Technologies*, 1(2), 99–104. <https://doi.org/10.1016/j.ddtec.2004.07.003>
- Kroeze, W. K., Sassano, M. F., Huang, X.-P., Lansu, K., McCorvy, J. D., Giguere, P. M., Sciaky, N., & Roth, B. L. (2015). PRESTO-TANGO: An open-source resource for interrogation of the druggable human GPCR-ome. *Nature Structural & Molecular Biology*, 22(5), 362–369. <https://doi.org/10.1038/nsmb.3014>

- Laroche, G., & Giguère, P. M. (2019). Measurement of β -Arrestin Recruitment at GPCRs Using the Tango Assay. In M. Tiberi (Ed.), *G Protein-Coupled Receptor Signaling: Methods and Protocols* (pp. 257–267). Springer.
https://doi.org/10.1007/978-1-4939-9121-1_14
- Leick, M., Catusse, J., Follo, M., Nibbs, R. J., Hartmann, T. N., Veelken, H., & Burger, M. (2010). CCL19 is a specific ligand of the constitutively recycling atypical human chemokine receptor CCR4-B. *Immunology*, 129(4), 536–546.
<https://doi.org/10.1111/j.1365-2567.2009.03209.x>
- Li, J., Ge, Y., Huang, J.-X., Strømgaard, K., Zhang, X., & Xiong, X.-F. (2020). Heterotrimeric G Proteins as Therapeutic Targets in Drug Discovery. *Journal of Medicinal Chemistry*, 63(10), 5013–5030.
<https://doi.org/10.1021/acs.jmedchem.9b01452>
- Lin, S., & Civelli, O. (2004). Orphan G protein-coupled receptors: Targets for new therapeutic interventions. *Annals of Medicine*, 36(3), 204–214.
<https://doi.org/10.1080/07853890310024668>
- Liu, Q.-F., Yu, H.-W., Sun, L.-L., You, L., Tao, G.-Z., & Qu, B.-Z. (2015). Apelin-13 upregulates Egr-1 expression in rat vascular smooth muscle cells through the PI3K/Akt and PKC signaling pathways. *Biochemical and Biophysical Research Communications*, 468(4), 617–621. <https://doi.org/10.1016/j.bbrc.2015.10.171>
- Lorenz, W., Lomansey, J. W., Collins, S., Regan, J. W., Caron, M. G., & Lefkowitz, R. J. (1990). Expression of three α 2-adrenergic receptor subtypes in rat tissues: Implications for α 2 receptor classification. *Molecular Pharmacology*, 38, 599–603.
- Luttrell, L. M., Ferguson, S. S., Daaka, Y., Miller, W. E., Maudsley, S., Della Rocca, G. J., Lin, F., Kawakatsu, H., Owada, K., Luttrell, D. K., Caron, M. G., & Lefkowitz, R. J. (1999). Beta-arrestin-dependent formation of beta2 adrenergic receptor-Src protein kinase complexes. *Science (New York, N.Y.)*, 283(5402), 655–661.
<https://doi.org/10.1126/science.283.5402.655>
- McGuire, J. (2004). Proteinase-Activated Receptor 2 (PAR2): A Challenging New Target for Treatment of Vascular Diseases. *Current Pharmaceutical Design*, 10(22), 2769–2778. <https://doi.org/10.2174/1381612043383656>
- McGuire, J. J., Dai, J., Andrade-Gordon, P., Triggle, C. R., & Hollenberg, M. D. (2002a). Proteinase-activated receptor-2 (PAR2): Vascular effects of a PAR2-derived activating peptide via a receptor different than PAR2. *Journal of Pharmacology and Experimental Therapeutics*, 303(3), 985–992.
<https://doi.org/10.1124/jpet.102.040352>

- McGuire, J. J., Dai, J., Andrade-Gordon, P., Triggle, C. R., & Hollenberg, M. D. (2002b). Proteinase-Activated Receptor-2 (PAR2): Vascular Effects of a PAR2-Derived Activating Peptide via a Receptor Different than PAR2. *Journal of Pharmacology and Experimental Therapeutics*, 303(3), 985–992. <https://doi.org/10.1124/jpet.102.040352>
- McGuire, J. J., Saifeddine, M., Triggle, C. R., Sun, K., & Hollenberg, M. D. (2004). 2-Furoyl-LIGRLO-amide: A Potent and Selective Proteinase-Activated Receptor 2 Agonist. *Journal of Pharmacology and Experimental Therapeutics*, 309(3), 1124–1131. <https://doi.org/10.1124/jpet.103.064584>
- McNeill, A. M., Zhang, C., Stanczyk, F. Z., Duckles, S. P., & Krause, D. N. (2002). Estrogen Increases Endothelial Nitric Oxide Synthase via Estrogen Receptors in Rat Cerebral Blood Vessels. *Stroke*, 33(6), 1685–1691. <https://doi.org/10.1161/01.STR.0000016325.54374.93>
- Meder, W., Wendland, M., Busmann, A., Kutzleb, C., Spodsberg, N., John, H., Richter, R., Schleuder, D., Meyer, M., & Forssmann, W. G. (2003). Characterization of human circulating TIG2 as a ligand for the orphan receptor ChemR23. *FEBS Letters*, 555(3), 495–499. [https://doi.org/10.1016/S0014-5793\(03\)01312-7](https://doi.org/10.1016/S0014-5793(03)01312-7)
- Meleka, M. M., Edwards, A. J., Xia, J., Dahlen, S. A., Mohanty, I., Medcalf, M., Aggarwal, S., Moeller, K. D., Mortensen, O. V., & Osei-Owusu, P. (2019). Anti-hypertensive mechanisms of cyclic depsipeptide inhibitor ligands for Gq/11 class G proteins. *Pharmacological Research*, 141, 264–275. <https://doi.org/10.1016/j.phrs.2019.01.012>
- Migeotte, I., Franssen, J.-D., Goriely, S., Willems, F., & Parmentier, M. (2002). Distribution and regulation of expression of the putative human chemokine receptor HCR in leukocyte populations. *European Journal of Immunology*, 32(2), 494–501. [https://doi.org/10.1002/1521-4141\(200202\)32:2<494::AID-IMMU494>3.0.CO;2-Y](https://doi.org/10.1002/1521-4141(200202)32:2<494::AID-IMMU494>3.0.CO;2-Y)
- Mihara, K., Ramachandran, R., Saifeddine, M., Hansen, K. K., Renaux, B., Polley, D., Gibson, S., Vanderboor, C., & Hollenberg, M. D. (2016). Thrombin-Mediated Direct Activation of Proteinase-Activated Receptor-2: Another Target for Thrombin Signaling. *Molecular Pharmacology*, 89(5), 606–614. <https://doi.org/10.1124/mol.115.102723>
- Mizuno, N., Abe, K., Morishita, Y., Yamashita, S., Segawa, R., Dong, J., Moriya, T., Hiratsuka, M., & Hirasawa, N. (2017). Pentanoic acid induces thymic stromal lymphopoietin production through Gq/11 and Rho-associated protein kinase signaling pathway in keratinocytes. *International Immunopharmacology*, 50, 216–223. <https://doi.org/10.1016/j.intimp.2017.06.024>

- Mizuno, N., & Itoh, H. (2009). Functions and Regulatory Mechanisms of Gq-Signaling Pathways. *Neurosignals*, 17(1), 42–54. <https://doi.org/10.1159/000186689>
- Mulvany, M. J., & Halpern, W. (1976). Mechanical properties of vascular smooth muscle cells in situ. *Nature*, 260(5552), 617–619. <https://doi.org/10.1038/260617a0>
- Nagy, B., Jr, Bhavaraju, K., Getz, T., Bynagari, Y. S., Kim, S., & Kunapuli, S. P. (2009). Impaired activation of platelets lacking protein kinase C- θ isoform. *Blood*, 113(11), 2557–2567. <https://doi.org/10.1182/blood-2008-07-169268>
- Nelson, G., Chandrashekar, J., Hoon, M. A., Feng, L., Zhao, G., Ryba, N. J. P., & Zuker, C. S. (2002). An amino-acid taste receptor. *Nature*, 416(6877), 199–202. <https://doi.org/10.1038/nature726>
- Ngo, T., Kufareva, I., Coleman, J. L., Graham, R. M., Abagyan, R., & Smith, N. J. (2016). Identifying ligands at orphan GPCRs: Current status using structure-based approaches. *British Journal of Pharmacology*, 173(20), 2934–2951. <https://doi.org/10.1111/bph.13452>
- Nguyen, L. P., Pan, J., Dinh, T. T., Hadeiba, H., O'Hara, E., Ebtikar, A., Hertweck, A., Gökmen, M. R., Lord, G. M., Jenner, R. G., Butcher, E. C., & Habtezion, A. (2015). Role and species-specific expression of colon T cell homing receptor GPR15 in colitis. *Nature Immunology*, 16(2), 207–213. <https://doi.org/10.1038/ni.3079>
- Niu, Q.-X., Chen, H.-Q., Chen, Z.-Y., Fu, Y.-L., Lin, J.-L., & He, S.-H. (2008). Induction of Inflammatory Cytokine Release from Human Umbilical Vein Endothelial Cells by Agonists of Proteinase-Activated Receptor-2. *Clinical and Experimental Pharmacology and Physiology*, 35(1), 89–96. <https://doi.org/10.1111/j.1440-1681.2007.04755.x>
- Novella, S., Dantas, A. P., Segarra, G., Medina, P., & Hermenegildo, C. (2012). Vascular Aging in Women: Is Estrogen the Fountain of Youth? *Frontiers in Physiology*, 3, 165. <https://doi.org/10.3389/fphys.2012.00165>
- Novensà, L., Novella, S., Medina, P., Segarra, G., Castillo, N., Heras, M., Hermenegildo, C., & Dantas, A. P. (2011). Aging Negatively Affects Estrogens-Mediated Effects on Nitric Oxide Bioavailability by Shifting ER α /ER β Balance in Female Mice. *PLoS ONE*, 6(9), e25335. <https://doi.org/10.1371/journal.pone.0025335>
- O'Dowd, B. F., Hnatowich, M., Regan, J. W., Leader, W. M., Caron, M. G., & Lefkowitz, R. J. (1988). Site-directed mutagenesis of the cytoplasmic domains of the human beta 2-adrenergic receptor. Localization of regions involved in G protein-receptor coupling. *Journal of Biological Chemistry*, 263(31), 15985–15992. [https://doi.org/10.1016/S0021-9258\(18\)37546-X](https://doi.org/10.1016/S0021-9258(18)37546-X)

- Oishi, A., Karamitri, A., Gerbier, R., Lahuna, O., Ahmad, R., & Jockers, R. (2017). Orphan GPR61, GPR62 and GPR135 receptors and the melatonin MT2 receptor reciprocally modulate their signaling functions. *Scientific Reports*, 7, 8990. <https://doi.org/10.1038/s41598-017-08996-7>
- Ostrowski, J., Kjelsberg, M. A., Caron, M. G., & Lefkowitz, R. J. (1992). Mutagenesis of the β 2-adrenergic receptor: How structure elucidates function. *Annual Reviews Pharmacology and Toxicology*, 32, 167–183.
- Otero, K., Vecchi, A., Hirsch, E., Kearley, J., Vermi, W., Del Prete, A., Gonzalvo-Feo, S., Garlanda, C., Azzolino, O., Salogni, L., Lloyd, C. M., Facchetti, F., Mantovani, A., & Sozzani, S. (2010). Non-redundant role of CCRL2 in lung dendritic cell trafficking. *Blood*, 116(16), 2942–2949. <https://doi.org/10.1182/blood-2009-12-259903>
- Pan, B., Wang, X., Nishioka, C., Honda, G., Yokoyama, A., Zeng, L., Xu, K., & Ikezoe, T. (2017). G-protein coupled receptor 15 mediates angiogenesis and cytoprotective function of thrombomodulin. *Scientific Reports*, 7, 692. <https://doi.org/10.1038/s41598-017-00781-w>
- Pierce, K. L., Premont, R. T., & Lefkowitz, R. J. (2002). Seven-transmembrane receptors. *Nature Reviews Molecular Cell Biology*, 3(9), 639–650. <https://doi.org/10.1038/nrm908>
- Rajagopal, S., Rajagopal, K., & Lefkowitz, R. J. (2010). Teaching old receptors new tricks: Biasing seven-transmembrane receptors. *Nature Reviews Drug Discovery*, 9(5), 373–386. <https://doi.org/10.1038/nrd3024>
- Ramachandran, R., Mihara, K., Mathur, M., Rochdi, M. D., Bouvier, M., DeFea, K., & Hollenberg, M. D. (2009). Agonist-Biased Signaling via Proteinase Activated Receptor-2: Differential Activation of Calcium and Mitogen-Activated Protein Kinase Pathways. *Molecular Pharmacology*, 76(4), 791–801. <https://doi.org/10.1124/mol.109.055509>
- Ramachandran, R., Noorbakhsh, F., DeFea, K., & Hollenberg, M. D. (2012). Targeting proteinase-activated receptors: Therapeutic potential and challenges. *Nature Reviews Drug Discovery*, 11(1), 69–86. <https://doi.org/10.1038/nrd3615>
- Reinscheid, R. K., Nothacker, H.-P., Bourson, A., Ardati, A., Henningsen, R. A., Bunzow, J. R., Grandy, D. K., Langen, H., Monsma, F. J., & Civelli, O. (1995). Orphanin FQ: A Neuropeptide That Activates an Opioidlike G Protein-Coupled Receptor. *Science*, 270(5237), 792–794. <https://doi.org/10.1126/science.270.5237.792>

- Robben, J. H., Fenton, R. A., Vargas, S. L., Schweer, H., Peti-Peterdi, J., Deen, P. M. T., & Milligan, G. (2009). Localization of the succinate receptor in the distal nephron and its signaling in polarized MDCK cells. *Kidney International*, 76(12), 1258–1267. <https://doi.org/10.1038/ki.2009.360>
- Saifeddine, M., Roy, S. S., Al-Ani, B., Triggle, C. R., & Hollenberg, M. D. (1998). Endothelium-dependent contractile actions of proteinase-activated receptor-2-activating peptides in human umbilical vein: Release of a contracting factor via a novel receptor. *British Journal of Pharmacology*, 125(7), 1445–1454. <https://doi.org/10.1038/sj.bjp.0702213>
- Samama, P., Cotecchia, S., Costa, T., & Lefkowitz, R. J. (1993). A mutation-induced activated state of the beta 2-adrenergic receptor. Extending the ternary complex model. *Journal of Biological Chemistry*, 268(7), 4625–4636. [https://doi.org/10.1016/S0021-9258\(18\)53442-6](https://doi.org/10.1016/S0021-9258(18)53442-6)
- Sanjana, N. E., Shalem, O., & Zhang, F. (2014). Improved vectors and genome-wide libraries for CRISPR screening. *Nature Methods*, 11(8), 783–784. <https://doi.org/10.1038/nmeth.3047>
- Schmidlin, F., Amadesi, S., Dabbagh, K., Lewis, D. E., Knott, P., Bunnett, N. W., Gater, P. R., Geppetti, P., Bertrand, C., & Stevens, M. E. (2002). Protease-Activated Receptor 2 Mediates Eosinophil Infiltration and Hyperreactivity in Allergic Inflammation of the Airway. *The Journal of Immunology*, 169(9), 5315–5321. <https://doi.org/10.4049/jimmunol.169.9.5315>
- Schnitzler, M. M. y, Storch, U., & Gudermann, T. (2016). Mechanosensitive Gq/11 Protein–Coupled Receptors Mediate Myogenic Vasoconstriction. *Microcirculation*, 23(8), 621–625. <https://doi.org/10.1111/micc.12293>
- Seawright, J. W., Sreenivasappa, H., Gibbs, H. C., Padgham, S., Shin, S. Y., Chaponnier, C., Yeh, A. T., Trzeciakowski, J. P., Woodman, C. R., & Trache, A. (2018). Vascular Smooth Muscle Contractile Function Declines With Age in Skeletal Muscle Feed Arteries. *Frontiers in Physiology*, 9, 856. <https://doi.org/10.3389/fphys.2018.00856>
- Seawright, J. W., Trache, A., Wilson, E., & Woodman, C. R. (2016). Short-duration increases in intraluminal pressure improve vasoconstrictor responses in aged skeletal muscle feed arteries. *European Journal of Applied Physiology*, 116(5), 931–937. <https://doi.org/10.1007/s00421-016-3350-x>
- Sehgel, N. L., Vatner, S. F., & Meininger, G. A. (2015). “Smooth Muscle Cell Stiffness Syndrome”—Revisiting the Structural Basis of Arterial Stiffness. *Frontiers in Physiology*, 6, 335. <https://doi.org/10.3389/fphys.2015.00335>

- Shalem, O., Sanjana, N. E., Hartenian, E., Shi, X., Scott, D. A., Mikkelsen, T., Heckl, D., Ebert, B. L., Root, D. E., Doench, J. G., & Zhang, F. (2014). Genome-Scale CRISPR-Cas9 Knockout Screening in Human Cells. *Science (New York, N.Y.)*, 343(6166), 84–87. <https://doi.org/10.1126/science.1247005>
- Shpacovitch, V. M., Seeliger, S., Huber-Lang, M., Balkow, S., Feld, M., Hollenberg, M. D., Sarma, V. J., Ward, P. A., Strey, A., Gerke, V., Sommerhoff, C. P., Vergnolle, N., & Steinhoff, M. (2007). Agonists of proteinase-activated receptor-2 affect transendothelial migration and apoptosis of human neutrophils. *Experimental Dermatology*, 16(10), 799–806. <https://doi.org/10.1111/j.1600-0625.2007.00605.x>
- Shpacovitch, V. M., Varga, G., Strey, A., Gunzer, M., Mooren, F., Buddenkotte, J., Vergnolle, N., Sommerhoff, C. P., Grabbe, S., Gerke, V., Homey, B., Hollenberg, M., Luger, T. A., & Steinhoff, M. (2004). Agonists of proteinase-activated receptor-2 modulate human neutrophil cytokine secretion, expression of cell adhesion molecules, and migration within 3-D collagen lattices. *Journal of Leukocyte Biology*, 76(2), 388–398. <https://doi.org/10.1189/jlb.0503221>
- Shukla, A. K., Xiao, K., & Lefkowitz, R. J. (2011). Emerging paradigms of β -arrestin-dependent seven transmembrane receptor signaling. *Trends in Biochemical Sciences*, 36(9), 457. <https://doi.org/10.1016/j.tibs.2011.06.003>
- Sriram, K., & Insel, P. A. (2018). G Protein-Coupled Receptors as Targets for Approved Drugs: How Many Targets and How Many Drugs? *Molecular Pharmacology*, 93(4), 251–258. <https://doi.org/10.1124/mol.117.111062>
- Stenton, G. R., Nohara, O., Déry, R. E., Vliagoftis, H., Gilchrist, M., Johri, A., Wallace, J. L., Hollenberg, M. D., Moqbel, R., & Befus, A. D. (2002). Proteinase-Activated Receptor (PAR)-1 and -2 Agonists Induce Mediator Release from Mast Cells by Pathways Distinct from PAR-1 and PAR-2. *Journal of Pharmacology and Experimental Therapeutics*, 302(2), 466–474. <https://doi.org/10.1124/jpet.302.2.466>
- Stiles, G. L., Caron, M. G., & Lefkowitz, R. J. (1984). Beta-adrenergic receptors: Biochemical mechanisms of physiological regulation. *Physiological Reviews*, 64(2), 661–743. <https://doi.org/10.1152/physrev.1984.64.2.661>
- Stockert, J. A., & Devi, L. A. (2015). Advancements in therapeutically targeting orphan GPCRs. *Frontiers in Pharmacology*, 6, 100. <https://doi.org/10.3389/fphar.2015.00100>
- Storch, U., Blodow, S., Gudermann, T., & Mederos y Schnitzler, M. (2015). Cysteinyl Leukotriene 1 Receptors as Novel Mechanosensors Mediating Myogenic Tone Together With Angiotensin II Type 1 Receptors—Brief Report. *Arteriosclerosis*,

- Thrombosis, and Vascular Biology*, 35(1), 121–126.
<https://doi.org/10.1161/ATVBAHA.114.304844>
- Sundström, L., Greasley, P. J., Engberg, S., Wallander, M., & Ryberg, E. (2013). Succinate receptor GPR91, a $G\alpha_i$ coupled receptor that increases intracellular calcium concentrations through PLC β . *FEBS Letters*, 587(15), 2399–2404.
<https://doi.org/10.1016/j.febslet.2013.05.067>
- Suply, T., Hannedouche, S., Carte, N., Li, J., Grosshans, B., Schaefer, M., Raad, L., Beck, V., Vidal, S., Hiou-Feige, A., Beluch, N., Barbieri, S., Wirsching, J., Lageyre, N., Hillger, F., Debon, C., Dawson, J., Smith, P., Lannoy, V., ... Bassilana, F. (2017). A natural ligand for the orphan receptor GPR15 modulates lymphocyte recruitment to epithelia. *Science Signaling*, 10(496), eaal0180.
<https://doi.org/10.1126/scisignal.aal0180>
- Suzuki, H., Motley, E. D., Eguchi, K., Hinoki, A., Shirai, H., Watts, V., Stemmle, L. N., Fields, T. A., & Eguchi, S. (2009). Distinct Roles of Protease-Activated Receptors in Signal Transduction Regulation of Endothelial Nitric Oxide Synthase. *Hypertension*, 53(2), 182–188.
<https://doi.org/10.1161/HYPERTENSIONAHA.108.125229>
- Tang, X., Wang, Y., Li, D., Luo, J., & Liu, M. (2012). Orphan G protein-coupled receptors (GPCRs): Biological functions and potential drug targets. *Acta Pharmacologica Sinica*, 33(3), 363–371. <https://doi.org/10.1038/aps.2011.210>
- Thibeault, P. E., & Ramachandran, R. (2020). Role of the Helix-8 and C-Terminal Tail in Regulating Proteinase Activated Receptor 2 Signaling. *ACS Pharmacology & Translational Science*, 3(5), 868–882. <https://doi.org/10.1021/acspsci.0c00039>
- Toma, I., Kang, J. J., Sipos, A., Vargas, S., Bansal, E., Hanner, F., Meer, E., & Peti-Peterdi, J. (2008). Succinate receptor GPR91 provides a direct link between high glucose levels and renin release in murine and rabbit kidney. *The Journal of Clinical Investigation*, 118(7), 2526–2534. <https://doi.org/10.1172/JCI33293>
- Touge, H., Chikumi, H., Igishi, T., Kurai, J., Makino, H., Tamura, Y., Takata, M., Yoneda, K., Nakamoto, M., Suyama, H., Gutkind, J. S., & Shimizu, E. (2007). Diverse activation states of RhoA in human lung cancer cells: Contribution of G protein coupled receptors. *International Journal of Oncology*, 30(3), 709–715.
<https://doi.org/10.3892/ijo.30.3.709>
- Tunaru, S., Kero, J., Schaub, A., Wufka, C., Blaukat, A., Pfeffer, K., & Offermanns, S. (2003). PUMA-G and HM74 are receptors for nicotinic acid and mediate its antilipolytic effect. *Nature Medicine*, 9(3), 352–355. <https://doi.org/10.1038/nm824>

- Turner, M. J., Mier, C. M., Spina, R. J., & Ehsani, A. A. (1999). Effects of Age and Gender on Cardiovascular Responses to Phenylephrine. *The Journals of Gerontology Series A: Biological Sciences and Medical Sciences*, 54(1), M17–M24. <https://doi.org/10.1093/gerona/54.1.M17>
- Uchiyama, K., Saito, M., Sasaki, M., Obara, Y., Higashiyama, S., & Nakahata, N. (2009). Thromboxane A2 receptor-mediated epidermal growth factor receptor transactivation: Involvement of PKC- δ and PKC- ϵ in the shedding of epidermal growth factor receptor ligands. *European Journal of Pharmaceutical Sciences*, 38(5), 504–511. <https://doi.org/10.1016/j.ejps.2009.09.016>
- Uemura, T., Kawasaki, T., Taniguchi, M., Moritani, Y., Hayashi, K., Saito, T., Takasaki, J., Uchida, W., & Miyata, K. (2006). Biological properties of a specific G α_q /11 inhibitor, YM-254890, on platelet functions and thrombus formation under high-shear stress. *British Journal of Pharmacology*, 148(1), 61–69. <https://doi.org/10.1038/sj.bjp.0706711>
- Uemura, T., Takamatsu, H., Kawasaki, T., Taniguchi, M., Yamamoto, E., Tomura, Y., Uchida, W., & Miyata, K. (2006a). Effect of YM-254890, a specific G α_q /11 inhibitor, on experimental peripheral arterial disease in rats. *European Journal of Pharmacology*, 536(1–2), 154–161. <https://doi.org/10.1016/j.ejphar.2006.02.048>
- Uemura, T., Takamatsu, H., Kawasaki, T., Taniguchi, M., Yamamoto, E., Tomura, Y., Uchida, W., & Miyata, K. (2006b). Effect of YM-254890, a specific G α_q /11 inhibitor, on experimental peripheral arterial disease in rats. *European Journal of Pharmacology*, 536(1–2), 154–161. <https://doi.org/10.1016/j.ejphar.2006.02.048>
- Vanti, W. B., Nguyen, T., Cheng, R., Lynch, K. R., George, S. R., & O'Dowd, B. F. (2003). Novel human G-protein-coupled receptors. *Biochemical and Biophysical Research Communications*, 305(1), 67–71. [https://doi.org/10.1016/S0006-291X\(03\)00709-5](https://doi.org/10.1016/S0006-291X(03)00709-5)
- Vergnolle, N., Hollenberg, M. D., Sharkey, K. A., & Wallace, J. L. (1999). Characterization of the inflammatory response to proteinase-activated receptor-2 (PAR2)-activating peptides in the rat paw. *British Journal of Pharmacology*, 127(5), 1083–1090. <https://doi.org/10.1038/sj.bjp.0702634>
- Vergnolle, N., Macnaughton, W. K., Al-Ani, B., Saifeddine, M., Wallace, J. L., & Hollenberg, M. D. (1998a). Proteinase-activated receptor 2 (PAR2)-activating peptides: Identification of a receptor distinct from PAR2 that regulates intestinal transport. *Proceedings of the National Academy of Sciences*, 95(13), 7766–7771. <https://doi.org/10.1073/pnas.95.13.7766>
- Vergnolle, N., Macnaughton, W. K., Al-Ani, B., Saifeddine, M., Wallace, J. L., & Hollenberg, M. D. (1998b). Proteinase-activated receptor 2 (PAR2)-activating

- peptides: Identification of a receptor distinct from PAR2 that regulates intestinal transport. *Proceedings of the National Academy of Sciences*, 95(13), 7766–7771. <https://doi.org/10.1073/pnas.95.13.7766>
- Vergnolle, N., Wallace, J. L., Bunnett, N. W., & Hollenberg, M. D. (2001). Protease-activated receptors in inflammation, neuronal signaling and pain. *Trends in Pharmacological Sciences*, 22(3), 146–152. [https://doi.org/10.1016/S0165-6147\(00\)01634-5](https://doi.org/10.1016/S0165-6147(00)01634-5)
- Wang, H., & He, S. (2006). Induction of lactoferrin and IL-8 release from human neutrophils by tryptic enzymes via proteinase activated receptor-2. *Cell Biology International*, 30(9), 688–697. <https://doi.org/10.1016/j.cellbi.2006.04.007>
- Watkins, L. R., & Orlandi, C. (2020). Orphan G Protein Coupled Receptors in Affective Disorders. *Genes*, 11(6), 694. <https://doi.org/10.3390/genes11060694>
- Weekley, L. B. (1993). Effects of melatonin on pulmonary and coronary vessels are exerted through perivascular nerves. *Clinical Autonomic Research*, 3(1), 45–47. <https://doi.org/10.1007/BF01819143>
- Weng, Y., Wang, J., Yang, Z., Xi, M., Duan, J., Guo, C., Yin, Y., Segawa, R., Moriya, T., Yonezawa, T., Cha, B. Y., Woo, J.-T., Wen, A., & Hirasawa, N. (2019). A steroid alkaloid derivative 02F04 upregulates thymic stromal lymphopoietin expression slowly and continuously through a novel Gq/11-ROCK-ERK1/2 signaling pathway in mouse keratinocytes. *Cellular Signalling*, 57, 58–64. <https://doi.org/10.1016/j.cellsig.2019.01.005>
- Wittamer, V., Franssen, J.-D., Vulcano, M., Mirjolet, J.-F., Le Poul, E., Migeotte, I., Brézillon, S., Tyldesley, R., Blanpain, C., Detheux, M., Mantovani, A., Sozzani, S., Vassart, G., Parmentier, M., & Communi, D. (2003). Specific Recruitment of Antigen-presenting Cells by Chemerin, a Novel Processed Ligand from Human Inflammatory Fluids. *The Journal of Experimental Medicine*, 198(7), 977–985. <https://doi.org/10.1084/jem.20030382>
- Xu, L., & Brink, M. (2016). MTOR, cardiomyocytes and inflammation in cardiac hypertrophy. *Biochimica et Biophysica Acta (BBA) - Molecular Cell Research*, 1863(7, Part B), 1894–1903. <https://doi.org/10.1016/j.bbamcr.2016.01.003>
- Yoshimura, T., & Oppenheim, J. J. (2011). Chemokine-like Receptor 1 (CMKLR1) and Chemokine (C-C motif) Receptor-like 2 (CCRL2); Two Multifunctional Receptors with Unusual Properties. *Experimental Cell Research*, 317(5), 674–684. <https://doi.org/10.1016/j.yexcr.2010.10.023>

Zhang, H., Nielsen, A. L., & Strømgaard, K. (2020). Recent achievements in developing selective Gq inhibitors. *Medicinal Research Reviews*, 40(1), 135–157.
<https://doi.org/10.1002/med.21598>

Appendices

Appendix 1: Animal use protocol



PI :	McGuire, John
Protocol #	2018-109
Status :	Approved (w/o Stipulation)
Approved :	10/01/2018
Expires :	10/01/2022
Title :	Novel receptor in blood vessels of mice

Curriculum Vitae

Name: Joselia Carlos

Education MSc in Medical Biophysics
University of Western Ontario
London, Ontario, Canada
2019 – present

BMSc in Medical Cell Biology
University of Western Ontario
London, Ontario, Canada
2014 – 2019

Honours and Awards Western Graduate Research Scholarship (\$4500/year)
2019 – 2020, 2020 – 2021

Western Scholarship of Excellence (\$2000)
2014

Research Experience Graduate Student Research Assistant
University of Western Ontario, London, ON
Dr. John McGuire, Medical Biophysics
2019 – present

Undergraduate Student Researcher
London Regional Cancer Program, Victoria Hospital, London, ON
Dr. Alison Allan, Anatomy and Cell Biology, Oncology
2018 – 2019

Undergraduate Student Researcher
London Regional Cancer Program, Victoria Hospital, London, ON
Dr. Eva Turley, Anatomy and Cell Biology, Oncology
2016 – 2018

Teaching Experience Graduate Teaching Assistant
MEDBIO 4700B
University of Western Ontario, London, ON
Jan 2020 – April 2021

Graduate Teaching Assistant
MEDBIO 3501A
University of Western Ontario, London, ON
Sept 2020 – Dec 2020

Extracurricular Activities Executive Committee Member
Science-to-Business Network, London Chapter, ON
Nov 2019 – Aug 2021

Professional Society Memberships
British Journal Pharmacology Society (2020 – 2021)

PUBLICATION HISTORY

Peer-Reviewed Manuscripts

1. Kitz, J., Lefebvre, C., **Carlos, J.**, Lowes, L. E., & Allan, A. L. (2021). Reduced Zeb1 Expression in Prostate Cancer Cells Leads to an Aggressive Partial-EMT Phenotype Associated with Altered Global Methylation Patterns. *International Journal of Molecular Sciences*, 22(23), 12840.
<https://doi.org/10.3390/ijms222312840>

Published Abstracts:

1. **Carlos, J.**, and McGuire, J., “Inhibitor of $G\alpha_{q,11}$ signalling blocks femoral artery smooth muscle contraction by trans-cinnamoyl-LIGRLO-amide in PAR2 knockout mice.” *Current Trends in Drug Discovery*. 9 – 10 June 2021. (United Kingdom; Virtual)
2. **Carlos, J.**, and McGuire, J., “The effects of G_q inhibitor YM-254890, sex, and age on mouse vascular smooth muscle contraction by a synthetic peptide.” *London Health Research Day*. 11 May 2021. (London, ON; Virtual).
3. **Carlos, J.**, and McGuire, J., “The effects of G_q inhibitor YM-254890, sex, and age on mouse vascular smooth muscle contraction by the synthetic peptide trans-cinnamoyl-LIGRLO-amide.” *Pharmacology 2020*. 14 – 18 Dec 2020. (United Kingdom; Virtual).
4. Kitz, J., Lowes, L.E., Goodale, D., Postenka, C., **Carlos, J.**, and Allan, A.L., “Influence of Zeb1 on the epithelial-to-mesenchymal transition and detection of circulating tumour cells in preclinical models of prostate cancer,” *Advances in Circulating Tumour Cells (ACTC) Meeting. Corfu, Greece*. 2 – 5 October 2019.
5. **Carlos, J.**, Kitz, J., and Allan, A.L., “Phenotypic and functional influence of Zeb1 knockdown in aggressive prostate cancer cells,” *Ontario Biology Day. London, Canada*. 23 March 2019.